Doctoral Dissertation

Studies on Fine Tuning of Lewis Acidity and Catalytic Activity Using Indium or *C*,*N*-Chelated Organoaluminum Complexes

Shuichi Nakao

January 2021

Department of Applied Chemistry
Graduate School of Engineering
Osaka University

Preface and Acknowledgements

The work of this thesis has been performed from 2015 to 2021 under the guidance of Prof. Dr. Makoto Yasuda at Department of Applied Chemistry, Graduated School of Engineering, Osaka University. The thesis describes development of Lewis acid-catalyzed reactions and novel Lewis acid catalysts based on fine tuning of Lewis acidity and catalytic activity of indium or *C*,*N*-chelated organoaluminum complexes.

First and foremost, I would like to express my sincerest gratitude to Prof. Dr. Makoto Yasuda for his precise guidance, helpful suggestions, and hearty encouragements throughout this work.

I would also like to thank Professors Dr. Toshiyuki Kida and Dr. Mamoru Fujitsuka for their helpful advice and kind assistance.

I really wish to make a grateful acknowledgement to Associate Prof. Dr. Yoshihiro Nishimoto for his intimate guidance, continuous advice, and kind encouragement.

I gratefully express acknowledgement to Assistant Prof. Dr. Akihito Konishi for his invaluable assistance, helpful suggestion, and stimulating discussion.

I would sincerely like to thank Prof. Dr. Suzanne Blum for giving me an opportunity of my overseas education in University of California, Irvine.

I would like to express my heartfelt thanks to Mr. Hiroshi Moriguchi, Dr. Nobuko Kanehisa, Dr. Kyoko Inoue, Dr. Hiroaki Tanaka, Mr. Kunihiko Kamon and Mr. Hiromi Ohi for giving me analytic assistance at the analytical instrumentation facility.

I am deeply thankful to Ms. Yoshimi Shinomiya for giving me her grateful support and heartwarming kindness.

Furthermore, I gratefully wish to thank Ms. Miki Saikai for her valuable discussion and active working. I also wish to acknowledge to all the members of Yasuda group for their hearty encouragement and constant support.

Finally, I would like to express my thanks to respectable parents, Hideaki Nakao and Yukari Nakao, for their understanding to my work, constant assistance, and financial support.

Shuichi Nakao

Department of Applied Chemistry
Graduate School of Engineering
Osaka University
2-1 Yamadaoka, Suita, Osaka 565-0871, JAPAN
January, 2021

List of Publications

1. Synthesis and Characterization of Pheox– and Phebox–Aluminum Complexes: Application as Tunable Lewis Acid Catalysts in Organic Reactions
   Y. Nishimoto, S. Nakao, S. Machinaka, F. Hidaka, M. Yasuda
   Chem. Eur. J. **2019**, *25*, 10792–10796.

2. $InBr_3$-Catalyzed Coupling Reaction between Electron-deficient Alkenyl Ethers with Silyl Enolates for Stereoselective Synthesis of 1,5-Dioxo-alk-2-enes
   S. Nakao, M. Saikai, Y. Nishimoto, M. Yasuda
   Eur. J. Org. Chem. **2021**, 77–81.

3. Tuning of Lewis Acidity of Phebox-Al Complexes by Substituents on the Benzene Backbone and Unexpected Photocatalytic Activity for Hydrodebromination of Aryl Bromide
   S. Nakao, Y. Nishimoto, M. Yasuda
   Chem. Lett. **2021**, DOI: 10.1246/cl.200894

Supplementary Publication

1. Borylative Heterocyclization without Air-Free Techniques
   C. Gao, S. Nakao, S. A. Blum
   J. Org. Chem. **2020**, *85*, 10350–10368.

Contents

General Introduction 1
References 5
Chapter 1. $InBr_3$-Catalyzed Coupling Reaction between Electron-Deficient Alkenyl Ethers with Silyl Enolates for Stereoselective Synthesis of 1,5-Dioxo-alk-2-enes 6
1-1. Introduction 6
1-2. Results and Discussion 7
1-3. Conclusion 15
1-4. Experimental Section 15
1-5. References 38
Chapter 2. Synthesis and Characterization of Pheox– and Phebox–Aluminum Complexes: Application as Tunable Lewis Acid Catalysts in Organic Reactions 42
2-1. Introduction 42
2-2. Results and Discussion 43
2-3. Conclusion 51
2-4. Experimental Section 51
2-5. References 75
Chapter 3. Phebox–Al Catalyzed Hydrodebromination Reaction under Visible Light Irradiation: Ligand-to-Ligand Charge Transfer through Aluminum Center 77
3-1. Introduction 77
3-2. Results and Discussions 78
3-3. Conclusion 84
3-4. Experimental Section 85
3-5. References 87
Conclusion 89

General Introduction

Lewis acids are important chemical species that are essential for various chemical transformations. In petrochemistry, solid acid catalysts, such as zeolites, are used in the catalytic cracking process of fuel oils,[1] which is one of the largest catalytic processes (Scheme 1A). Lewis acids have also been used in organic synthesis for many years, for example in Friedel-Crafts alkylation reactions (Scheme 1B),[2] and are still used as essential catalysts for various molecular transformations.[3]

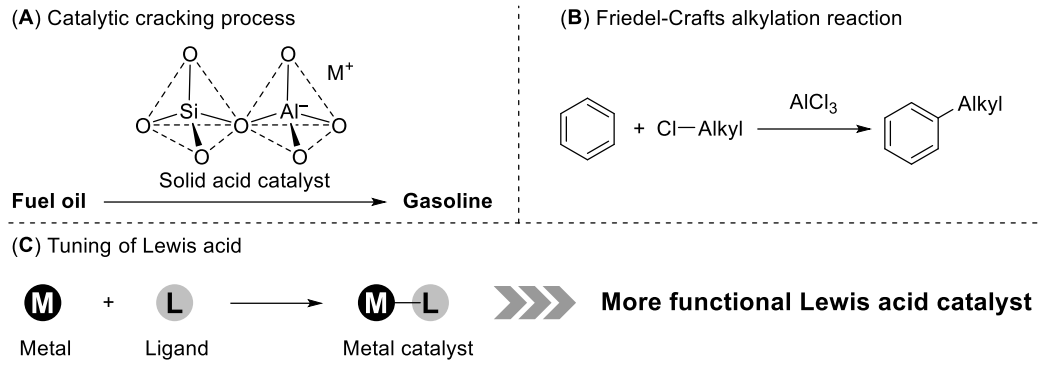

Scheme 1. Lewis acid catalysis

Thus, Lewis acid catalysts are one of the most important catalysts in chemical processes. Therefore, the improvement of reactivity, selectivity, and versatility in catalytic processes still remains an important issue. To precisely control the properties of the Lewis acid, the selection of the metal center, which is the Lewis acidic site, and the design of the ligands are necessary for the development of highly functionalized Lewis acid catalysts (Scheme 1C).

The Lewis acidity is an important factor in tuning the catalytic activity, but the higher Lewis acidity does not necessarily have a positive effect on catalytic activity. Piers and coworkers reported that $PhB(C_6F_5)_2$, which has lower Lewis acidity than $B(C_6F_5)_3$, has higher catalytic activity in allylation of aldehydes (Table 1).[4] That is because lower Lewis acidity promotes the release of products and regeneration of catalyst.

Table 1. Lewis acid-catalyzed allylation of aldehyde

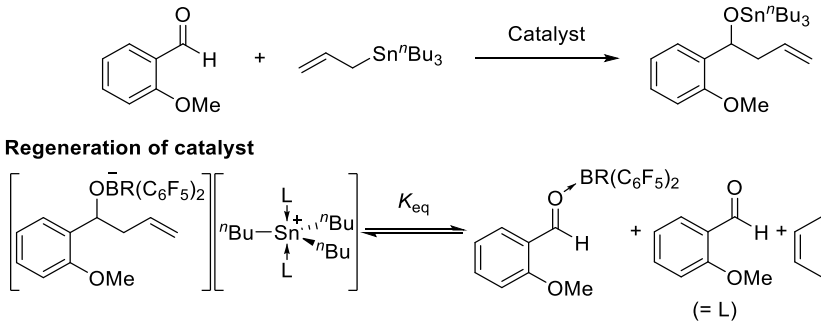

Catalyst	Lewis acidity[a]	Conversion [%]	K_{eq}
$B(C_6F_5)_3$	0.68	21	6.0×10^{-5}
$PhB(C_6F_5)_2$	0.54	100	3.0×10^{-3}

[a] Lewis acidity was evaluated by Childs' method.[5] The stronger the acidity of the Lewis acid, the larger is the value.

In the Lewis acid-catalyzed Morita–Baylis–Hillman reaction, Aggrwal and coworkers reported that $La(OTf)_3$ with a lower Lewis acidity had a higher catalytic activity than $Sc(OTf)_3$ (Table 2).[6] Thus, it is important to select a catalyst with an appropriate Lewis acidity for the Lewis acid-catalyzed reaction.

Table 2. Lewis acid-catalyzed Morita–Baylis–Hillman reaction

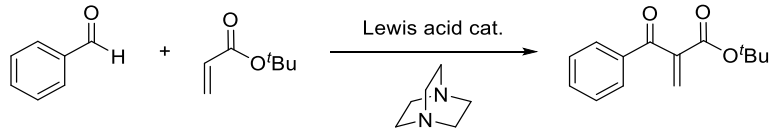

Lewis acid cat.	Lewis acidity [eV][a]	k_{rel}[b]
None	–	1
Sc(OTf)3	1.00	3.3
Ln(OTf)3	0.82	4.7

[a] Lewis acidity was evaluated by fluorescence maxima of 10-methylacridone–metal ion salt complexes.[7] The stronger the acidity of the Lewis acid, the larger is the value. [b] Relative to reactions using 100 mol % DABCO as a catalyst and no Lewis acid.

In the case of tuning the Lewis acidity by a metal center, the Lewis acidity and its catalytic activity would be drastically changed. Kobayashi and coworkers reported the inversion of the substrate-selectivity in the competitive reaction between aldehydes and aldimines (Table 3).[8,9] $Yb(OTf)_3$ catalyzed the reaction of aldimines selectively. On the other hand, typical Lewis acids such as $SnCl_4$ and $TiCl_4$ catalyzed aldehydes selectively.

Table 3. Inversion of selectivity in competitive reaction between aldehyde and aldimine

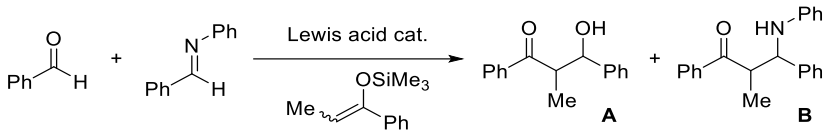

Lewis acid cat.	**A**/**B**
$SnCl_4$	>99/1
$TiCl_4$	>99/1
$Yb(OTf)_3$	<1/>99

Our group reported that InI_3 exhibited the different cyclization mode (Scheme 2 right)[10] from *B*-chloro catecolborane in the cyclic oxymetalation (Scheme 2 left).[11] In the cyclization of methyl 2-ethynylbenzoate, the use of InI_3 led to a 6-*endo* cyclization, giving an isocoumarin derivative. In contrast, the use of chloro catecolborane resulted in the formation of a 5-*exo* cyclization product.

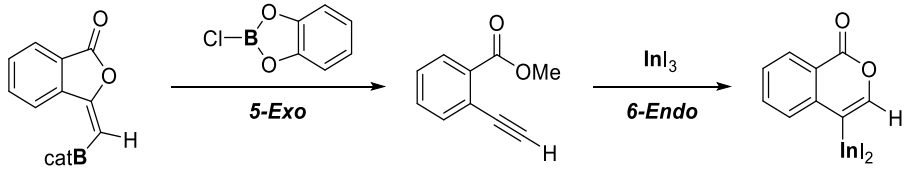

Scheme 2. Changing regioselectivity of cyclization of Methyl 2-ethynylbenzoate

Thus, to control the selectivity between considerably different substrates or at considerably different locations, drastic changes in Lewis acidity by changing a kind of metals could be effective, but more precise control of Lewis acidity is required to control the selectivity between similar substrates or similar reaction paths.

The ligand is also an important factor for the control of a Lewis acidity. In the ligand design of triarylboranes, it is expected that the electron affinity and Lewis acidity of the boron complexes are improved by introduction of pentachlorophenyl groups which are more electron-withdrawing than a pentafluorophenyl group. In fact, replacing the pentafluorophenyl groups with pentachlorophenyl groups increases the electrophilicity of the boron center, but decreases the Lewis acidity (Scheme 3).[12] This is due to the increase in steric repulsion between chlorine atoms due to the structural change caused by the coordination of the Lewis base. Not only the electrophilic properties of the metal center, but also the structural changes caused by the interaction with Lewis bases must be considered in ligand design. Therefore, the establishment of the comprehensive design or modification guidelines of ligands is an important issue.

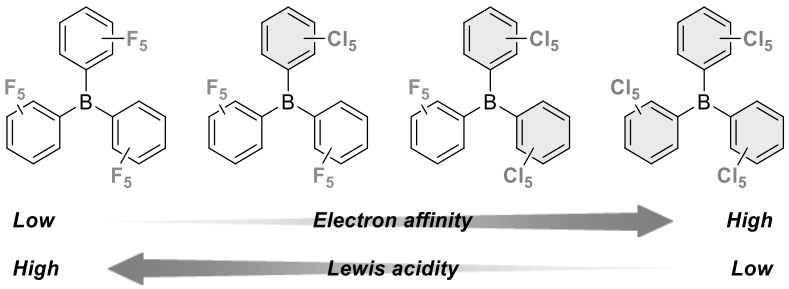

Scheme 3. Orthogonal change of Lewis acidity with electron affinity

Based on the strategy of fine tuning of Lewis acidity by the metal center and the ligand, I developed a new Lewis acid catalyzed reaction and novel Lewis acid catalysts. In addition, I also designed ligands to give functionality to the catalyst. This thesis consists of the following chapters.

Chapter 1 describes the $InBr_3$-catalysed coupling reaction between electron-deficient alkenyl ethers with silyl enolates for stereoselective synthesis of 1,5-dioxo-alk-2-enes. This reaction occurs through addition–elimination mechanism and gives coupling products stereoselectively.

Chapter 1: $InBr_3$-catalysed coupling reaction between electron-deficient alkenyl ethers with silyl enolates for stereoselective synthesis of 1,5-dioxo-alk-2-enes

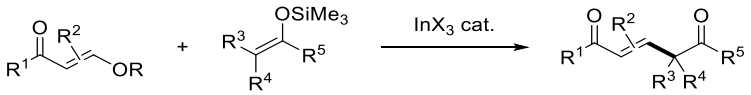

Chapter 2 focuses on aluminum, which is the cheaper and more abundant metal, as a metal center and its Lewis acidity is controlled by the ligand. I synthesized and characterized *C*,*N*-chelated organoaluminum complexes, Pheox– and Phebox–aluminum complexes. These complexes acted as tunable Lewis acid catalysts in organic reactions.

Chapter 2: Synthesis and characterization of Pheox– and Phebox–aluminum complexes: Application as tunable Lewis acid catalysts in organic reactions

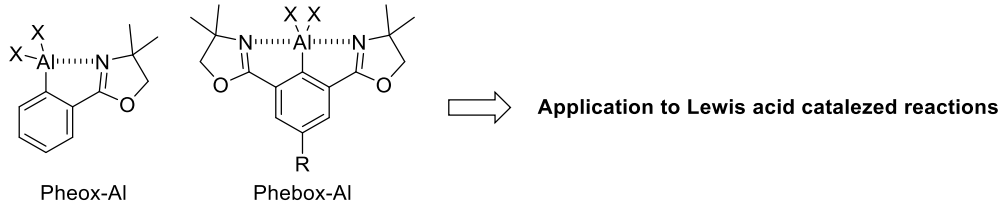

Another application of Phebox–Al complexes is mentioned in Chapter 3. Phebox–Al complexes catalyzed hydrodebromination reaction of aryl bromides efficiently under visible light irradiation was developed. Substrate recognition not depending on reduction potential was achieved due to the Lewis acidic site of Al complexes.

Chapter 3: Phebox–Al catalyzed hydrodebromination reaction under visible light irradiation: Ligand-to-ligand charge transfer through aluminum center

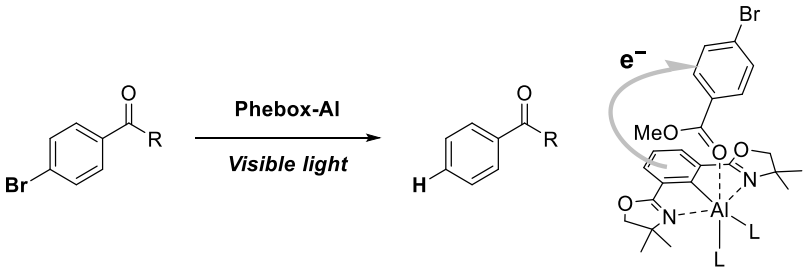

References

[1] W. Vermeiren, J. P. Gilson, *Top. Catal.* **2009**, *52*, 1131–1161.

[2] E. Ador, J. Crafts, *Berichte der Dtsch. Chem. Gesellschaft* **1877**, *10*, 2173–2176.

[3] H. Yamamoto, Ed., *Lewis Acids in Organic Synthesis*, Wiley, **2000**.

[4] D. J. Morrison, W. E. Piers, *Org. Lett.* **2003**, *5*, 2857–2860.

[5] R. F. Childs, D. L. Mulholland, A. Nixon, *Can. J. Chem.* **1982**, *60*, 801–808.

[6] V. K. Aggarwal, A. Mereu, G. J. Tarver, R. McCague, *J. Org. Chem.* **1998**, *63*, 7183–7189.

[7] S. Fukuzumi, K. Ohkubo, *J. Am. Chem. Soc.* **2002**, *124*, 10270–10271.

[8] S. Kobayashi, S. Nagayama, *J. Am. Chem. Soc.* **1997**, *119*, 10049–10053.

[9] S. Kobayashi, S. Nagayama, *J. Org. Chem.* **1997**, *62*, 232–233.

[10] Y. Kita, T. Yata, Y. Nishimoto, K. Chiba, M. Yasuda, *Chem. Sci.* **2018**, *9*, 6041–6052.

[11] D. J. Faizi, A. Issaian, A. J. Davis, S. A. Blum, *J. Am. Chem. Soc.* **2016**, *138*, 2126–2129.

[12] A. E. Ashley, T. J. Herrington, G. G. Wildgoose, H. Zaher, A. L. Thompson, N. H. Rees, T. Krämer, D. Öhare, *J. Am. Chem. Soc.* **2011**, *133*, 14727–14740.

Chapter 1. $InBr_3$-Catalyzed Coupling Reaction between Electron-Deficient Alkenyl Ethers with Silyl Enolates for Stereoselective Synthesis of 1,5-Dioxo-alk-2-enes

1-1. Introduction

Catalytic cross-coupling via the transformation of C–O bonds to C–C bonds has been an important pursuit of organic chemists for the past twenty years in attempts to replace organic halides with more environmentally benign oxygen-based electrophiles such as alcohol, arenol, and enol derivatives.[1,2] In particular, the coupling between enol derivatives and enolate nucleophiles is one of the most significant of these reactions, because the α-alkenyl carbonyl compounds produced in this process are recognized as valuable building blocks for pharmaceuticals, natural products, and organic materials (Scheme 1A),[3] but robust C–O bonds make this catalytic reaction a challenge.[4] Thus far, the report of $GaBr_3$-catalyzed coupling reactions of enol derivatives with ketene silyl acetals that were established by our group remains the only description of the availability of electron-rich enol derivatives (Scheme 1B).[5] As far as electron-deficient enol derivatives are concerned, the Michael addition/elimination reaction system using 2-carbonylalkenyl ethers is the sole methodology (Scheme 1C).[6,7,8] A severely narrow scope of substrates, however, restricts both the generality and the diversity of this reaction system. In fact, either a polyhalogenated acyl group or two electron-withdrawing groups on enol derivatives is necessary, and enolate nucleophiles are limited to stabilized alkali metal enolates such as those from 1,3-diketone and β-keto ester derivatives,[6] phosphoranylideneacetates,[7] and 2-oxoethylpyridinium salts.[8] Therefore, a strategy that could achieve more versatile reactions is highly desirable. In this study, we overcame these limitations and developed an $InBr_3$-catalyzed coupling reaction between 2-carbonylalkenyl ethers and silyl enolates (Scheme 1D). Various alkenyl ethers substituted by only one carbonyl group are applicable to this reaction. The availability of useful silyl enolates is a notable advantage over previously reported reactions. It is noteworthy that the corresponding alk-2-ene-1,5-diones were produced with alkene moieties that have perfect stereoselectivity.

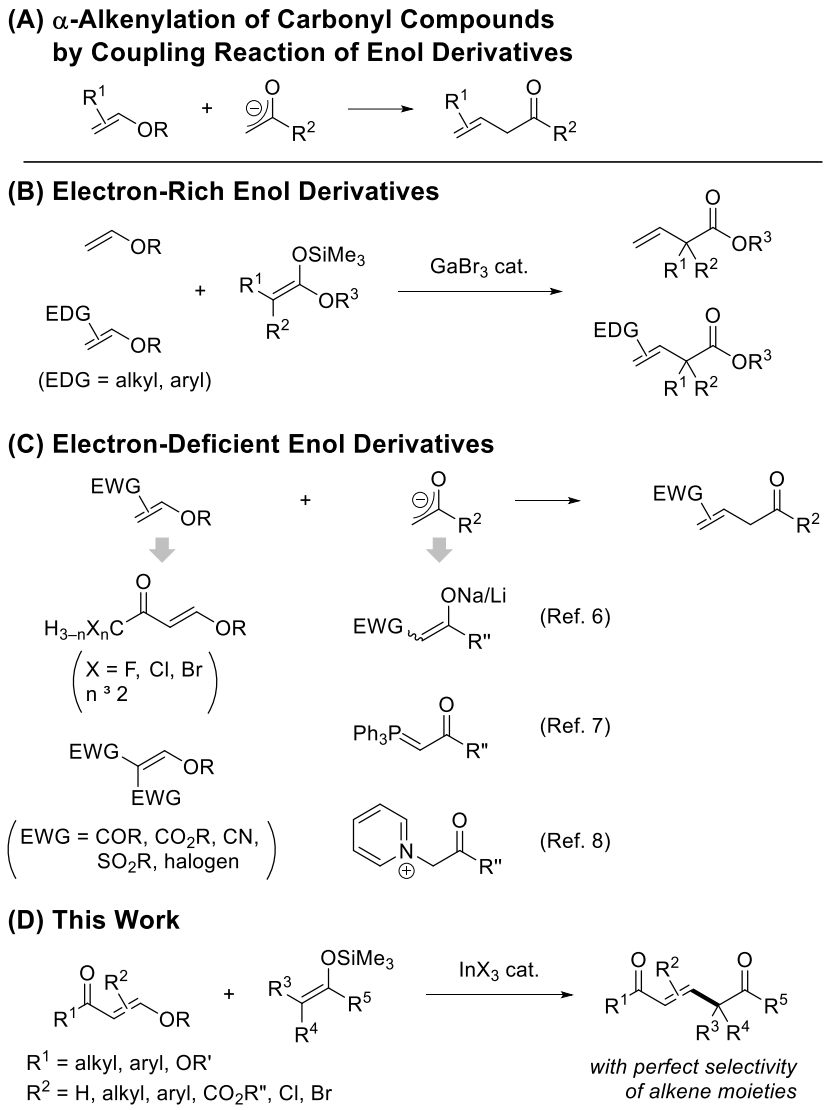

Scheme 1. Coupling reaction between enol derivatives and enolate nucleophiles.

1-2. Results and Discussion

The electron-donating effect of an alkoxy group reduces electrophilicity of enol derivatives. Therefore, reported reactions require quite strong or two electron-withdrawing groups on enol derivatives and high-nucleophilic enolate species. A simple and promising strategy to solve this problem would be the enhancement of electrophilicity of electron-withdrawing group by Lewis acids. However, there is no report for Lewis acid-catalyzed system because typical Lewis acids are deactivated by substrates (2-carbonylalkenyl ethers and enolate nucleophiles), products, and by-products due to their coordinating sites which interacts with the strong Lewis acids. Our and other groups have revealed that moderate-Lewis acidic indium and gallium salts have an important property of fast ligand exchange to be not tightly trapped by one substrate but to flexibly interact with various coordinating sites in the reaction system.[5,9,10] Therefore, indium and gallium catalysts have a

possibility to achieve a desired reaction course when a suitable reaction system is designed. In Table 1, we started from investigation of indium and gallium salts in the reaction of alkenyl ether **1a** with ketene silyl acetal **2a**.[11] To our delight, indium halides exhibited the effective catalytic activity (Entries 1–3). $InBr_3$ was the best catalyst to give an excellent yield of the desired product **3aa** (Entry 2). Gallium halides possessed slightly less activity than indium halides (Entries 4–6). The use of $In(OTf)_3$ and $Ga(OTf)_3$ resulted in low yields (Entries 7 and 8). Typical group 13 Lewis acids, $BF_3{\cdot}OEt_2$ and $AlCl_3$, hardly gave **3aa** (Entries 9 and 10). Transition metal salts such as zinc, scandium, iron, palladium, gold salts were less effective to give sluggish results (Entries 11–17). The cationic InI_2 catalyst generated from InI_3 and $AgSbF_6$ was less effective in the present coupling reaction (Entry 18).[12] The catalyst-free conditions afforded no products (Entry 19).

Table 1. Investigation of metal salt catalysts in coupling reaction of alkenyl ether 1a with ketene silyl acetal **2a**.[a]

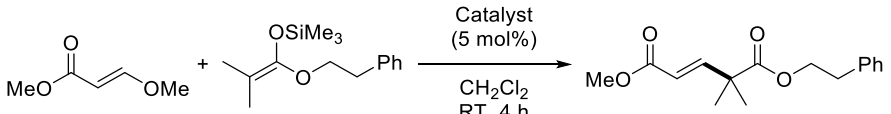

Entry	Catalyst	Yield of 3aa		Entry	Catalyst	Yield of 3aa
1	$InCl_3$	4%		10	$AlCl_3$	0%
2	$InBr_3$	93%	(84%)	11	$ZnCl_2$	0%
3	InI_3	63%		12	$ZnBr_2$	0%
4	$GaCl_3$	0%		13	$Sc(OTf)_3$	21%
5	$GaBr_3$	84%		14	$FeCl_3$	0%
6	GaI_3	72%		15	$PdCl_2$	0%
7	$In(OTf)_3$	10%[c]		16	AuCl	0%
8	$Ga(OTf)_3$	8%		17	$AuCl_3$	0%
9	$BF_3{\cdot}OEt$	10%		18[d]	$InI_3 + AgSbF_6$	16%
				19	none	0%

[a] **1a** (0.5 mmol), **2a** (0.75 mmol), Catalyst (0.025 mmol), CH_2Cl_2 (1 mL), room temperature, 4 h. [b] The yields of **3aa** were measured by ^1H NMR analysis of the crude mixture. The isolated yield is shown in a parenthesis. [c] 24 h. [d] InI_3 (5 mol%) and $AgSbF_6$ (5 mol%) were used.

We used typical methods to compare the $InBr_3$-catalyzed reaction (Scheme 2). As mentioned above, a catalytic amount of $InBr_3$ gave **3aa** in an excellent yield in the reaction of **1a** with **2a** (Scheme 2A). A typical Mukaiyama-type reaction with $TiCl_4$[13] resulted in the recovery of **1a** without the formation of **3aa** (Scheme 2B). A fluoride anion[14] is known to mediate the addition of silyl enolates to α,β-unsaturated carbonyl compounds, but tetrabutylammonium fluoride was ineffective in this

reaction (Scheme 2C). The use of lithium enolate **4** also gave a poor result (Scheme 2D).[15] Under Reformatsky-type reaction conditions, product **5** was obtained neither at room temperature nor at 50 °C, although an over-reaction of **5** with the zinc enolate proceeded at 50 °C to give undesired product **7** in 32% yield (Scheme 2E).[16] A comparison study revealed that, rather than strong Lewis acid catalysts and highly nucleophilic enolates, moderate Lewis acidic $InBr_3$ and moderate nucleophilic silyl enolates efficiently achieved the desired coupling reaction.

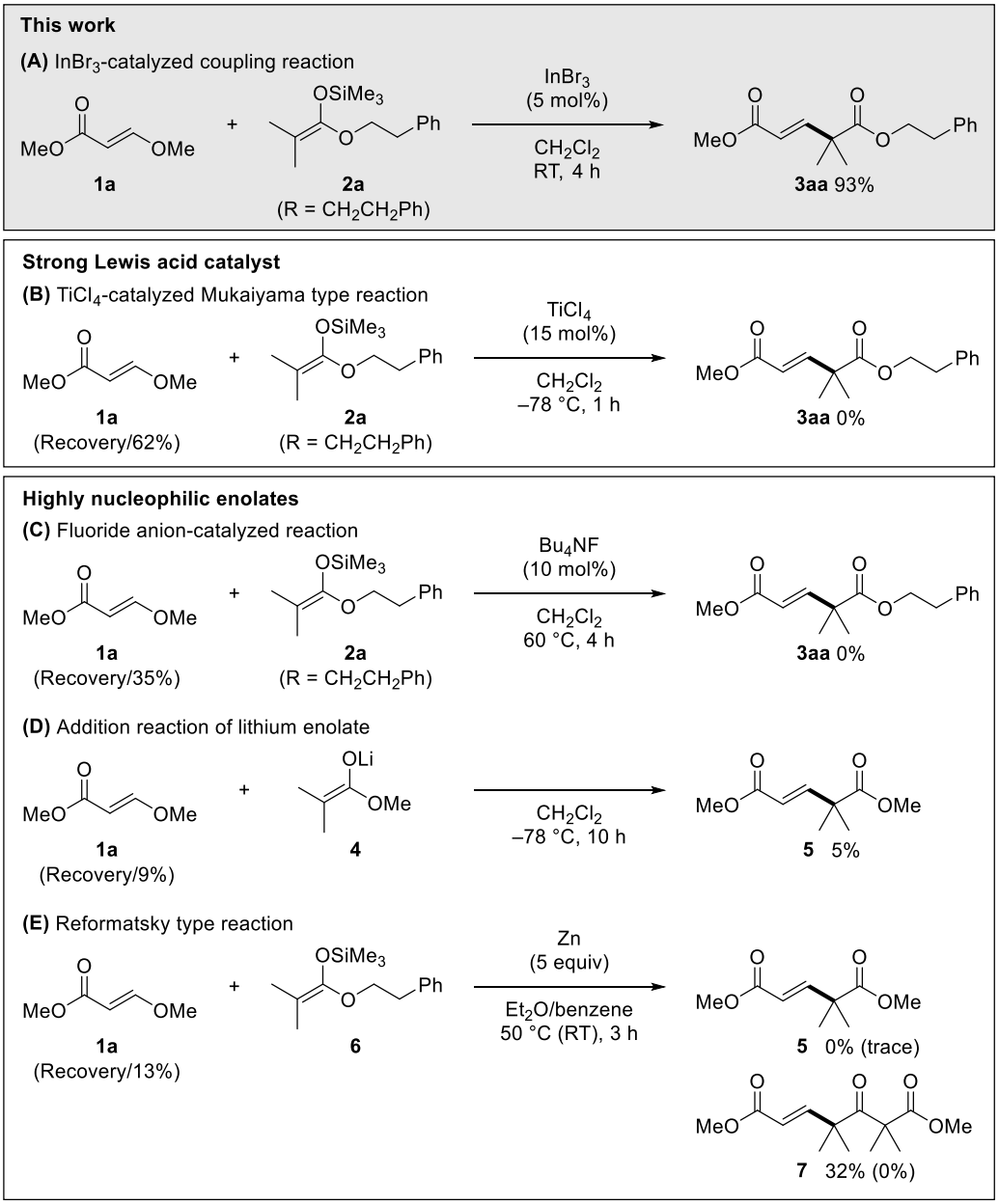

Scheme 2. Comparison among $InBr_3$-catalyzed reaction and typical methods

With the optimal conditions in hand (Entry 2, Table 1), we explored the scope of alkenyl ethers **1** (Scheme 3). Various 2-carbonylalkenyl ethers were applicable to this reaction system, and the single stereoisomers for alkene moieties were selectively furnished in all cases. Acetyl and benzoyl groups were tolerated and the desired products **3ba** and **3ca** were obtained in 61 and 88% yields, respectively. The coupling reactions using 1- or 2-alkylsubstituted alkenyl ethers occurred in moderate yields (**3da**, **3ea**, and **3fa**). Phenyl-substituted substrates reacted effectively (**3gj**). The halogen-substituted alkenyl ethers were also suitable substrates, affording the corresponding products **3ha** and **3ia**. In a reaction using a 2,2-di(methoxycarbonyl)-substituted substrate, $GaBr_3$ instead of $InBr_3$ worked as an efficient catalyst to afford a high yield of **3ja**. The alkynyl group at the 2-position was compatible in this coupling reaction (**3kj**). It is noted that an *E*/*Z*-mixture of alkenyl ether **1l** led to the exclusive yield of *E*-isomer product **3la**.[17]

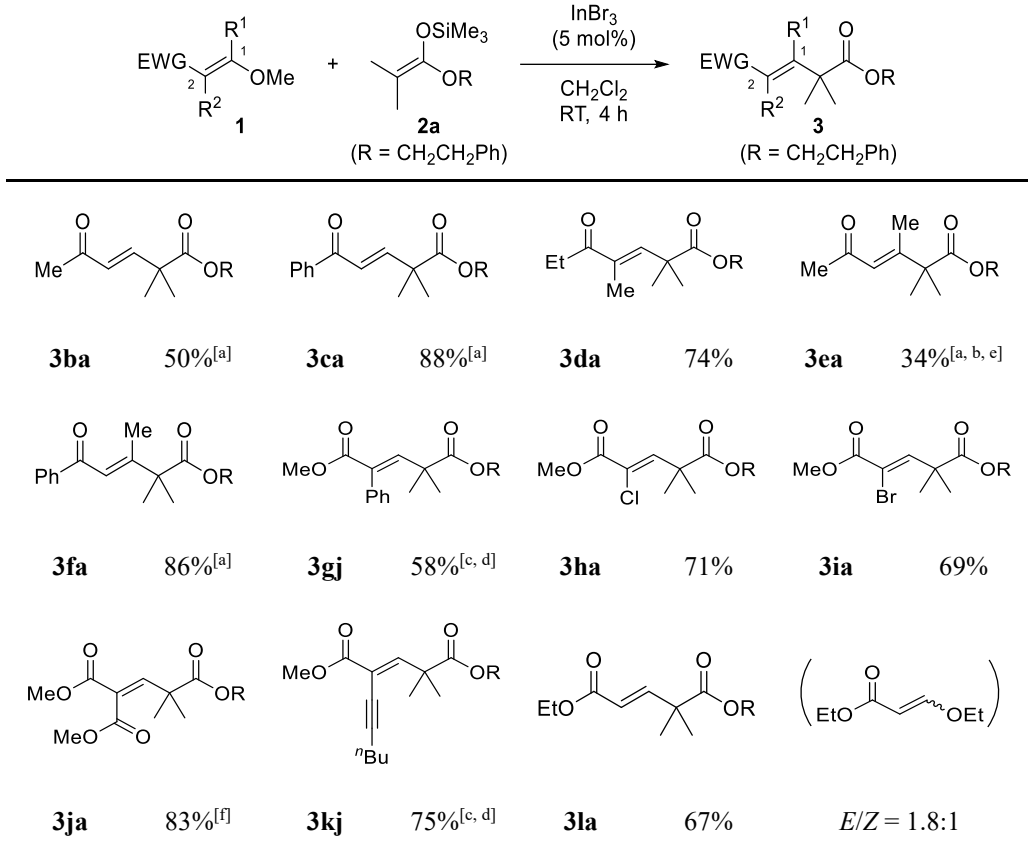

Scheme 3. Scope of alkenyl ethers **1** in the coupling of **2a**. Standard conditions: **1** (0.5 mmol), **2a** (0.5–0.75 mmol), $InBr_3$ (0.025 mmol), CH_2Cl_2 (1 mL), 4 h. Isolated yields are shown. [a] 0 °C, 2 h. [b] $In(OTf)_3$ instead of $InBr_3$. [c] $InBr_3$ (10 mol%) was used. [d] Ketene silyl acetal **2j** (R = Me) was used. [e] The NMR yield is shown. [f] $GaBr_3$ instead of $InBr_3$ was used. 2 h.

The scope of ketene silyl acetals **2** in the coupling reaction of alkenyl ether **1b** was investigated (Table 2). Disubstituted ketene silyl acetals **2b**, **2c** and **2d** afforded the corresponding α-alkenyl esters in yields that ranged from moderate to high (Entries 1–3). Butylketene silyl acetal **2e** and unsubstituted ketene silyl acetal **2f** were applicable to afford products **3be** (Entry 4) and **3bf** (Entry 5) in 49 and 97% yields, respectively, although the alkene moiety of **3bf** was isomerized. The coupling with cyclic ketene silyl acetal **2g** proceeded to give product **3bg** in 52% yield (Entry 6). Silyl enol ethers acted as efficient nucleophiles. The desired products **3bh** and **3bi** were selectively obtained in the reactions using **2h** and **2i**, respectively (Entries 7 and 8).

Table 2. Scope of ketene silyl acetals **2** in the reaction with **1b**.[a]

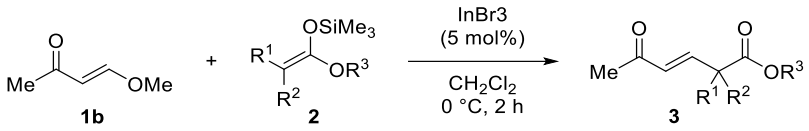

Entry	**2**	**3**	Yield of **3**
1	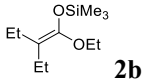 **2b**	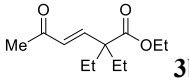 **3bb**	81%
2	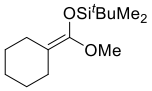 **2c**	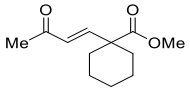 **3bc**	70%
3	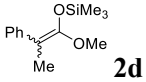 **2d**	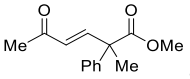 **3bd**	78%
4	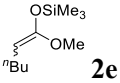 **2e**	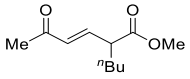 **3be**	46%[b, c]
5	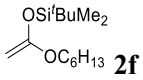 **2f**	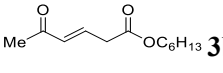 **3bf** 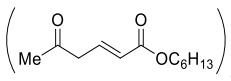 **3bf'**	97% (81;19)[b]
6	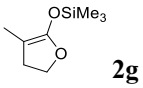 **2g**	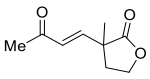 **3bg**	52%
7	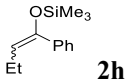 **2h**	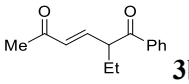 **3bh**	54%[d]

8	 **2i**	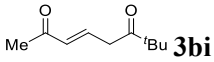 **3bi**	56%[b]

[a] **1b** (0.5 mmol), **2** (0.6 mmol), $InBr_3$ (0.025 mmol), CH_2Cl_2 (1 mL), 0 °C, 2 h. Isolated yields are shown. [b] The yield and the ratio of products determined by ^1H NMR analysis in crude products are shown. [c] Room temperature. [d] 6 h.

We monitored the reaction progress via ^1H NMR spectroscopy to gain insight into the mechanism (Scheme 4). In the reaction of alkenyl ether **1b** with ketene silyl acetal **2j**, the 1,4-addition of **2j** to **1b** readily proceeded at −60 °C to give silyl enol ether intermediate **8**. Then, an elimination of the MeO group took place at −20 °C with the formation of coupling product **9**.[18]

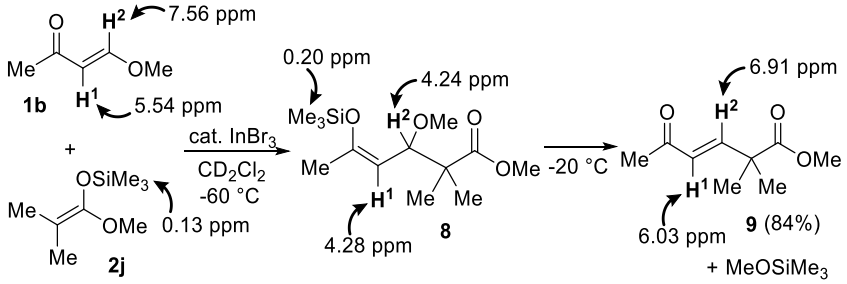

Scheme 4. Monitoring reaction progress and silyl enol intermediate by ^1H NMR spectroscopy.

Based on these results, a plausible reaction mechanism is illustrated in Scheme 5i. $InBr_3$ activates alkenyl ether **1** via coordination of the carbonyl group of **1** to the indium center. The 1,4-addition of silyl enolate **2** to **1** activated by $InBr_3$ gives indium enolate **12**. Then, silyl enol ether **13** is generated via the exchange of $InBr_3$ with Me_3Si group. Finally, $InBr_3$ mediates the elimination of the R^5O group (**14**) to give coupling product **15**. The explanation about the selective production of *E*-isomer **15** via the elimination of Me_3SiOR^5 from the *E*/*Z*-mixture of intermediate **13** is shown in Scheme 5ii.[19] The elimination of Me_3SiOR^5 from the *Z*-isomer of **13** proceeds via the six-membered ring transition state TS **A** to avoid the steric repulsion between the Br atom on the indium center and the substituent $CR^1R^2(COR^3)$, giving the *Z*-isomer of **15**. In the case of the *E*-isomer of **13**, the elimination occurs via acyclic transition state TS **B** to afford the *Z*-isomer of **15**.

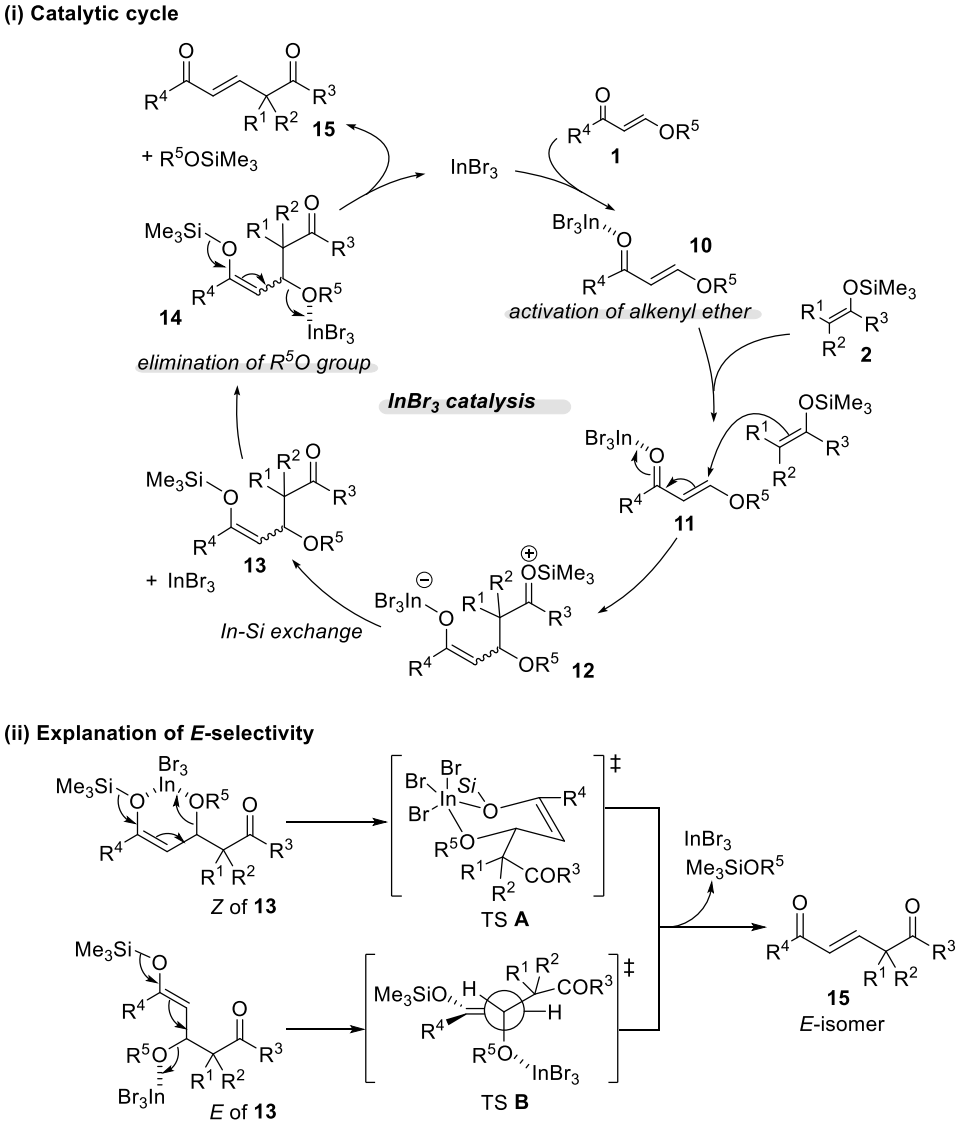

Scheme 5. Plausible mechanism of the $InBr_3$-catalyzed coupling of 2-carbonylalkenyl ethers with silyl enolates.

As catalysts, strong Lewis acids such as $TiCl_4$ (Scheme 2B) and $AlCl_3$ (Table 1, Entry 10) suffer from a detrimental interaction with either silyl enolate **2** or product **9** so that the catalytic reaction hardly proceeds (Scheme 6i). On the other hand, lithium enolates could cause a 1,4-addition to **1** (Scheme 2D), but the alkoxy (R^5O) group could not be released without the assistance of Lewis acids, and an anionic polymerization of **1** would occur (Scheme 6ii).[20] It is noteworthy that moderate Lewis acidic $InBr_3$ capably performs both the activation of alkenyl ethers (**10**) and the elimination[21] of the R^5O group (**14**) in the presence of various coordinative functional groups.

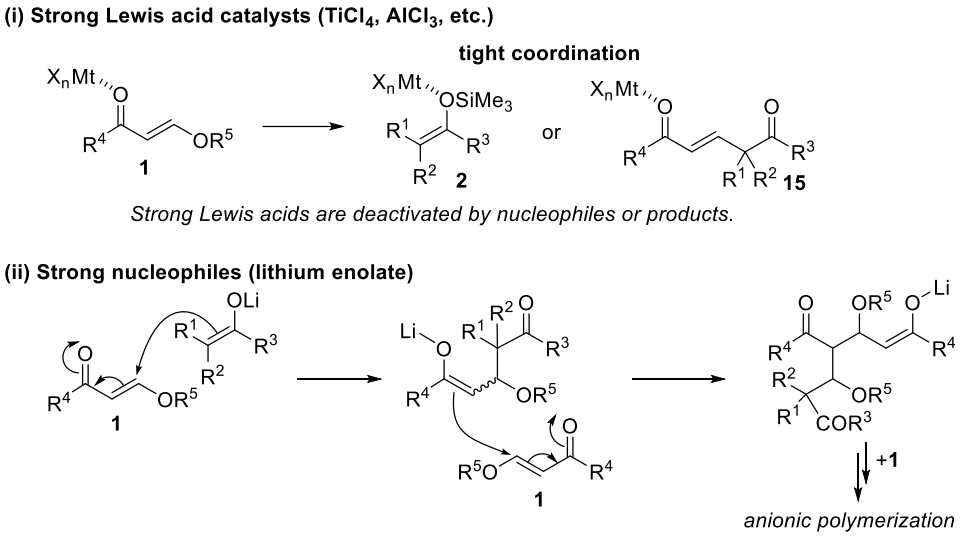

Scheme 6. Problems of other reaction systems

The reductive transformation of alk-2-ene-1,5-diones, which were endowed with alkene moieties that have perfect stereoselectivity via the present reaction, was demonstrated toward the construction of 1,5-hydroxyalk-2-ene structures that are important in molecules with biological relevance (Scheme 7).[22] The $InBr_3$-catalyzed coupling between alkenyl ether **1d** and ketene silyl acetal **2k** gave alk-2-ene-1,5-dione **3dk** with *E*-selectivity. Then, the reduction of **3dk** by $LiAlH_4$ afforded 1,5-hydroxyalk-2-ene **16** with the retention of the *E*-configuration. The structure of **16** is included in berkleasmins that are eremophilane sesquiterpenoids from a saprobic fungus, and these have exhibited cytotoxic activity against cancer cell lines as well as antimalarial activity.[23]

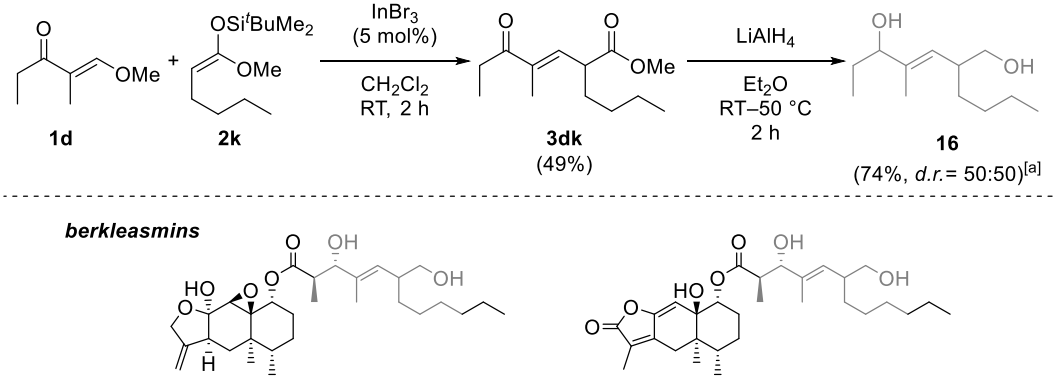

Scheme 7. Application to the construction of 1,5-hydroxyalk-2-ene structure included in berkleasmins. [a] The isolated yield is shown. The diastereoselectivity determined by ^{1}H NMR analysis in crude products is shown.

1-3. Conclusion

In conclusion, we established an $InBr_3$-catalyzed coupling reaction of 2-carbonylalkenyl ethers with silyl enolates to give the corresponding alk-2-ene-1,5-diones that feature alkene moieties with perfect stereoselectivity. The scope of the substrates is wide, and various functional groups are compatible with this reaction system. The observation of the silyl enolate intermediate by in situ ^1H NMR study revealed that the present reaction proceeded via 1,4-addition of silyl enolates to alkenyl ethers and elimination of silyl alkoxides. The reductive transformation of the synthesized alk-2-ene-1,5-diones enabled ready access to valuable compounds in organic synthesis such as 1,5-dihydroxyalk-2-enes.

1-4. Experimental Section

General

NMR spectra were recorded on a JEOL-AL400 and a JEOL-ECS400 spectrometers (400 MHz for ^1H, and 100 MHz for ^{13}C) and a Bruker AVANCE III spectrometer (600 MHz for ^1H, and 150 MHz for ^{13}C). Chemical shifts were reported in ppm on the δ scale relative to tetramethylsilane (δ = 0 for ^1H NMR) and residual $CHCl_3$ (δ = 77.0 for ^{13}C NMR) as an internal reference. Coupling constants were quoted in Hz (J). ^1H NMR Spectroscopy splitting patterns were designated as singlet (s), doublet (d), triplet (t), quartet (q). Splitting patterns that could not be interpreted or easily visualized were designated as multiplet (m) or broad (br). New compounds were characterized by ^1H, ^{13}C, ^{13}C off-resonance techniques, COSY, HMQC, and HMBC. Stereochemistry of alkene moieties in some compounds was determined by NOE or NOESY. Infrared (IR) spectra were recorded on a JASCO FT/IR-6200 Fourier transform infrared spectrophotometer. Column chromatographies were performed with silica gel. Purification by recycle HPLC was performed on SHIMADZU recycle HPLC system (SPD-20A, RID-10A, DGU-20A, LC-6AD, and FCV-20H2) and Japan Analytical Industry Co. (NEXT recycling preparative HPLC). Reactions were carried out in dry solvents under nitrogen atmosphere, unless otherwise stated. Reagents were purchased from Aldrich or Tokyo Chemical Industry Co., Ltd. (TCI), Wako Pure Chemical Industries, Ltd., and used after purification by distillation or used without purification for solid substrates.

Materials

Dehydrated solvents were purchased from Wako Pure Chemical Industries and used as obtained. Alkenyl ethers (**1a**, **1b**, **1d**, **1j**, **1k**) and silyl enol ether **2j** were purchased. The preparation and characterization of new compounds, alkenyl ethers **1l** and silyl kenete acetal **2f**and **2k** were described below. Other alkenyl ethers (**1c**,[24] **1e**,[25] **1f**,[26] **1g**,[27] **1h**,[27] **1i**[27]) and silyl enolates (**2a**,[28] **2b**,[29] **2c**,[30] **2d**,[29] **2e**,[29] **2g**,[31] **2h**,[32] **2i**[33]) were synthesized by the reported methods, and spectroscopic data matches that reported in the literature (references are shown below). All metal salt catalysts were purchased and used as obtained.

Alkenyl ethers

(1k) methyl (*E*)-2-(methoxymethylene)oct-3-ynoate

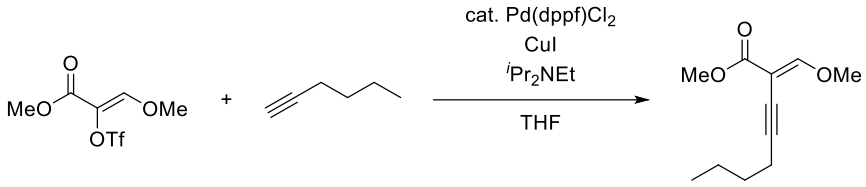

We modified the coupling reaction developed by Tanabe (H. Nakatsuji, R. Kamada, H. Kitaguchi, Y. Tanabe, *Adv. Synth. Catal.* **2017**, *359*, 3865.). 1-Hexyne (12 mmol, 0.992 g) and *i*Pr$_2$NEt (3 mL) were added to a stirred solution of trifluoromethanesulfonyloxy ester (3.06 mmol, 0.808 g), CuI (0.474 mmol, 0.0903 g), and Pd(dppf)Cl$_2$ (0.156 mmol, 0.104 g) in THF (2 mL) at 80 °C, and the mixture was stirred at same temperature for 14 h. Water was added to the mixture, which was extracted with AcOEt. The combined organic phase was washed with water, brine, dried over Na_2SO_4 and concentrated. The obtained crude product was purified by SiO_2-column chromatography (hexane–AcOEt) to give the desired product (0.347 g, 59%).

IR (neat) 1716 cm^{-1}; ^{1}H NMR (400 MHz, $CDCl_3$) 7.62 (s, 1H), 3.95 (s, 3H), 3.76 (s, 3H), 2.43 (t, J = 7.2 Hz, 2H), 1.61–1.41 (m, 4H), 0.92 (t, J = 7.2 Hz, 3H); ^{13}C NMR (100 MHz, $CDCl_3$) 166.7 (s), 165.8 (d), 97.5 (s), 95.7 (s), 70.9 (s), 62.4 (q), 51.9 (q), 30.7 (t), 21.9 (t), 19.4 (t), 13.6 (q); HRMS (CI, 70 eV) Calculated ($C_{11}H_{17}O_3$) 197.1178 Found: 197.1176.

(2f) ketene *tert*-butyldimethylsilyl hexyl acetal

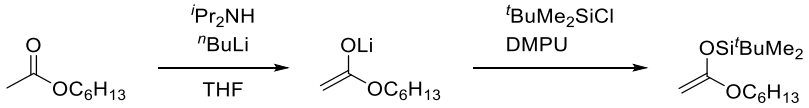

To diisopropylamine (7.13 g, 70.4 mmol) was added a solution of *n*BuLi (42 mL, 1.6 M in hexane) and THF (75 mL) at 0 ºC. The resulted solution was stirred for 10 min at room temperature to prepare the LDA solution. Then, a solution of hexyl acetate (8.57 g, 59.4 mmol) was slowly added to the LDA solution at −78 ºC. After the solution was stirred for 30 min at −78 ºC, DMPU (*N*,*N*'-dimethylpropyleneurea) (12 mL) was added to the reaction mixture, and then the solution of *t*BuMe$_2$SiCl (10.0 g, 66.3 mmol) was added, and the reaction mixture was stirred for 17 h at from −78 ºC to room temperature. The solvent was evaporated, and pentane (150 mL) was added to the residual mixture. The pentane solution was washed with H_2O, saturated $CuSO_4$ aq, saturated $NaHCO_3$ aq, followed by brine and was dried over $MgSO_4$. The solution was concentrated and the obtained crude oil was purified by distillation (b.p. 76–85 ºC, 1.2 mmHg) to give the desired product (15.0 g, 98%).

IR (neat) 1653 cm^{-1}; ^{1}H NMR (400 MHz, $CDCl_3$) 3.67 (t, J = 6.5 Hz, 2H), 3.21 (d, J = 2.6 Hz, 1H), 3.06 (d, J = 2.6 Hz, 1H), 1.66 (quintet, J = 6.5 Hz, 2H), 1.43–1.28 (m, 6H), 0.93 (s, 9H), 0.89 (t, J = 7.0 Hz, 3H), 0.17 (s, 6H); ^{13}C NMR (100 MHz, $CDCl_3$) 161.4 (s), 67.7 (t), 60.3 (t), 31.5 (t), 28.8 (t),

25.8 (t), 25.6 (q), 22.6 (t), 18.1 (s), 13.9 (q), −4.59 (q); HRMS (CI, 70 eV) Calculated ($C_{14}H_{31}O_2Si$) 259.2093 Found: 259.2098.

(2k) *n*-butylketene *tert*-butyldimethylsilyl methyl acetal

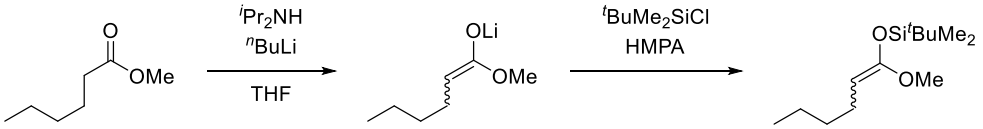

To the solution of diisopropylamine (2.7 mL, 19.5 mmol) in THF (18 mL) was added *n*-BuLi (1.6 M in hexane, 10 mL, 16 mmol) at 0 °C, and then the reaction mixture was stirred for 30 min at 0 °C. Methyl hexanoate (15 mmol, 2.00 g) was added at −78 °C, and the reaction mixture was stirred at −78 °C for 1 h. The solution of *t*BuMe$_2$SiCl (2.42 g, 16 mmol) and HMPA (hexamethylphosphoric triamide) (5.4 mL) in THF (6 mL) was added at −78 °C, and then the reaction mixture was stirred at room temperature for 1 h. The volatiles were evaporated and hexane (20 mL) was poured into the residual crude product. The organic layer was washed with cooled water (10 mL) five times, dried over $MgSO_4$, and concentrated. The crude product was purified by distillation to give the desired silyl ketene acetal (2.47 g, 10.1 mmol, 67%, *E*/*Z* mixture: 85:15).

IR (neat) 1683 cm^{-1}; ^{1}H NMR (400 MHz, $CDCl_3$) major isomer 3.64 (t, J = 7.5 Hz, 1H), 3.51 (s, 3H), 1.97–1.91 (m, 2H), 1.34–1.22 (m, 4H), 0.94–0.86 (m, 12H), 0.17 (s, 6H), minor isomer 3.45 (s, 3H), 3.42 (t, J = 7.3 Hz, 1H), 1.97–1.91 (m, 2H), 1.34–1.22 (m, 4H), 0.94–0.86 (m, 12H), 0.13 (s, 6H); ^{13}C NMR (100 MHz, $CDCl_3$) major isomer 153.7 (s), 85.3 (d), 54.8 (q), 32.9 (t), 25.62 (q), 24.2 (t), 22.23 (t), 18.1 (s), 13.9 (q), −5.1 (q), minor isomer 156.6, 75.7, 54.3, 33.2, 25.59, 24.3, 22.28, 18.0, 13.9, −4.4; HRMS (CI, 70 eV) major isomer Calculated ($C_{13}H_{29}O_2Si$) 245.1937 ([M + H]) Found: 245.1933.

<u>Products</u>

(3aa) 1-methyl 5-phenethyl (E)-4,4-dimethylpent-2-enedioate

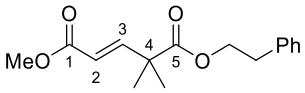

To a solution of $InBr_3$ (0.028 mmol, 0.0099 g) and dimethylketene phenethyl trimethylsilyl acetal (0.584 mmol, 0.155 g) in CH_2Cl_2 (1 mL) was added methyl (*E*)-3-methoxyacrylate (0.482 mmol, 0.0560 g) at 0 °C. The mixture was stirred for 4 h at room temperature and then quenched by water (3 mL) and CH_2Cl_2 (3 mL). The mixture was extracted with ethyl acetate (10 mL x 3). The collected organic layers were dried over $MgSO_4$. The solvent was evaporated and the residue was purified by silica gel column chromatography (hexane/ethyl acetate) to give the product as a colorless liquid (112 mg, 84%).

IR (neat) 1728, 1652 cm^{-1}; ^{1}H NMR (400 MHz, $CDCl_3$) 7.31–7.19 (m, 5H, Ph), 7.08 (d, J = 16.0 Hz, 1H, 3-H), 5.82 (d, J = 16.0 Hz, 1H, 2-H), 4.30 (t, J = 7.2 Hz, 2H, $COOCH_2$), 3.75 (s, 3H, OMe), 2.94

(t, J = 7.2 Hz, 2H, CH_2Ph), 1.31 (s, 6H, 4-Me_2); ^{13}C NMR (100 MHz, $CDCl_3$) 174.6 (s), 166.8 (s), 151.5 (d, C-3), 137.5 (s), 128.9 (d), 128.4 (d), 126.5 (d), 119.2 (d, C-2), 65.6 (t), 51.6 (q, OMe), 44.6 (s, C-4), 34.9 (t, *C*H_2Ph), 24.3 (q, 4-Me_2); HRMS (CI, 70 eV) Calculated ($C_{16}H_{21}O_4$) 277.1440 Found: 277.1435.

(3ba) Phenethyl (*E*)-2,2-dimethyl-5-oxohex-3-enoate

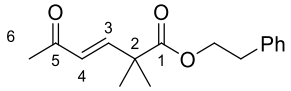

To a solution of $InBr_3$ (0.025 mmol, 0.0084 g) and dimethylketene phenethyl trimethylsilyl acetal (0.590 mmol, 0.156 g) in dichloromethane (1 mL) was added (*E*)-4-methoxybut-3-en-2-one (0.549 mmol, 0.0550 g) at 0 °C. The mixture was stirred for 2 h at 0 °C and then quenched by H_2O (3 mL) and CH_2Cl_2 (3 mL). The mixture was extracted with ethyl acetate (10 mL x 3). The collected organic layers were dried over $MgSO_4$. The solvent was evaporated and the residue was purified by silica gel column chromatography (hexane/ethyl acetate = 75:25, column length 11 cm) to give the product as a colorless liquid (70.6 mg, 50%).

IR (neat) 1734, 1719 cm^{-1}; ^{1}H NMR (400 MHz, $CDCl_3$) 7.31–7.19 (m, 5H, Ph), 6.88 (d, J = 16.4 Hz, 1H, 3-H), 6.04 (d, J = 16.4 Hz, 1H, 4-H), 4.33 (t, J = 7.2 Hz, 2H, CO_2CH_2), 2.95 (t, J = 7.2 Hz, 2H, CH_2Ph), 2.24 (s, 3H, 6-H_3), 1.32 (s, 6H, 2-Me_2); ^{13}C NMR (100 MHz, CDCl3) 198.6 (s, C-5), 174.7 (s, C-1), 150.3 (d, C-3), 137.5 (s), 128.9 (d), 128.7 (d, C-4), 128.4 (d), 126.6 (d), 65.6 (t, CO_2CH_2), 44.6 (s), 34.9 (t, *C*H_2Ph), 27.1 (q, C-6), 24.4 (q, 2-Me_2); HRMS (CI, 70 eV) Calculated ($C_{16}H_{21}O_3$) 261.1491 Found: 261.1495.

(3ca) phenethyl (*E*)-2,2-dimethyl-5-oxo-5-phenylpent-3-enoate

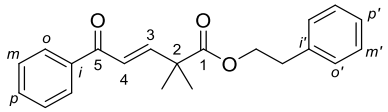

To a solution of $InBr_3$ (0.020 mmol, 0.0072 g) and trimethyl{(2-methyl-1-phenethoxyprop-1-en-1-yl)oxy}silane (0.584 mmol, 0.155 g) in dichloromethane (1 mL) was added (*E*)-3-methoxy-1-phenylprop-2-en-1-one (0.526 mmol, 0.0848 g) at 0 °C. The mixture was stirred for 2 h at 0 °C and then quenched by water (3 mL) and CH_2Cl_2 (3 mL). The mixture was extracted with ethyl acetate (10 mL x 3). The collected organic layers were dried over $MgSO_4$. The solvent was evaporated and the residue was purified by silica gel column chromatography (hexane/ethyl acetate) to give the product as a colorless liquid (150 mg, 88%).

IR (neat) 1731, 1673 cm^{-1}; ^{1}H NMR (400 MHz, $CDCl_3$) 7.90 (d, J = 7.2 Hz, 2H, *o*), 7.55 (t, J = 7.2 Hz, 1H, *p*), 7.45 (t, J = 7.2 Hz, 2H, *m*), 7.30–7.14 (m, 5H, CH_2CH_2*Ph*), 7.13 (d, J = 15.7 Hz, 1H, 3-H), 6.83 (d, J = 15.7 Hz, 1H, 4-H), 4.32 (t, J = 7.0 Hz, 2H, CH_2CH_2Ph), 2.93 (t, J = 7.0 Hz, 2H,

CH_2CH_2Ph), 1.38 (s, 6H, 2-Me_2); ^{13}C NMR (100 MHz, $CDCl_3$) 190.6 (C, C-5), 174.6 (C, C-1), 151.4 (CH, C-3), 137.6 (CH), 137.4 (CH), 132.7 (CH, *o*), 128.8 (CH), 128.5 (CH), 128.4 (CH), 128.3 (CH), 126.5 (CH), 123.5 (CH, C-4), 65.5 (CH_2, CH_2CH_2Ph), 44.9 (C, C-2), 34.9 (CH_2, CH_2CH_2Ph), 24.4 (CH_3, 2-Me_2); HRMS (CI, 70 eV) Calculated ($C_{21}H_{23}O_3$) 323.1647 ($[M + H]^+$) Found: 323.1653.

(3da) phenethyl (*E*)-2,2,4-trimethyl-5-oxohept-3-enoate

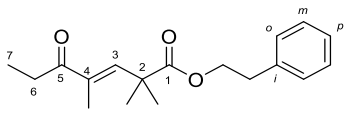

To a solution of $InBr_3$ (0.026 mmol, 0.0091 g) and trimethyl{(2-methyl-1-phenethoxyprop-1-en-1-yl)oxy}silane (0.506 mmol, 0.1339 g) in dichloromethane (1 mL) was added (*E*)-1-methoxy-2-methylpent-1-en-3-one (0.505 mmol, 0.0647g) at 0 °C. The mixture was stirred for 2 h at room temperature and then quenched by water (3 mL) and CH_2Cl_2 (3 mL). The mixture was extracted with ethyl acetate (10 mL x 3). The collected organic layers were dried over $MgSO_4$. The solvent was evaporated and the residue was purified by silica gel column chromatography (hexane/ethyl acetate) to give the product as a colorless liquid (107.8 mg, 74%).

IR (neat) 1727, 1680 cm^{-1}; ^1H NMR (400 MHz, $CDCl_3$) 7.29-7.17 (m, 5H, Ph), 6.54 (s, 1H, 3-H), 4.31 (t, *J* = 6.8 Hz, 2H, OCH_2CH_2Ph), 2.92 (t, *J* = 6.8 Hz, 2H, OCH_2CH_2Ph), 2.65 (q, *J* = 7.2 Hz, 2H, 6-H_2), 1.57 (s, 3H, 4-Me), 1.36 (s, 6H, 2-Me_2), 1.09 (t, *J* = 7.2 Hz, 3H, 7-H_3); ^{13}C NMR (100 MHz, $CDCl_3$) 202.5 (s, C-5), 176.2 (s, C-1), 144.7 (d, C-3), 137.7 (s, C-4), 137.7 (s, *i*), 128.8 (d), 128.4 (d), 126.6 (d), 65.6 (t, OCH_2CH_2Ph), 43.3 (s, C-2), 34.9 (t, OCH_2CH_2Ph), 30.5 (t, C-6), 26.4 (q, 2-Me_2), 12.0 (q, 4-Me), 8.6 (q, C-7); HRMS (EI, 70 eV) Calculated ($C_{18}H_{24}O_3$) 288.1725 Found: 288.1724.

The stereochemistry of the alkene moiety was determined by NOE.

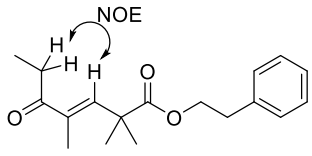

(3ea) phenethyl (*E*)-2,2,3-trimethyl-5-oxohex-3-enoate

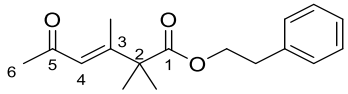

To a solution of $In(OTf)_3$ (0.0154 mmol, 0.0087 g) and trimethyl{(2-methyl-1-phenethoxy-prop-1-en-1-yl)oxy}silane (0.723 mmol, 0.191 g) in CH_2Cl_2 (1 mL) was added (*E*)-4-methoxypent-3-en-2-one (0.499 mmol, 0.0570 g) at 0 °C. The mixture was stirred for 2 h at 0 °C and then quenched by CH_2Cl_2 (3 mL) and water (3 mL). The mixture was extracted with CH_2Cl_2 (10 mL x 4). The collected organic layer was dried over $MgSO_4$. The solvent was evaporated and the NMR yield and the ratio in the crude

product were determined by ^{1}H NMR using 1,1,2,2-tetrachloroethane as an internal standard (NMR yield 34%). The residue was purified by column chromatography (hexane/ethyl acetate = 85:15) and then the product was given (colorless oil, 35.1 mg, 26%).

IR (neat) 1731 cm^{-1}, 1691 cm^{-1}, 1614 cm^{-1}; ^{1}H NMR (400 MHz, $CDCl_3$) 7.28–7.16 (m, 5H, Ph), 6.13 (s, 1H, 4-H), 4.28 (t, J = 6.8 Hz, 2H, OCH_2CH$_2$Ph), 2.90 (t, J = 6.8 Hz, 2H, OCH$_2$CH_2Ph) 2.19 (s, 3H, 6-H$_3$), 1.97 (s, 3H, 3-Me), 1.30 (s, 6H, 2-Me$_2$); ^{13}C NMR (100 MHz, $CDCl_3$) 198.6 (s, C-5), 175.0 (s, C-1), 158.0 (s, C-3), 137.3 (s, *i*), 128.6 (d), 128.2 (d), 126.3 (d, *p*), 121.7 (d, C-4), 65.2 (t, OCH_2CH$_2$Ph), 49.8 (s, C-2), 34.6 (t, OCH$_2$CH_2Ph), 31.9 (q, C-6), 23.9 (q, 2-Me$_2$), 16.8 (q, 3-Me); HRMS (EI, 70 eV) Calculated ($C_{17}H_{22}O_3$) 274.1569 Found: 274.1565.

The stereochemistry of the alkene moiety was determined by NOE.

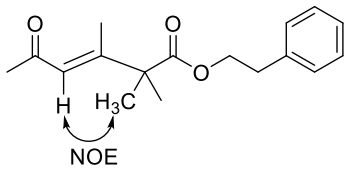

(3fa) phenethyl (*E*)-2,2,3-trimethyl-5-oxo-5-phenylpent-3-enoate

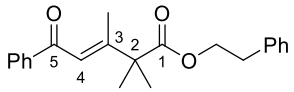

To a solution of $InBr_3$ (0.022 mmol, 0.0079 g) and trimethyl{(2-methyl-1-phenethoxyprop-1-en-1-yl)oxy}silane (0.580 mmol, 0.153 g) in dichloromethane (1 mL) was added (*E*)-3-methoxy-1-phenylbut-2-en-1-one (0.514 mmol, 0.0906 g) at 0 °C. The mixture was stirred for 2 h at 0 °C and then quenched by water (3 mL) and CH_2Cl_2 (3 mL). The mixture was extracted with ethyl acetate (10 mL x 3). The collected organic layers were dried over $MgSO_4$. The solvent was evaporated and the residue was purified by silica gel column chromatography (hexane/ethyl acetate = 77:23) to give the product as a colorless liquid (149.4 mg, 86%).

IR (neat) 1730, 1664 cm^{-1}; ^{1}H NMR (400 MHz, $CDCl_3$) 7.91 (d, J = 6.8 Hz, 2H), 7.53 (t, J = 6.8 Hz, 1H), 7.44 (t, J = 6.8 Hz, 2H), 7.24-7.16 (m, 5H), 6.75 (s, 1H, 4-H), 4.32 (t, J = 6.8 Hz, 2H), 2.92 (t, J = 6.8 Hz, 2H), 2.00 (s, 3H, 3-Me), 1.40 (s, 6H, 2-Me$_2$); ^{13}C NMR (100 MHz, $CDCl_3$) 192.2 (s, C-5), 175.2 (s, C-1), 158.3 (s), 138.9 (s), 137.4 (s), 132.4 (d), 128.7 (d), 128.4 (d), 128.3 (d), 128.1 (d), 126.4 (d), 119.8 (d, C-4), 65.4 (t), 50.1 (s), 34.8 (t), 24.2 (q, 2-Me$_2$), 17.1 (q, 3-Me); HRMS (CI, 70 eV) Calculated ($C_{22}H_{24}O_3$) 336.1725 (M^+) Found: 336.1727.

The stereochemistry of the alkene moiety was determined by NOE.

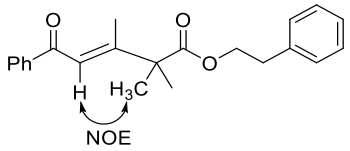

(3gj) dimethyl (*E*)-4,4-dimethyl-2-phenylpent-2-enedioate

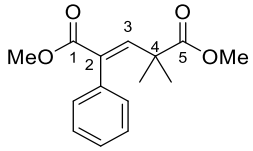

To a solution of $InBr_3$ (0.0561 mmol, 0.0199 g) and dimethylketene methyl trimethylsilylacetal (0.649 mmol, 0.113 g) in CH_2Cl_2 (1 mL) was added methyl (*E*)-3-methoxy-2-phenylacrylate (0.527 mmol, 0.101 g) at 0 °C. The mixture was stirred for 4 h at room temperature and then quenched by CH_2Cl_2 (3 mL) and water (3 mL). The mixture was extracted with CH_2Cl_2 (10 mL x 4). The collected organic layer was dried over $MgSO_4$. The solvent was evaporated and the residue was purified by column chromatography (hexane/ethyl acetate) and then the product was given (colorless oil, 79.6 mg, 58%).

IR (neat) 1734, 1717 cm^{-1}; ^1H NMR (400 MHz, $CDCl_3$) 7.35–7.30 (m, 3H), 7.11–7.09 (m, 2H), 7.07 (s, 1H, 3-H), 3.71 (s, 3H, 1-OMe), 3.29 (s, 3H, 5-OMe), 1.28 (s, 6H, 4-Me_2); ^{13}C NMR (100 MHz, $CDCl_3$) 175.3 (s, C-5), 167.9 (s, C-1), 147.3 (d, C-3), 134.4 (s), 133.1 (s), 129.8 (d), 127.7 (d), 127.6 (d), 52.3 (q, 1-OMe), 51.7 (q, 5-OMe), 43.9 (s, C-4), 26.9 (q, 4-Me); HRMS (CI, 70 eV) Calculated ($C_{15}H_{19}O_4$) 263.1283 Found: 263.1284.

The stereochemistry of the alkene moiety was determined by NOESY.

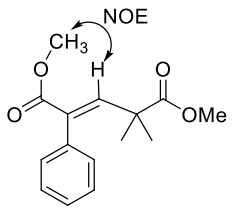

(3ha) 1-methyl 5-phenethyl (Z)-2-chloro-4,4-dimethylpent-2-enedioate

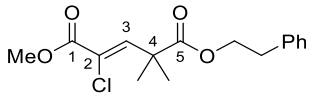

To a solution of $InBr_3$ (0.047 mmol, 0.0165 g) and trimethyl{(2-methyl-1-phenethoxyprop-1-en-1-yl)oxy}silane (0.760 mmol, 0.201 g) in dichloromethane (1 mL) was added methyl (Z)-2-chloro-3-methoxyacrylate (0.491 mmol, 0.0666 g) at 0 °C. The mixture was stirred for 4 h at room temperature

and then quenched by water (3 mL) and CH_2Cl_2 (3 mL). The mixture was extracted with ethyl acetate (10 mL x 3). The collected organic layers were dried over $MgSO_4$. The solvent was evaporated and the residue was purified by silica gel column chromatography (hexane/ethyl acetate) to give the product as a colorless liquid (107.7 mg, 71%).

IR (neat) 1734, 1698 cm^{-1}; ^1H NMR (400 MHz, $CDCl_3$) 7.29–7.18 (m, 5H, Ph), 7.11 (s, 1H, 3-H), 4.32 (t, J = 7.2 Hz, 2H), 3.83 (s, 3H, OMe), 2.94 (t, J = 7.2 Hz, 2H), 1.40 (s, 3H, 4-Me_2); ^{13}C NMR (100 MHz, $CDCl_3$) 174.6 (s, C-5), 162.8 (s, C-1), 145.2 (d, C-3), 137.6 (s), 128.8 (d), 128.3 (d), 126.4 (d), 124.6 (s), 65.7 (t), 53.2 (q, OMe), 43.8 (s), 34.8 (t), 24.9 (q, 4-Me_2); HRMS (EI, 70 eV) Calculated ($C_{16}H_{19}ClO_4$) 310.0972 (M^+) Found 310.0969.

The stereochemistry of the alkene moiety was determined by NOESY.

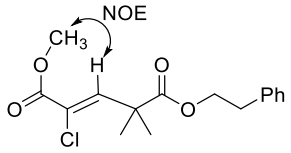

(3ia) 1-methyl 5-phenethyl (Z)-2-bromo-4,4-dimethylpent-2-enedioate

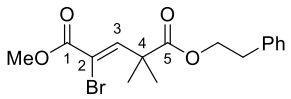

To a solution of $InBr_3$ (0.028 mmol, 0.0099 g) and dimethylketene phenethyl trimethylsilyl acetal (0.746 mmol, 0.197 g) in dichloromethane (1 mL) was added methyl (*Z*)-2-bromo-3-methoxyacrylate (0.491 mmol, 0.0958 g) at 0 °C. The mixture was stirred for 4 h at room temperature and then quenched by water (3 mL) and CH_2Cl_2 (3 mL). The mixture was extracted with ethyl acetate (10 mL x 3). The collected organic layers were dried over $MgSO_4$. The solvent was evaporated and the residue was purified by silica gel column chromatography (hexane/ethyl acetate) to give the product as a colorless liquid (121 mg, 69%).

IR (neat) 1734, 1718 cm^{-1}; ^1H NMR (400 MHz, $CDCl_3$) 7.42 (s, 1H, 3-H), 7.30–7.19 (m, 5H, Ph), 4.33 (t, J = 8.0 Hz, 2H, CO_2CH_2), 3.84 (s, 3H, OMe), 2.95 (t, J = 8.0 Hz, 2H, CH_2Ph), 1.42 (s, 3H, 4-Me_2); ^{13}C NMR (100 MHz, $CDCl_3$) 174.6 (s), 162.9 (s), 149.0 (d, C-3), 137.7 (s), 128.9 (d), 128.4 (d), 126.5 (d), 115.7 (s), 65.8 (t, COO*C*H_2), 53.5 (q, OMe), 45.0 (s), 34.9 (t, *C*H_2Ph), 25.1 (q, 4-Me_2); HRMS (CI, 70 eV) Calculated ($C_{16}H_{20}BrO_4$) 355.0545 ($[M + H]^+$) Found: 355.0540.

The stereochemistry of the alkene moiety was determined by NOESY.

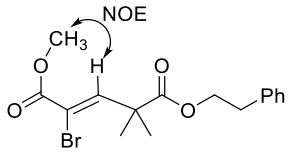

(3ja) 1,1-dimethyl 3-phenethyl 3-methylbut-1-ene-1,1,3-tricarboxylate

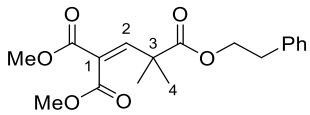

To a solution of $GaBr_3$ (0.028 mmol, 0.088 g) and dimethylketene phenethyl trimethylsilylacetal (0.770 mmol, 0.204 g) in CH_2Cl_2 (1 mL) was added dimethyl 2-(methoxymethylene)malonate (0.483 mmol, 0.0841 g) at 0 °C. The mixture was stirred for 2 h at room temperature and then quenched by CH_2Cl_2 (3 mL) and water (3 mL). The mixture was extracted with CH_2Cl_2 (10 mL x 4). The collected organic layers were dried over $MgSO_4$. The solvent was evaporated and the residue was purified by column chromatography (hexane/ethyl acetate) and then the product was given (colorless oil, 0.133 mg, 83%).

IR (neat) 1733 cm^{-1}; ^1H NMR (400 MHz, $CDCl_3$) 7.30-7.19 (m, 5H, Ph), 7.04 (s, 1H, 2-H), 4.28 (t, J = 7.3 Hz, 2H, $COOCH_2$), 3.80 (s, 3H, OMe), 3.74 (s, 3H, OMe), 2.93 (t, J = 7.3 Hz, 2H, CH_2Ph), 1.36 (s, 6H, 4-H_3 and 3-Me); ^{13}C NMR (100 MHz, $CDCl_3$) 174.2 (s), 16.5 (s), 164.4 (s), 151.0 (d, C-2), 137.6 (s), 128.9 (d), 128.4 (d), 126.8 (s), 126.5 (d), 65.5 (t, $COOCH_2$), 52.6 (q), 52.1 (q), 44.3 (s), 34.8 (t, CH_2Ph), 25.5 (q, C-4 and 3-Me); HRMS (CI, 70 eV) Calculated ($C_{18}H_{23}O_6$) 335.1495 ($[M + H]^+$) Found: 335.1490.

(3kj) dimethyl (*E*)-2-(hex-1-yn-1-yl)-4,4-dimethylpent-2-enedioate

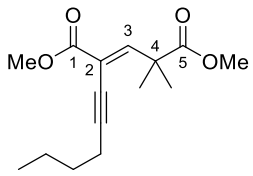

To a solution of $InBr_3$ (0.0505 mmol, 0.0179 g) and dimethylketene methyl trimethylsilylacetal (0.759 mmol, 0.132 g) in CH_2Cl_2 (1 mL) was added methyl methyl (*E*)-2-(methoxymethylene)oct-3-ynoate (0.504 mmol, 0.0989 g) at 0 °C. The mixture was stirred for 4 h at room temperature and then quenched by CH_2Cl_2 (3 mL) and water (3 mL). The mixture was extracted with ethyl acetate (10 mL x 4). The collected organic layers were dried over $MgSO_4$. The solvent was evaporated and the residue was purified by column chromatography (hexane/ethyl acetate) and then the product was given (colorless oil, 100 mg, 75%).

IR (neat) 1734, 1719 cm^{-1}; ^1H NMR (400 MHz, $CDCl_3$) 7.17 (s, 1H, 3-H), 3.79 (s, 3H, 1-OMe), 3.69 (s, 5-OMe), 2.38 (t, J = 7.2 Hz, 2H), 1.63–1.38 (m, 4H), 1.44 (s, 6H, 4-Me_2), 0.93 (t, J = 7.2 Hz, 3H); ^{13}C NMR (100 MHz, $CDCl_3$) 175.6 (s, C-5), 165.5 (s, C-1), 153.9 (d, C-3), 117.2 (s), 100.6 (s), 73.3 (s, C-2), 52.5 (q, 1-OMe), 52.1 (q, 5-OMe), 44.1 (s, C-4), 30.2 (t), 25.2 (q, 4-Me_2), 21.9 (t), 19.3 (t), 13.5 (q); HRMS (CI, 70 eV) Calculated ($C_{15}H_{23}O_4$) 267.1596 Found: 267.1593.

The stereochemistry of the alkene moiety was determined by NOESY.

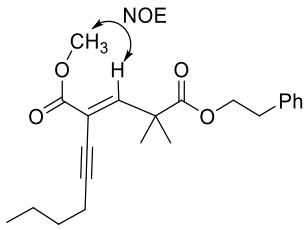

(3la) 1-ethyl 5-phenethyl (*E*)-4,4-dimethylpent-2-enedioate

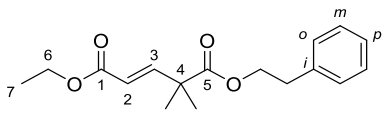

To a solution of $InBr_3$ (0.026 mmol, 0.0093 g) and trimethyl{(2-methyl-1-phenethoxyprop-1-en-1-yl)oxy}silane (0.588 mmol, 0.156 g) in dichloromethane (1 mL) was added *E*/*Z* mixture of ethyl 3-ethoxyacrylate (0.482 mmol, 0.0695 g, *E*/*Z* = 1.8:1) at 0 °C. The mixture was stirred for 4 h at room temperature and then quenched by water (3 mL) and CH_2Cl_2 (3 mL). The mixture was extracted with ethyl acetate (10 mL x 3). The collected organic layers were dried over $MgSO_4$. The solvent was evaporated and the residue was purified by silica gel column chromatography (hexane/ethyl acetate) to give the product as a colorless liquid (93.6 mg, 67%).

IR (neat) 1732, 1719 cm^{-1}; ^1H NMR (400 MHz, $CDCl_3$) 7.30–7.19 (m, 5H, Ph), 7.07 (d, J = 15.9 Hz, 1H, 3-H), 5.82 (d, J = 15.9 Hz, 1H, 2-H), 4.30 (t, J = 6.8 Hz, 2H, C$H_2$$CH_2$Ph), 4.20 (q, J = 7.2 Hz, 2H, 6-H_2), 2.93 (t, J = 6.8 Hz, 2H, CH_2CH_2Ph), 1.30 (s, 6H, 4-Me_2), 1.30 (t, J = 7.2 Hz, 3H, 7-H_3); ^{13}C NMR (100 MHz, $CDCl_3$) 174.6 (s, C-1), 166.3 (s, C-5), 151.2 (d, C-3), 137.5 (s, *i*), 128.9 (d), 128.3 (d), 126.5 (d), 119.6 (d, C-2), 65.5 (t, C$H_2$$CH_2$Ph), 60.3 (t, C-6), 44.5 (s, C-2), 34.9 (t, CH_2CH_2Ph), 24.3 (q, 2-Me_2), 14.1 (q, C-7); HRMS (CI, 70 eV) Calculated ($C_{17}H_{23}O_4$) 291.1596 ([M + H]) Found: 291.1594.

(3bb) ethyl (*E*)-2,2-diethyl-5-oxohex-3-enoate

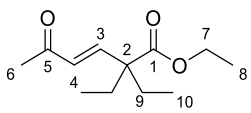

To a solution of $InBr_3$ (0.025 mmol, 0.0084 g) and diethylketene ethyl trimethylsilyl acetal (0.582

mmol, 0.129 g) in dichloromethane (1 mL) was added (*E*)-4-methoxybut-3-en-2-one (0.506 mmol, 0.0507 g) at 0 °C. The mixture was stirred for 2 h at 0 °C and then quenched by H_2O (3 mL) and CH_2Cl_2 (3 mL). The mixture was extracted with ethyl acetate (10 mL x 3). The collected organic layers were dried over $MgSO_4$. The solvent was evaporated and the residue was purified by silica gel column chromatography (hexane/ethyl acetate) to give the product as a colorless liquid (86.7 mg, 81%).

IR (neat) 1727, 1680 cm^{-1}; ^1H NMR : (400 MHz, $CDCl_3$) 7.03 (d, J = 16.9 Hz, 1H, 3-H), 6.10 (d, J = 16.9 Hz, 1H, 4-H), 4.20 (q, J = 7.2 Hz, 2H, 7-H_2), 2.31 (s, 3H, 6-H_3), 1.89–1.69 (m, 4H, 9-H_2 x 2), 1.28 (t, J = 7.2 Hz, 3H, 8-H_3), 0.81 (t, J = 7.5 Hz, 6H, 10-H_3 x 2); ^{13}C NMR (100 MHz, $CDCl_3$) 198.7 (C, C-5), 174.1 (C, C-1), 148.8 (CH, C-3), 130.5 (CH, C-4), 61.0 (CH_2, C-7), 53.2 (C, C-2), 29.5 (CH_2, C-9), 26.9 (CH_3, C-6), 14.2 (CH_3, C-8), 8.9 (CH_3, C-10); HRMS (EI, 70 eV) Calculated ($C_{12}H_{20}O_3$) 212.1412 ($[M]^+$) Found: 212.1416.

(3bc) methyl (*E*)-1-(3-oxobut-1-en-1-yl)cyclohexane-1-carboxylate

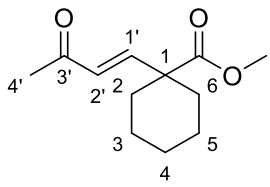

To a solution of $InBr_3$ (0.023 mmol, 0.0081 g) and 1-methoxy-1-*tert*-butyldimethylsilyloxymethylenecyclohexane (0.584 mmol, 0.150 g) in dichloromethane (1 mL) was added (*E*)-4-methoxybut-3-en-2-one (0.562 mmol, 0.0563 g) at 0 °C. The mixture was stirred for 2 h at 0 °C and then quenched by saturated $NaHCO_3$ aq (3 mL) and CH_2Cl_2 (3 mL). The mixture was extracted with ethyl acetate (10 mL x 3). The collected organic layers were dried over $MgSO_4$. The solvent was evaporated and the residue was purified by silica gel column chromatography (hexane/ethyl acetate) to give the product as a colorless liquid (83.0 mg, 70%).

IR (neat) 1732, 1679 cm^{-1}; ^1H NMR (400 MHz, $CDCl_3$) 6.70 (d, J = 16.2 Hz 1H, 1'-H), 6.09 (d, J = 16.2 Hz, 1H, 2'-H), 3.72 (s, 3H, OCH_3) 2.27 (s, 3H, 4'-H_3), 2.17–2.12 (m, 2H), 1.63–1.25 (m, 8H); ^{13}C NMR (100 MHz, $CDCl_3$) 198.4 (C, C-3'), 174.1 (C, *C*$OOCH_3$), 149.9 (CH, C-1'), 129.9 (CH, C-2'), 52.3 (CH_3, OCH_3), 49.5 (C, C-1), 33.4 (CH_2), 27.4 (CH_3, C-4'), 25.3 (CH_2), 22.9 (CH_2); HRMS (CI, 70 eV) Calculated ($C_{12}H_{19}O_3$) 211.1334 ([M + H]) Found: 211.1329.

(3bd) methyl (*E*)-2-methyl-5-oxo-2-phenylhex-3-enoate

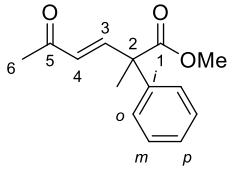

To a solution of $InBr_3$ (0.025 mmol, 0.0090 g) and trimethyl{(1-methoxy-2-phenylprop-1-en-1-yl)oxy}silane (0.609 mmol, 0.144 g) in dichloromethane (1 mL) was added (*E*)-4-methoxybut-3-en-2-one (0.495 mmol, 0.0496 g) at 0 °C. The mixture was stirred for 2 h at 0 °C and then quenched by water (3 mL). The mixture was extracted with ethyl acetate (10 mL x 3). The collected organic layers were dried over $MgSO_4$. The solvent was evaporated and the residue was purified by silica gel column chromatography (hexane/ethyl acetate) to give the product as a colorless liquid (89.7 mg, 78%).

IR (neat) 1735, 1680 cm^{-1}; ^1H NMR (400 MHz, $CDCl_3$) 7.37–7.20 (m, 6H, 2-Ph and 3-H), 6.05 (d, *J* = 16.4 Hz, 1H, 4-H), 3.75 (s, 3H, OCH_3), 2.32 (s, 3H, 6-H_3), 1.72 (s, 3H, 2-Me); ^{13}C NMR (100 MHz, $CDCl_3$) 198.5 (C, C-5), 174.0 (C, C-1), 149.3 (CH, C-3), 141.5 (C, *i*), 130.3 (CH, C-4), 128.8 (CH), 127.5 (CH), 126.3 (CH), 53.3 (C, C-2), 52.8 (CH_3, OCH_3), 27.3 (CH_3, 6-C), 23.2 (CH_3, 2-Me); HRMS (EI, 70 eV) Calculated ($C_{14}H_{16}O_3$) 232.1099 Found: 232.1097.

(3be) methyl (*E*)-2-butyl-5-oxohex-3-enoate, (methyl (*E*)-2-butyl-5-oxohex-2-enoate)

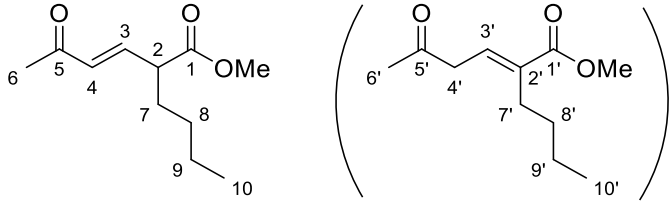

To a solution of $InBr_3$ (0.024 mmol, 0.0084 g) and trimethyl{(1-methoxyhex-1-en-1-yl)oxy}silane (0.590 mmol, 0.118 g) in dichloromethane (1 mL) was added (*E*)-4-methoxybut-3-en-2-one (0.480 mmol, 0.0481 g) at room temperature. The mixture was stirred for 2 h at room temperature and then quenched by water (3 mL) and CH_2Cl_2 (3 mL). The mixture was extracted with ethyl acetate (10 mL x 3). The collected organic layers were dried over $MgSO_4$. The solvent was evaporated and the NMR yield and the ratio in the crude product were determined by ^1H NMR using 1,1,2,2-tetrachloroethane as an internal standard (total yield 46%, target product/regio isomer = >99:1). The crude product was purified by silica gel column chromatography (hexane/ethyl acetate) to give the product (target product/ regio isomer = 88:12) as a colorless liquid (41.5 mg, 44%). The regio isomer was afforded via isomerization of the target product through the silica gel column.

IR (neat) 1738, 1680 cm^{-1}; ^1H NMR (400 MHz, $CDCl_3$) target product 6.75 (dd, *J* = 16.3, 8.6 Hz, 1H, 3-H), 6.11 (d, *J* = 16.3 Hz, 1H, 4-H), 3.72 (s, 3H, OCH_3), 3.17 (q, *J* = 8.6 Hz, 1H, 2-H), 2.28 (s, 3H, 6-H_3), 1.89–1.80 (m, 1H, 7-H^A), 1.67–1.58 (m, 1H, 7-H^B), 1.40–1.21 (m, 4H), 0.93–0.88 (t, *J* = 7.3

Hz, 3H, 10-H_3), regio isomer 6.92 (t, *J* = 7.6 Hz, 1H), 3.75 (s, 3H, OCH_3), 3.34 (d, *J* = 7.6 Hz, 2H, 4'-H), 2.22 (s, 3H, 6'-H_3), 1.67–1.58 (m, 2H), 1.40–1.21 (m, 4H), 0.93–0.88 (t, *J* = 7.3 Hz, 3H, 10'-H_3); ^{13}C NMR (100 MHz, $CDCl_3$) target product 198.2 (s, C-5), 173.1 (s, C-1), 144.2 (d, C-3), 132.6 (d, C-4), 52.2 (q, 1-OCH_3), 48.8 (d, C-2), 31.8 (t, C-7), 29.2 (t), 27.0 (q, C-6), 22.3 (t), 13.8 (q, C-10), regio isomer 204.7, 167.7, 135.4, 132.6, 51.8, 43.0, 31.2, 30.0, 26.9, 22.6, 13.9; HRMS (EI, 70 eV) terget product Calculated ($C_{11}H_{18}O_3$) 198.1256 Found: 198.1258, regio isomer Calculated ($C_{11}H_{18}O_3$) 198.1256 Found: 198.1259.

(3bf) hexyl (*E*)-5-oxohex-3-enoate

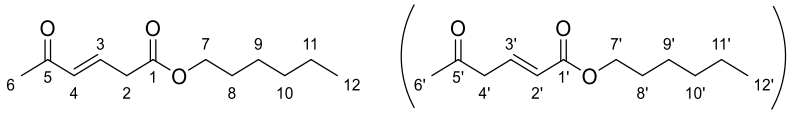

To a solution of $InBr_3$ (0.025 mmol, 0.0089 g) and *tert*-butyl[{1-(hexyloxy)vinyl}oxy]dimethylsilane (0.614 mmol, 0.1588 g) in dichloromethane (1 mL) was added (*E*)-4-methoxybut-3-en-2-one (0.519 mmol, 0.0520 g) at 0 °C. The mixture was stirred for 2 h at 0 °C and then quenched by water (3 mL) and CH_2Cl_2 (3 mL). The mixture was extracted with ethyl acetate (10 mL x 3). The collected organic layers were dried over $MgSO_4$. The solvent was evaporated and the NMR yield and the ratio in the crude product were determined by ^1H NMR using 1,1,2,2-tetrachloroethane as an internal standard (total yield 97%, target product/regio isomer = 81:19). The crude product was purified by silica gel column chromatography (hexane/ethyl acetate) to give the product with the isomer (target product/isomer = 79:21) as a colorless liquid (62.1 mg, 56%).

IR (neat) 1737, 1703, 1680, 1634 cm^{-1}; ^1H NMR (400 MHz, $CDCl_3$) target product 6.90–6.82 (dt, *J* = 16.2, 7.0 Hz, 1H, 3-H), 6.14 (dt, *J* = 16.2, 2.4 Hz, 1H, 4-H), 4.15–4.10 (t, *J* = 6.8 Hz, 2H, 7-H_2), 3.26 (dd, *J* = 7.0, 2.4 Hz, 2H, 2-H_2), 2.28 (s, 3H, 6-H_3), 1.67–1.60 (m, 2H, 8-H_2), 1.36–1.25 (m, 6H, 9-H_2, 10-H_2, 11-H_2), 0.893 (t, *J* = 6.7 Hz, 3H, 12-H_3), regio isomer 7.06–6.98 (dt, *J* = 15.7, 7.3 Hz,1H, 3'-H), 5.90 (dt, *J* = 15.7, 2.4 Hz, 1H, 2'-H), 4.15–4.10 (t, *J* = 6.8 Hz, 2H, 7'-H_2), 3.34 (dd, *J* = 7.3, 2.4 Hz, 2H, 4'-H_2), 2.21 (s, 2H, 6'-H_3), 1.67–1.60 (m, 2H, 8'-H_2), 1.36–1.25 (m, 6H, 9'-H_2, 10'-H_2, 11'-H_2), 0.888 (t, *J* = 6.9 Hz, 3H, 12'-H_3); ^{13}C NMR (100 MHz, $CDCl_3$) target product 197.9 (C, C-5), 169.9 (C, C-1), 138.8 (CH, C-3), 133.8 (CH, C-4), 65.3 (CH_2, C-7), 37.5 (CH_2, C-2), 31.27 (CH_2), 28.4 (CH_2, C-8), 26.7 (CH_3, C-6), 25.4 (CH_2), 22.40 (CH_2), 13.86 (CH_3, C-12), regio isomer 204.2 (C), 165.8 (C), 139.6 (CH), 124.9 (CH), 64.6 (CH_2), 46.3 (CH_2), 31.32 (CH_2), 29.8 (CH_3), 28.5 (CH_2), 25.5 (CH_2), 22.42 (CH_2), 13.88 (CH_3); HRMS (CI, 70 eV) target product Calculated ($C_{12}H_{21}O_3$) 213.1491 ([M + H]) Found: 213.1492, regio isomer Calculated ($C_{12}H_{21}O_3$) 213.1491 ([M + H]) Found: 213.1493.

(3bg) (*E*)-3-methyl-3-(3-oxobut-1-en-1-yl)dihydrofuran-2(3*H*)-one

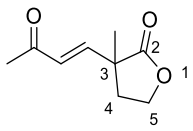

To a solution of $InBr_3$ (0.0256 mmol, 0.0091 g) and trimethyl((3-methyl-4,5-dihydrofuran-2-yl)oxy)silane (0.609 mmol, 0.105 g) in dichloromethane (1 mL) was added (*E*)-4-methoxybut-3-en-2-one (0.559 mmol, 0.056 g) at 0 °C. The mixture was stirred for 2 h at room temperature and then quenched by water (3 mL) and CH_2Cl_2 (3 mL). The mixture was extracted with ethyl acetate (10 mL x 3). The collected organic layers were dried over $MgSO_4$. The solvent was evaporated and the residue was purified by silica gel column chromatography (hexane/ethyl acetate) to give the product as a colorless liquid (48.5 mg, 52%).

IR (neat) 1775, 1680 cm^{-1}; ^1H NMR (400 MHz, $CDCl_3$) 6.77 (d, J = 16.8 Hz, 1H), 6.14 (d, J = 16.8 Hz, 1H), 4.34–4.22 (m, 2H), 2.43–2.36 (m, 1H), 2.25 (s, 3H), 2.25–2.18 (m, 1H), 1.40 (s, 3H); ^{13}C NMR (100 MHz, $CDCl_3$) 197.6 (s), 177.9 (s), 145.3 (d), 130.2 (d), 64.9 (t), 45.0 (s), 35.0 (t), 27.6 (q), 22.5 (q); HRMS (CI, 70 eV) Calculated ($C_9H_{13}O_3$) 169.0865 Found: 169.0863.

(3bh) (*E*)-2-ethyl-1-phenylhex-3-ene-1,5-dione

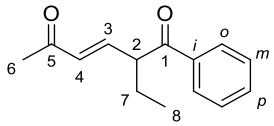

To a solution of $InBr_3$ (0.025 mmol, 0.0084 g) and trimethyl{(1-phenylbut-1-en-1-yl)oxy}silane (0.589 mmol, 0.130 g) in dichloromethane (1 mL) was added (*E*)-4-methoxybut-3-en-2-one (0.534 mmol, 0.0535 g) at 0 °C. The mixture was stirred for 6 h at 0 °C and then quenched by saturated $NaHCO_3$ aq (3 mL) and CH_2Cl_2 (3 mL). The mixture was extracted with ethyl acetate (10 mL x 3). The collected organic layers were dried over $MgSO_4$. The solvent was evaporated and the crude product was purified by silica gel column chromatography (hexane/ethyl acetate) to give the product with the isomerization as a colorless liquid (62.6 mg, 54%).

IR: (neat) 1680, 1621 cm^{-1}; ^1H NMR (400 MHz, $CDCl_3$) 7.95 (d, J = 7.6 Hz, 2H, *o*), 7.60 (t, J = 7.6 Hz, 1H, *m*), 7.49 (t, J = 7.6 Hz, 2H, *p*), 6.89 (dd, J = 16.2, 8.5 Hz, 1H, 3-H), 6.16 (d, J = 16.2 Hz, 1H, 4-H), 4.13 (q, J = 8.5 Hz, 1H, 2-H), 2.26 (s, 3H, 6-H_3), 2.06–1.96 (m, 1H, 7-H), 2.06–1.96 (m, 1H, 7-H^A), 1.79–1.69 (m, 1H, 7-H^B), 0.95 (t, J = 7.4 Hz, 3H, 8-H_3); ^{13}C NMR (100 MHz, $CDCl_3$) 199.4 (C), 198.2 (C), 145.3 (CH), 136.2 (C), 133.5 (CH), 133.0 (CH), 128.7 (CH), 128.3 (CH), 51.7 (CH, C-2), 26.7 (CH_3, C-6), 25.7 (CH_2), 11.7 (CH_3, C-8); HRMS (EI, 70 eV) Calculated ($C_{14}H_{16}O_2$) 216.1150 Found: 216.1153.

(3bi) (*E*)-7,7-dimethyloct-3-ene-2,6-dione

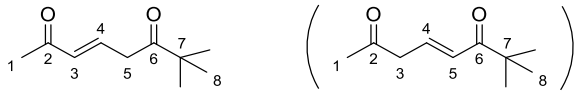

To a solution of $InBr_3$ (0.050 mmol, 0.0177 g) and {(3,3-dimethylbut-1-en-2-yl)oxy}trimethylsilane (0.600 mmol, 0.103 g) in dichloromethane (1 mL) was added (*E*)-4-methoxybut-3-en-2-one (0.531 mmol, 0.0504 g) at 0 °C. The mixture was stirred for 2 h at 0 °C and then quenched by water (3 mL) and CH_2Cl_2 (3 mL). The mixture was extracted with ethyl acetate (10 mL x 3). The collected organic layers were dried over $MgSO_4$. The solvent was evaporated and the NMR yield of the target product was determined by ^1H NMR using 1,1,2,2-tetrachloroethane as an internal standard (56% yield), and the regio isomer was not observed in the crude product. The crude product was purified by silica gel column chromatography (hexane/ethyl acetate) to give the mixture of the target product and the regio isomer as a light-yellow liquid (32.4 mg, total yield 36%, target product/regio isomer = 65:35). The regio isomer was afforded via isomerization of the target product through the silica gel column.

IR (neat) 1707, 1675, 1626 cm^{-1}; ^1H NMR (400 MHz, $CDCl_3$) target product 6.93 (dt, J = 15.9, 7.0 Hz, 1H, 4-H), 6.09 (d, J = 15.9 Hz, 1H, 3-H), 3.47 (d, J = 7.0 Hz, 2H, 5-H_2), 2.29 (s, 3H, 1-H_3), 1.18 (s, 9H, 8-H_3 and 7-Me_2), regio isomer 7.02–6.92 (m, 1H, 4-H), 6.59 (d, J = 15.9 Hz, 1H, 3-H), 3.35 (d, J = 7.0 Hz, 2H, 5-H_2), 2.21 (s, 3H, 1-H_3), 1.16 (s, 9H, 8-H_3 and 7-Me_2); ^{13}C NMR (100 MHz, $CDCl_3$) target product 211.8 (s, C-6), 198.2 (s, C-2), 140.8 (d, C-4), 133.9 (d, C-3), 44.5 (s, C-7), 39.6 (t, C-5), 26.4 (q, C-1), 26.1 (q, C-8), regio isomer 204.5 (s), 203.4 (s), 137.7 (d), 127.5 (d), 46.8 (t), 42.9 (s), 29.8 (q), 25.9 (q); HRMS (CI, 70 eV) target product Calculated ($C_{10}H_{17}O_2$) 169.1229 ([M + H]) Found: 169.1231, regio isomer Calculated ($C_{10}H_{17}O_2$) 169.1229 ([M + H]) Found: 169.1233.

(3dj) methyl (*E*)-2-butyl-4-methyl-5-oxohept-3-enoate

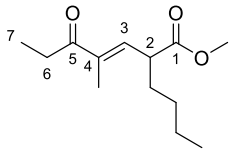

To a solution of $InBr_3$ (0.101 mmol, 0.0359 g) and *tert*-butyl((1-methoxyhex-1-en-1-yl)oxy)dimethylsilane (0.760 mmol, 0.713 g) in dichloromethane (4 mL) was added (*E*)-1-methoxy-2-methylpent-1-en-3-one (1.92 mmol, 0.2456 g) at 0 °C. The mixture was stirred for 2 h at room temperature and then quenched by water (3 mL) and CH_2Cl_2 (3 mL). The mixture was extracted with ethyl acetate (10 mL x 3). The collected organic layers were dried over $MgSO_4$. The solvent was evaporated and the residue was purified by silica gel column chromatography (hexane/ethyl acetate = 80:20, column length 11 cm) to give the product as a colorless liquid (211 mg, 49%).

IR (neat) 1739, 1677 cm^{-1}; ^1H NMR (400 MHz, $CDCl_3$) 6.45 (d, J = 9.7 Hz, 1H, 3-H), 3.57 (s, 3H, OMe), 3.34–3.28 (m, 1H, 2-H), 2.59 (q, J = 7.2 Hz, 2H, 6-H_2), 1.76–1.65 (m, 4H, 1-H^A and 4-Me),

1.52–1.43 (m, 1H, 1-H^B), 1.24–1.08 (m, 4H 2-H_2 and 3-H_2), 0.96 (t, J = 7.2 Hz, 3H), 0.76 (t, J = 7.2 Hz, 3H); ^{13}C NMR (100 MHz, $CDCl_3$) 201.8 (s, C-5), 173.3 (s, C-1), 138.1 (s), 137.9 (d, C-3), 51.7 (q, OMe), 45.2 (d, C-2), 32.1 (t), 30.3 (t), 28.9 (t), 22.2 (t), 13.5 (q), 11.5 (q), 8.3 (q); HRMS (EI, 70 eV) Calculated ($C_{13}H_{22}O_3$) 226.1569 (M^+) Found 226.1567.

The stereochemistry of the alkene moiety was determined by NOE.

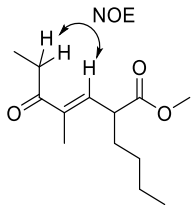

(16) (*E*)-2-butyl-4-methylhept-3-ene-1,5-diol

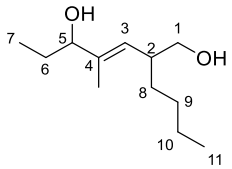

To a solution of $LiAlH_4$ (1.12 mmol, 0.0425 g) in Et_2O (3.2 mL) was added the Et_2O solution of methyl (*E*)-2-butyl-4-methyl-5-oxohept-3-enoate (0.25 M, 1.2 mL) at 0 °C. The mixture was stirred for 1 h at room temperature and stirred for 1 h at 50 ℃ and then quenched by water (3 mL) and 10% NaOH aq (6 mL) at 0 ℃. The mixture was extracted with Et_2O (10 mL x 3). The collected organic layers were dried over Na_2SO_4. The solvent was evaporated and the NMR yield and the ratio in the crude product was determined by ^{1}H NMR using 1,1,2,2-tetrachloroethane as an internal standard (>99% yield, diastereomer ratio = 50:50). The crude product was purified by column chromatography (hexane/ethyl acetate = 40:60 for one diastereomer (**A)**, hexane/ethyl acetate = 20:80 for the other diastereomer (**B)**, column length 11 cm) and then the product was given (diastereomer **A**: colorless oil, 28.8 mg, 48%, diastereomer **B**: colorless oil, 15.9 mg, 26%).

IR (neat) diastereomer **A** 3361 cm^{-1}; diastereomer **B** 3597 cm^{-1};

^{1}H NMR (400 MHz, $CDCl_3$) diastereomer **A** 5.13 (d, J = 9.7 Hz, 1H, 3-H), 3.94 (t, J = 6.5 Hz, 1H, 5-H), 3.54 (dd, J = 10.4, 5.6 Hz, 1H, 1-H^A), 3.35 (dd, J = 10.1, 8.2 Hz, 1H, 1-H^B), 2.57-2.49 (m, 1H, 2-H), 1.64 (s, 3H, 4-Me), 1.60-1.52 (m, 2H, 6-H_2), 1.44-1.38 (m, 1H, 8-H^A), 1.30-1.22 (m, 4H, 9-H_2, 10-H_2), 1.22-1.12 (m, 1H, 8-H^B), 0.87 (t, J = 7.0 Hz, 3H), 0.86 (t, J = 7.5 Hz, 3H), diastereomer **B** 5.07 (d, J = 9.9 Hz, 1H, 3-H), 3.92 (t, J = 7.1 Hz, 1H, 5-H), 3.58 (dd, J = 10.4, 5.0 Hz, 1H, 1-H^A), 3.33 (dd, J = 10.4, 8.9 Hz, 1H, 1-H^B), 2.55–2.49 (m, 1H, 2-H), 1.62 (s, 3H, 4-Me), 1.61–1.50 (m, 2H, 6-H_2), 1.38–1.08 (m, 6H, 8-H_2, 9-H_2, 10-H_2), 1.31–1.15 (m, 4H, 9-H_2, 10-H_2), 0.86 (t, J = 7.1 Hz, 3H, 11-H_3), 0.83 (t, J = 7.4 Hz, 3H, 7-H_3); ^{13}C NMR (100 MHz, $CDCl_3$) diastereomer **A** 140.2 (C, C-4),

127.4 (CH, C-3), 78.5 (CH, C-5), 66.6 (CH_2, C-1), 40.7 (CH, C-2), 31.3 (CH_2, C-8), 29.4 (CH_2), 27.8 (CH_2, C-6), 22.8 (CH_2), 14.0 (CH_3, C-11), 12.8 (CH_3, 4-Me), 9.9 (CH_3, C-7), diastereomer **B** 139.8 (C, C-4), 129.5 (CH, C-3), 80.0 (CH, C-5), 66.7 (CH_2, C-1), 40.6 (CH, C-2), 31.2 (CH_2, C-8), 29.3 (CH_2, C-9), 27.3 (CH_2, C-6), 22.7 (CH_2, C-10), 14.0 (CH_3, C-11), 11.1 (CH_3, 4-Me), 10.0 (CH_3, C-7); HRMS (EI, 70 eV) diastereomer **A** Calculated ($C_{12}H_{24}O_2$) 200.1776 Found: 200.1778, diastereomer **B** Calculated ($C_{12}H_{24}O_2$) 200.1776 Found: 200.1773.

The stereochemistry of the alkene moiety in both diastereomers was determined by NOE.

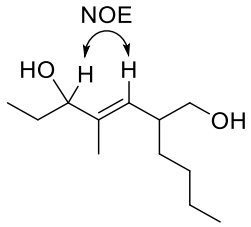

General procedures

Coupling reaction of 1a with 2a (Table 1)

To a solution of $InBr_3$ (0.025 mmol) and silyl enolate **2a** (0.6 mmol) in dichloromethane (1 mL) was added **1a** (0.5 mmol) at room temperature. The mixture was stirred for 2 h at room temperature and then the reaction was quenched by saturated $NaHCO_3$ aq (3 mL). The mixture was extracted with ethyl acetate (10 mL x 3). The collected organic layers were dried over $MgSO_4$. The volatiles were evaporated and the NMR yield of the desired product **3aa** was determined by ^1H NMR using 1,1,2,2-tetrachloroethane as an internal standard. The purification was performed by silica gel column chromatography to give the pure product **3aa**. The isolated yield of **3aa** was calculated with the weight of the pure product.

Comparison among $InBr_3$-catalyzed reaction and typical methods (Scheme 2)

$TiCl_4$-catalyzed Mukaiyama type reaction (Scheme 2B)

To a solution of alkenyl ether **1a** (0.5 mmol) and silyl enolate **2a** (0.65 mmol) in CH_2Cl_2 (1 mL) was added a solution of $TiCl_4$ in CH_2Cl_2 (1 M, 0.075 mL) at −78 °C. Then, the reaction mixture was stirred at −78 °C for 1 h. Water was poured into the reaction mixture. The mixture was extracted with ethyl acetate (10 mL x 3). The collected organic layers were dried over $MgSO_4$. The volatiles were evaporated and the NMR yield of the desired product and the recovery of **1a** was determined by ^1H NMR using 1,1,2,2-tetrachloroethane as an internal standard.

We referred to the reported papers[34] to carry out this experiment.

Fluoride anion-catalyzed reaction (Scheme 2C)

To a solution of silyl enolate **2a** (0.5 mmol) in THF (1 mL), tetrabutylammonium fluoride (1 M in THF, 0.05 mL, 10 mol%) was added dropwise under argonatmosphere, followed by addition of alkenyl

ether **1a** (0.5 mmol). The resulting solution was stirred for 4 h at 60 °C. The mixture was cooled to room temperature, filtration under diminished pressure. Water was poured into the reaction mixture. The mixture was extracted with ethyl acetate (10 mL x 3). The collected organic layers were dried over $MgSO_4$. The volatiles were evaporated and the NMR yield of the desired product and the recovery of **1a** was determined by ^{1}H NMR using 1,1,2,2-tetrachloroethane as an internal standard.

We referred to the reported paper[35] to carry out this experiment.

Addition reaction of lithium enolate (Scheme 2D)

To *n*-BuLi (1.6 M solution in hexane, 3.75 mL, 6 mmol) in THF (5 mL) was added diisopropylamine (6 mmol) at 0 °C. The reaction mixture was stirred for 15 min at 0 °C. Then to reaction mixture was added methyl isobutyrate (5 mmol) dropwise at −78 °C to generate the corresponding lithium enolate **4**. After stirred for 30 min at the same temperature, alkenyl ether **1a** (5 mmol) was added dropwise. The reaction mixture was stirred for overnight at −78 °C. Then, water was poured into the reaction mixture. The mixture was extracted with ethyl acetate (10 mL x 3). The collected organic layers were dried over $MgSO_4$. The volatiles were evaporated and the NMR yield of the desired product and the recovery of **1a** was determined by ^{1}H NMR using 1,1,2,2-tetrachloroethane as an internal standard.

We referred to the reported papers[36] to carry out this experiment.

Reformatsky type reaction (Scheme 2E)

Methyl 2-bromo-2-methylpropanoate **6** (0.77 mmol) was added to the solution of alkenyl ether **1a** (0.5 mmol) and zinc powder (2.4 mmol) in Et_2O (0.15 mL) and benzene (0.6 mL) at room temperature. The reaction mixture was stirred at 50 °C for 3 h. Then, the mixture was cooled to room temperature and 5% HCl aq (5 mL) was added. The mixture was extracted with Et_2O (10 mL x 3). The collected organic layers were dried over $MgSO_4$. The volatiles were evaporated and the NMR yield of the desired product and the recovery of **1a** was determined by ^{1}H NMR using 1,1,2,2-tetrachloroethane as an internal standard.

We referred to the reported paper[37] to carry out this experiment.

Compound 7

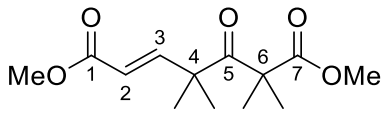

IR (neat) 1749, 1734, 1717 cm^{-1}; ^{1}H NMR (400 MHz, $CDCl_3$) 7.10 (d, J = 15.4 Hz, 1H, 3-H), 6.23 (d, J = 15.4 Hz, 1H, 2-H), 3.71 (s, 3H), 3.70 (s, 3H), 1.39 (s, 6H), 1.35 (s, 6H); ^{13}C NMR (100 MHz, $CDCl_3$) 196.3 (s, C-5), 175.2 (s), 174.2 (s), 150.8 (d, C-3), 122.3 (d, C-2), 54.6 (s), 52.40 (q), 52.35 (q), 44.8 (s), 24.5 (q), 21.8 (q); HRMS (CI, 70 eV) Calculated ($C_{13}H_{21}O_5$) 257.1389 Found: 257.1391.

NMR studies on the coupling reactions (Scheme 4A)

NMR study of the reaction between alkenyl ether 1b and silyl enolate 2j

The preparation of the reaction mixture was performed in a glove box filled with nitrogen. The solution of silyl enolate **2j** (1.0 mmol) and alkenyl ether **1b** (1.2 mmol) in CD_2Cl_2 (2 mL) was prepared (Solution **A**). The suspension of $InBr_3$ (0.03 mmol) in CD_2Cl_2 (0.4 mL) was prepared (Solution **B**). Solution **A** (0.6 mL) was added into a sealable NMR tube, and then the Solution **A** in the tube was cooled to −92 °C with a dry ice/methanol bath. Solution **B** (0.4 mL) was added into the tube containing Solution **A** (0.6 mL) at −92 °C. The reaction progress was observed by NMR spectroscopy at from −60 °C to 20 °C (NMR spectra are shown in Scheme 9) Compound **9** was produced in 84% yield.

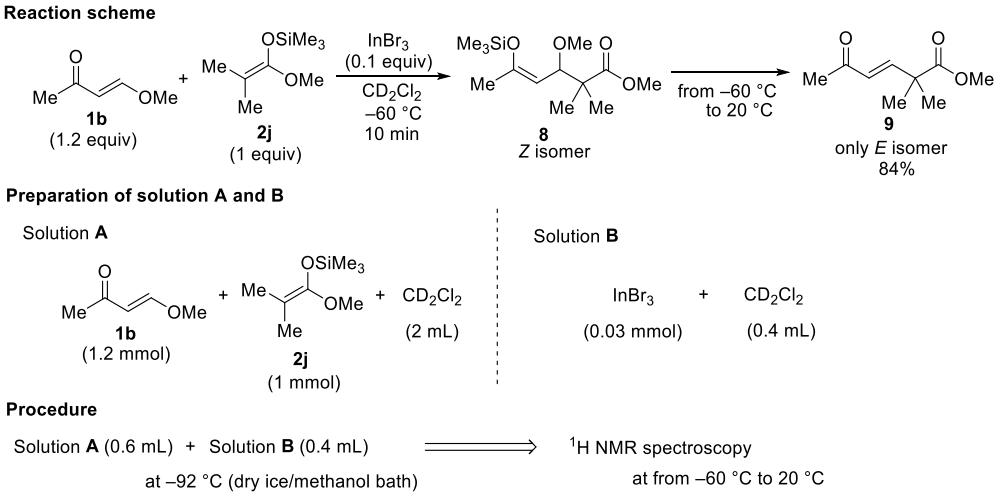

Scheme 8. The coupling reaction for the NMR studies.

VT NMR study

At −60 °C, $InBr_3$-catalyzed 1,4-addition of **2j** to **1b** occurred to produce intermediate **8**. The elimination of Me_3SiOMe from **8** started at −20 °C, and then the reaction completed at room temperature.

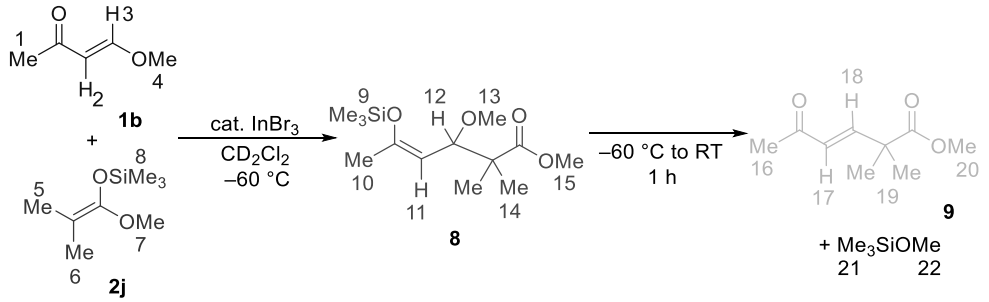

^1H NMR (400 MHz, CD_2Cl_2)

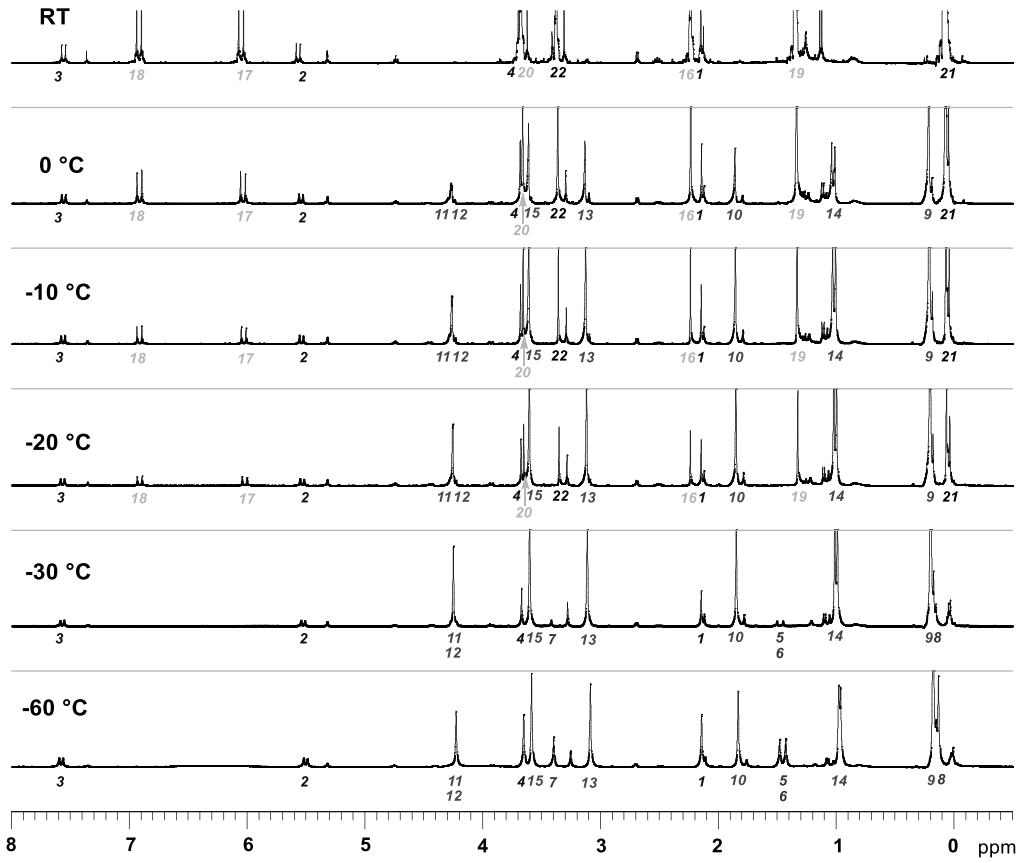

Scheme 9. Observation of the reaction progress by VT-NMR.

Assignment of intermediate 8

Assignment of ^{1}H NMR spectrum of intermediate **8** was carried out by using reference compound **A**. Chemical shifts of characteristic protons (9, 11, 12, 13) in intermediate **8** are reasonably consistent with the corresponding chemical shifts (9', 11', 12', 13') of reference compound **A**.[38]

intermediate 8

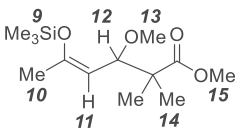

11: 4.28 ppm, d, *J* = 9.4 Hz, 1H
12: 4.24 ppm, d, *J* = 9.4 Hz, 1H
15: 3.61 ppm, s, 3H
13: 3.12 ppm, s, 3H
10: 1.85 ppm, s, 3H
14: 1.03 and 1.00 ppm, s, 6H
9: 0.20 ppm, s, 9H

reference compound A

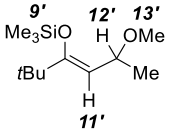

11': 4.50 ppm, d, *J* = 9.0 Hz
12': 4.07 ppm, dq, *J* = 9.4 and 6.5 Hz
13': 3.22 ppm, s
9': 0.24 ppm, s

^{1}H NMR chart at −10 °C

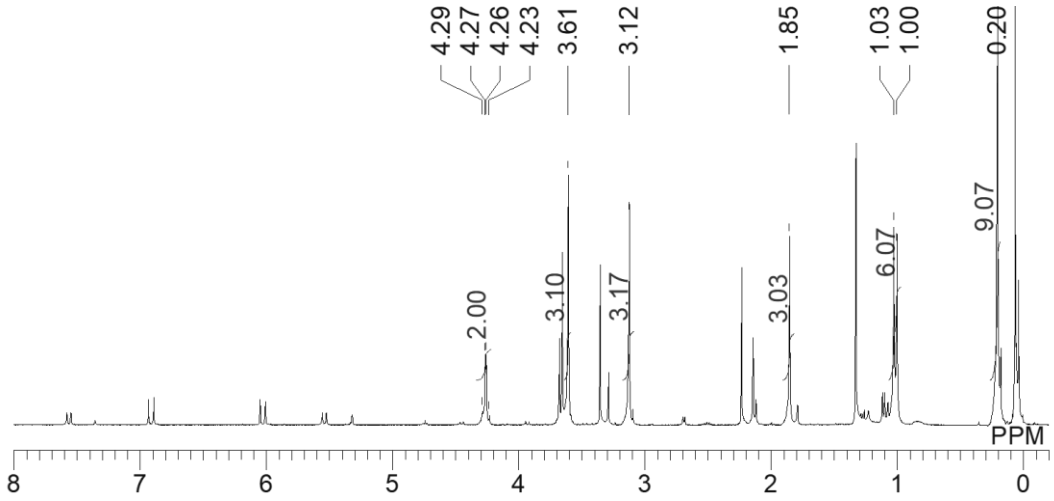

Plausible mechanism to explain stereoselectivity of coupling product

The reaction of alkenyl ether 1b with silyl enolate 2a (Scheme 4, Mechanism A)

It is possible that the reaction of **1** with **2** gives the *E*/*Z*-mixture of silyl enolate intermediate **13** although only *E*-isomer of the intermediate in the reaction of **1b** with **2j** was observed in ^{1}H NMR experiment (Scheme 4A). The proposed mechanism is shown below to explain the selective generation of the *E*-isomer of coupling product via the elimination of Me_3SiOR^5 from the *E*/*Z*-mixture of silyl enolate intermediate **13**.

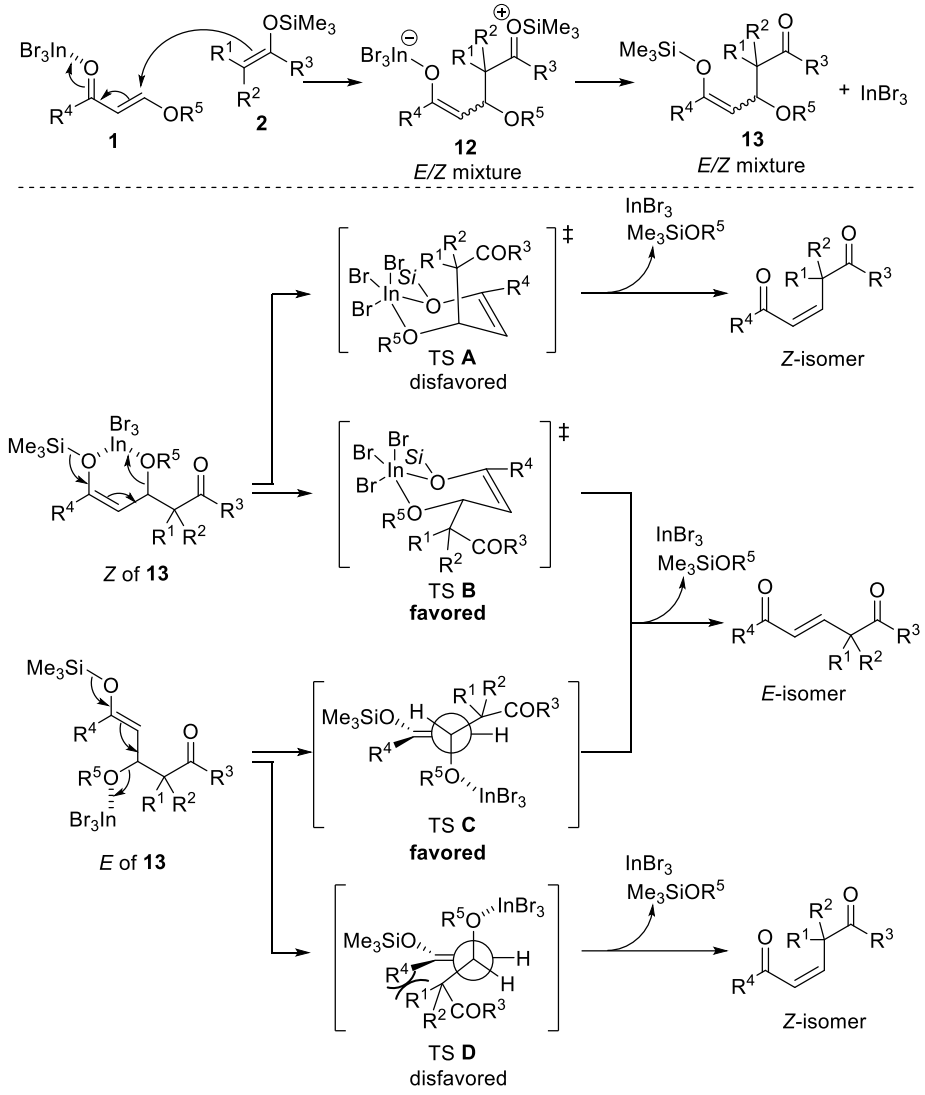

Scheme 10. Plausible mechanism for the stereoselective elimination step.

The $InBr_3$-catalyzed elimination of Me_3SiOMe from the *Z*-isomer of intermediate **13** proceeds via the six-membered ring transition state like TS **A** and TS **B**. The paths via TS **A** and TS **B** give the *Z*-isomer and the *E*-isomer of the coupling product, respectively. TS **A** is less stable than TS **B** because of the steric repulsion between the Br atom on the indium center and the substituents (R^1, R^2, and COR^3)

derived from **2** at the *pseude* axial position. Therefore, the *Z*-isomer of **10** selectively gives the *E*-isomer product via TS **B**. In the case of the *E*-isomer of **13**, the elimination occurs via acyclic transition state like TS **C** and TS **D**. In these transition states, the C–OR^5 bond, which has been cleaving, is perpendicular to the plane containing the Si–O–C=C structure. The path via TS **C** and TS **D** gives the *E*-isomer and the *Z*-isomer of the coupling product, respectively. TS **D** is less stable than TS **C** because of 1,3-allylic strain between R^4 group and the substituents (R^1, R^2, and COR^3) derived from **2**. Thus, the *E*-isomer of **10** selectively gives the *E*-isomer product via TS **C**.

The reaction of *E*/*Z* mixture of alkenyl ether 1o with silyl enolate 2a (Scheme 3, product 3la)

E/*Z* mixture of alkenyl ether **1l** gave only *E*-isomer of the coupling product **3la**. Also, *E*/*Z* mixture of the silyl enolate intermediate would be generated in this reaction. Thus, the elimination of Me_3SiOEt from the silyl enolate intermediate selectively gives *E*-isomer of the coupling product **3la** via the reaction path similar to the reaction of **1b** with **2a** as shown above.

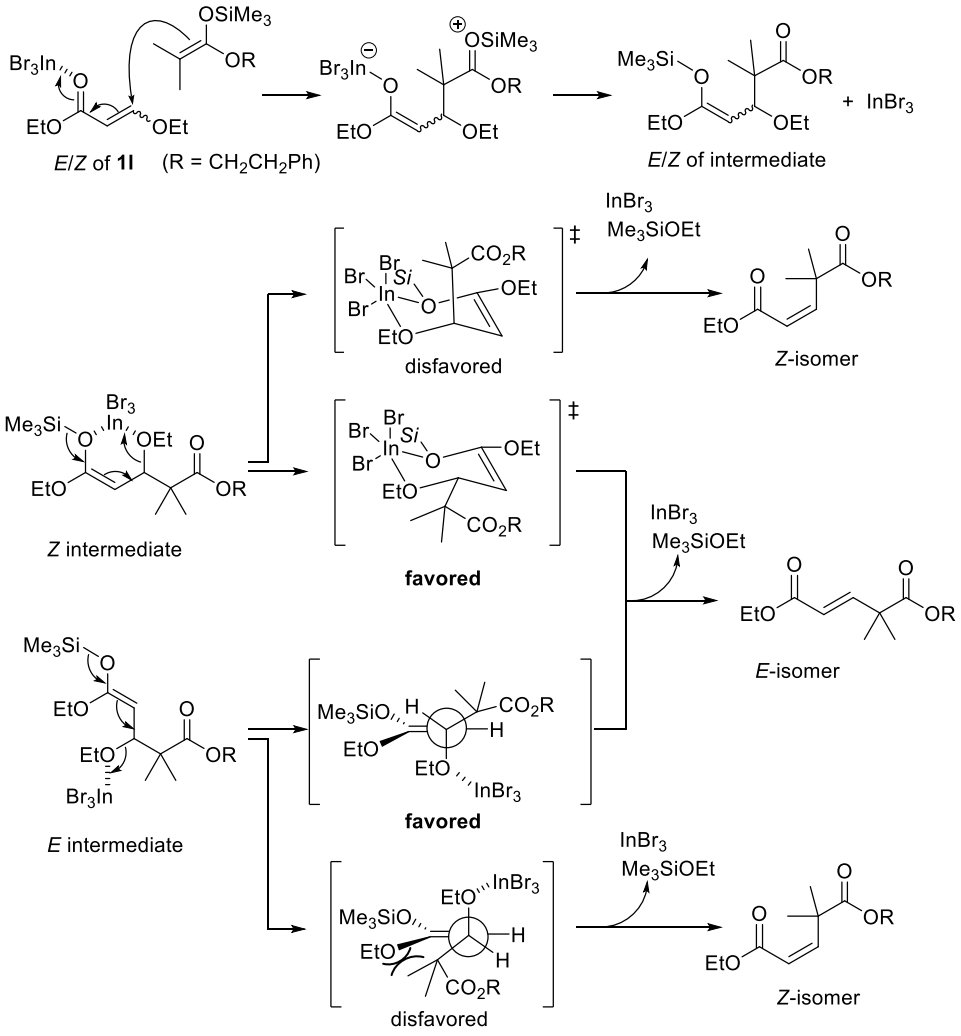

Scheme 11. Plausible mechanism for the E/Z mixture of alkenyl ether.

1-5. References

[1] For select reviews on transition metal catalyzed cross coupling using oxygen-based electrophiles, see: a) B. M. Rosen, K. W. Quasdorf, D. A. Wilson, N. Zhang, A. M. Resmerita, N. K. Garg, V. Percec, *Chem. Rev.* **2011**, *111*, 1346; b) J. Yamaguchi, K. Muto, K. Itami, *Eur. J. Org. Chem.* **2013**, 19; c) J. Cornella, C. Zarate, R. Martin, *Chem. Soc. Rev.* **2014**, *43*, 8081; d) M. Tobisu, N. Chatani, *Acc. Chem. Res.* **2015**, *48*, 1717; e) E. J. Tollefson, L. E. Hanna, E. R. Jarvo, *Acc. Chem. Res.* **2015**, *48*, 2344; f) E. Bisz, M. Szostak, *ChemSusChem* **2017**, *10*, 3964; g) N. A. Butt, W. Zhang, *Chem. Soc. Rev.* **2015**, *44*, 7929. B. M. Trost, M. L. Crawley, *Chem. Rev.* **2003**, *103*, 2921.

[2] For a review on Lewis acid catalyzed cross coupling using oxygen-based electrophiles, see: a) E. Emer, R. Sinisi, M. G. Capdevila, D. Petruzziello, F. De Vincentiis, P. G. Cozzi, *Eur. J. Org. Chem.* **2011**, 647; For select recent reports, see: b) Y. Di, T. Yoshimura, S. Naito, Y. Kimura, T. Kondo, *ACS Omega* **2018**, *3*, 18885; c) R. Fujihara, K. Nakata, *Eur. J. Org. Chem.* **2018**, *2018*, 6566. B. Rubial, A. Ballesteros, J. M. González, *Eur. J. Org. Chem.* **2018**, *2018*, 6194; d) R. Umeda, T. Jikyo, K. Toda, I. Osaka, Y. Nishiyama, *Tetrahedron Lett.* **2018**, *59*, 1121; f) S. Yaragorla, A. Pareek, R. Dada, A. I. Almansour, N. Arumugam, *Tetrahedron Lett.* **2016**, *57*, 5841; g) M. Saito, N. Tsuji, Y. Kobayashi, Y. Takemoto, *Org. Lett.* **2015**, *17*, 3000; h) N. Allali, V. Mamane, *Tetrahedron Lett.* **2012**, *53*, 2604; i) Z.-Q. Liu, Y. Zhang, L. Zhao, Z. Li, J. Wang, H. Li, L.-M. Wu, *Org. Lett.* **2011**, *13*, 2208; j) G. Chen, Z. Wang, J. Wu, K. Ding, *Org. Lett.* **2008**, *10*, 4573.

[3] For select recent report, see; a) B. Li, Y. Kuang, J. B. He, R. Tang, L. L. Xu, C. H. Leung, D. L. Ma, X. Qiao, M. Ye, *J. Nat. Prod.* **2020**, *83*, 45; b) J. P. Leea, M. G. Kang, J. Y. Lee, J. M. Oh, S. C. Baek, H. H. Leem, D. Park, M. L. Cho, H. Kim, *Bioorg. Chem.* **2019**, *89*, 103043; c) M. Isaka, P. Chinthanom, R. Suvannakad, T. Thummarukcharoen, T. Feng, J. K. Liu, *Phytochem. Lett.* **2019**, *29*, 178; d) H. Li, X. Han, J. Zhang, Y. Dong, S. Xu, Y. Bao, C. Chen, Y. Feng, Q. Cui, W. Li, *J. Nat. Prod.* **2019**, *82*, 3340; e) K. Georgousakia, N. Tsafantakisa, S. Gumenib, I. Gonzalezc, T. A. Mackenziec, F. Reyesc, C. Lambertd, I. P. Trougakosb, O. Genilloudc, N. Fokialakisa, *Bioorg. Med. Chem. Lett.* **2020**, *30*, 126952; f) C. de los Reyes, M. J. Ortega, H. Zbakh, V. Motilva, E. Zubía, *J. Nat. Prod.* **2016**, *79*, 395; g) T. J. Rettenmaier, H. Fan, J. Karpiak, A. Doak, A. Sali, B. K. Shoichet, J. A. Wells, *J. Med. Chem.* **2015**, *58*, 8285; h) F. Olivon, H. Palenzuela, E. Girard-Valenciennes, J. Neyts, C. Pannecouque, F. Roussi, I. Grondin, P. Leyssen, M. Litaudon, *J. Nat. Prod.* **2015**, *78*, 1119; i) R. B. Williams, V. L. Norman, M. O'Neil-Johnson, S. Woodbury, G. R. Eldridge, C. M. Starks, *J. Nat. Prod.* **2015**, *78*, 2074; j) O. Corminboeuf, X. Leroy, *J. Med. Chem.* **2015**, *58*, 537.

[4] Pd-catalyzed dimerization of silyl enol ethers, see; C. Chen, R. F. Jordan, *J. Am. Chem. Soc.* **2010**, *132*, 10254.

[5] a) Y. Nishimoto, Y. Kita, H. Ueda, H. Imaoka, K. Chiba, M. Yasuda, A. Baba, *Chem. Eur. J.* **2016**, *22*, 11837; b) Y. Nishimoto, H. Ueda, M. Yasuda, A. Baba, *Angew. Chem. Int. Ed.* **2012**, *51*, 8073.

[6] a) J. N. Desrosiers, C. B. Kelly, D. R. Fandrick, L. Nummy, S. J. Campbell, X. Wei, Xudong; M. Sarvestani, L. Heewon, S. Alexander, S. Sanjit, Z. Xingzhong, G. Nelu, M. Shengli, J. J. Song, C. H. Senanayake, *Org. Lett.* **2014**, *16*, 1724; b) M. Birch, S. Birtles, L. K. Buckett, P. D. Kemmitt, G. J. Smith, T. J. D. Smith, A. V. Turnbull, S. J. Y. Wang, *J. Med. Chem.* **2009**, *52*, 1558; c) T, Dyachenko, *Russ. J. Org. Chem.* **2003**, 39, 1174; d) L. E. Kiss, H. S. Ferreira, D. A. Learmonth, *Org. Lett.* **2008**, *10*, 1835; e) N. A. Tolmachova, I. I. Gerus, S. I. Vdovenko, G. Haufe, Y. A. Kirzhner, *Synthesis* **2007**, *24*, 3797; f) N. Zanatta, R. Barichello, H. G. Bonacorso, M. A. P. Martins, *Synthesis* **1999**, 765; g) A. Schwartz, Z. Pál, L. Szabó, K. Simon, I. Hermecz, Z. Mészáros, *J. Heterocyclic Chem.* **1987**, *24*, 645.

[7] I. S. Kondratov, I. I. Gerus, M. V. Furmanova, S. I. Vdovenko, I. Sergey, V. P. Kukhar, *Tetrahedron* **2007**, *63*, 7246.

[8] a) C. M. Abuhaie, A. Ghinet, A. Farce, J. Dubois, P. Gautret, B. Rigo, D. Belei, E. Bîcu, *Eur. J. Med. Chem.* **2013**, *59*, 101; b) C. M. Abuhaie, A. Ghinet, A. Farce, J. Dubois, B. Rigo, E. Bîcu, *Bioorg. Med. Chem. Lett.* **2013**, *23*, 5887; c) Y. Matsuda, K. Katou, C. Motokawa, T. Uemura, *Heterocycles* **2000**, *53*, 213; d) Y. Matsuda, K. Katou, T. Nishiyori, T. Uemura, M. Urakami, *Heterocycles* **1997**, 45, 2197; e) Y. Matsuda, Y. Chiyomaru, C. Motokawa, T. Nishiyori, *Heterocycles* **1995**, *41*, 329; f) Y. Matsuda, M. Yamashita, K. Takahashi, S. Ide, K. Torisu, K. Furuno, *Heterocycles* **1992**, *33*, 295; g) Y. Matsuda, H. Gotou, K. Katou, H. Matsumoto, M. Yamashita, K. Takahashi, S. Ide, Heterocycles, **1990**, *31*, 977; h) M. Watanabe, T. Kinoshita; S. Furukawa, *Chem. Pharm. Bull.* **1975**, *23*, 82; i) M. Watanabe, M. Baba, T. Kinoshita; S. Furukawa, *Chem. Pharm. Bull.* **1976**, *24*, 2421; j) G. B. Payne, *J. Org. Chem.* **1968**, *33*, 3517.

[9] Our recent reports, see; a) Y. Kita, T. Yata, Y. Nishimoto, M. Yasuda, *J. Org. Chem.* **2018**, *83*, 740; b) Y. Nishimoto, A. Okita, A. Baba, M. Yasuda, *Molecules* **2016**, *21*, 1330; c) Y. Nishimoto, T. Nishimura, M. Yasuda, *Chem. Eur. J.* **2015**, *21*, 18301; d) Y. Inamoto, Y. Kaga, Y. Nishimoto, M. Yasuda, A. Baba, *Chem. Eur. J.* **2014**, *37*, 11664; e) Y. Onishi, Y. Nishimoto, M. Yasuda, A. Baba, *Org. Lett.* **2014**, *16*, 1176.

[10] Reviews; a) S. R. Pathipat, A. van der Werf, N. Selander, *Synthesis* **2017**, *49*, 4931; b) J. P. Sestelo, L. A. Sarandeses, M. M. Martínez, L. Alonso-Marañón, *Org. Biomol. Chem.* **2018**, *16*, 5733; c) S. Dagorne, C. Fliedel and P. de Frémont, in *Encyclopedia of Inorganic and Bioinorganic Chemistry*, John Wiley & Sons, Ltd, 2011, DOI: 10.1002/9781119951438.eibc2416; d) J. S. Yadav, A. Antony, J. George, B. V. Subba Reddy, *Eur. J. Org. Chem.* **2010**, 591.

[11] Details of the optimization of reaction conditions are described in the Experimental section.

[12] a) K. Surendra, E. J. Corey, *J. Am. Chem. Soc.* **2014**, *136*, 10918; b) B. Michelet, J. Colard-Itté, G. Thiery, R. Guillot, C. Bour, V. Gandon, *Chem. Commun.* **2015**, *51*, 7401; c) J. Tian, Y. Chen, M. Vayer, A. Djurovic, R. Guillot, R. Guermazi, S. Dagorne, C. Bour, V. Gandon, *Chem. Eur. J.* **2020**, *26*, 12831.

[13] a) A. R. Lippert, J. Kaeobamrung, J. W. Bode, *J. Am. Chem. Soc.* **2006**, *128*, 14738; b) D. R. Williams, S. Patnaik, G. S. Cortez, *Heterocycles* **2007**, *72*, 213; c) I. Matsuda, *J. Organomet. Chem.* **1987**, *321*, 307.

[14] N. Li, X. Y. Dong, J. L. Zhang, K. Yang, Z. J. Zheng, W. Q. Zhang, Z. W. Gao, L. W. Xu, *RSC Adv.* **2017**, *7*, 50729.

[15] a) E. J. Corey, P. A. Magriotis, *J. Am. Chem. Soc.* **1987**, *109*, 287; b) A. Natarajan, D. Ng, Z. Yang, M. A. Garcia-Garibay, *Angew. Chem. Int. Ed.* **2007**, *46*, 6485; c) D. Gray, T. Gallagher, *Angew. Chem. Int. Ed.* **2006**, 45, 2419; d) C. H. Heathcock, D. A. Oare, *J. Org. Chem.* **1985**, *50*, 3022.

[16] V. V. Shchepin, D. V. Fotin, *Russ. J. Org. Chem.* **2005**, *41*, 1011.

[17] The plausible explanation for the selective production of *E*-isomer **3la** from *E*/*Z*-mixture of alkenyl ether **1l** is described in the Experimental section (Scheme 11).

[18] The details of NMR studies are shown in the Experimental section (Scheme 8).

[19] Full explanation about the selective production of *E*-isomer **15** from *E*/*Z*-mixture of enolate intermediates **13** is described in the Experimental section (Scheme 10).

[20] a) P. Vlček, L. Lochmann, *Prog. Polym. Sci.* **1999**, *24*, 793; b) L. Dvořánek, P. Vlček, *Polym. Bull.* **1993**, *31*, 393.

[21] Hydrogen-bond-activated Pd-mediated elimination of alkoxy groups at the allylic position in the coupling between allylic ethers and carbonyl compounds was reported. X. Huo, M. Quan, G. Yang, X. Zhao, D. Liu, Y. Liu, W. Zhang, *Org. Lett.* **2014**, *16*, 1570.

[22] Selected papers; a) E. Schievano, E. Morelato, C. Facchin, S. Mammi, *J. Agric. Food Chem.* **2013**, *61*, 1747; b) P. Ciminiello, C. Dell'Aversano, E. D. Iacovo, E. Fattorusso, M. Forino, L. Grauso, L. Tartaglione, F. Guerrini, L. Pezzolesi, R. Pistocchi, S. Vanucci, *J. Am. Chem. Soc.* **2012**, *134*, 1869; c) I. Paterson, N. M. Gardner, K. G. Poullennec, A. E. Wright, *J. Nat. Prod.* **2008**, *71*, 364.

[23] a) T. Suga, M. Shiina, Y. Asami, M. Iwatsuki, T. Yamamoto, K. Nonaka, R. Masuma, H. Matsui, H. Hanaki, S. Iwamoto, H. Onodera, K. Shiomi, S. Ōmu, *J. Antibiot.* **2016**, *69*, 605; b) M. Isaka, U. Srisanoh, S. Veeranondha, W. Choowong, S. Lumyong, *Tetrahedron* **2009**, *65*, 8808.

[24] Spectroscopic data: A. Clerici, N. Pastori, O. Porta, *Tetrahedron* **2001**, *57*, 217. Synthetic procedure: F. Shi, S. Luo, Z. Tao, L. He, J. Yu, S. Tu, L. Gong, *Org. Lett.* **2011**, *13*, 4680. S. Son, G. C. Fu, *J. Am. Chem. Soc*. **2007**, *129*, 1046.

[25] R. Chong, P. S. Clozy, *Tetrahedron Lett.* **1966**, *7*, 741.

[26] Spectroscopic data: M. R. Detty, H. R. Luss, J. M. McKelvey, S. M. Geer, *J. Org. Chem*. **1986**, *51*, 1692. T. Nishio, Y. Omote, *Synthesis* **1980**, 1013. Synthetic procedure: See ref 25.

[27] Spectroscopic data and synthetic procedure: H. Nakatsuji, R. Kamada, H. Kitaguchi, Y. Tanabe, *Adv. Synth. Catal.* **2017**, *359*, 3865.

[28] Spectroscopic data and synthetic procedure: D. Katayev, V. Matoušek, R. Koller, A. Togni, *Org. Lett.* **2015**, *17*, 5898.

[29] Spectroscopic data and synthetic procedure: Y. Nishimoto, Y. Kita, H. Ueda, H. Imaoka, K. Chiba, M. Yasuda, A. Baba, *Chem. Eur. J.* **2016**, *22*, 11837.

[30] Spectroscopic data and synthetic procedure: A. Romanens, G. Bélanger, *Org. Lett.* **2015**, *17*, 322.

[31] Spectroscopic data and synthetic procedure: F. Zhou, H. Yamamoto, *Angew. Chem. Int. Ed.* **2016**, *55*, 8970.

[32] Spectroscopic data and synthetic procedure: H. Kuroda, E. Hanaki, H. Izawa, M. Kano, H. Itahashi, *Tetrahedron* **2004**, *60*, 1913.

[33] Spectroscopic data and synthetic procedure: N. Esumi, K. Suzuki, Y. Nishimoto, M. Yasuda, *Org. Lett.* **2016**, *18*, 5704.

[34] a) A. R. Lippert, J. Kaeobamrung, J. W. Bode, *J. Am. Chem. Soc.* **2006**, *128*, 14738; b) D. R. Williams, S. Patnaik, G. S. Cortez, *Heterocycles* **2007**, *72*, 213; c) I. Matsuda, *J. Organomet. Chem.* **1987**, *321*, 307.

[35] N. Li, X. Y. Dong, J. L. Zhang, K. Yang, Z. J. Zheng, W. Q. Zhang, Z. W. Gao, L. W. Xu, *RSC Adv.* **2017**, *7*, 50729.

[36] a) E. J. Corey, P. A. Magriotis, *J. Am. Chem. Soc.* **1987**, *109*, 287; b) A. Natarajan, D. Ng, Z. Yang, M. A. Garcia-Garibay, *Angew. Chem. Int. Ed.* **2007**, *46*, 6485; c) D. Gray, T. Gallagher, *Angew. Chem. Int. Ed.* **2006**, 45, 2419; d) C. H. Heathcock, D. A. Oare, *J. Org. Chem.* **1985**, *50*, 3022.

[37] V. V. Shchepin, D. V. Fotin, *Russ. J. Org. Chem.* **2005**, *41*, 1011.

[38] T. Bach, K. Jödicke, K. Kather, R. Fröhlich, *J. Am. Chem. Soc.* **1997**, *119*, 2437.

Chapter 2. Synthesis and Characterization of Pheox– and Phebox–Aluminum Complexes: Application as Tunable Lewis Acid Catalysts in Organic Reactions

2-1. Introduction

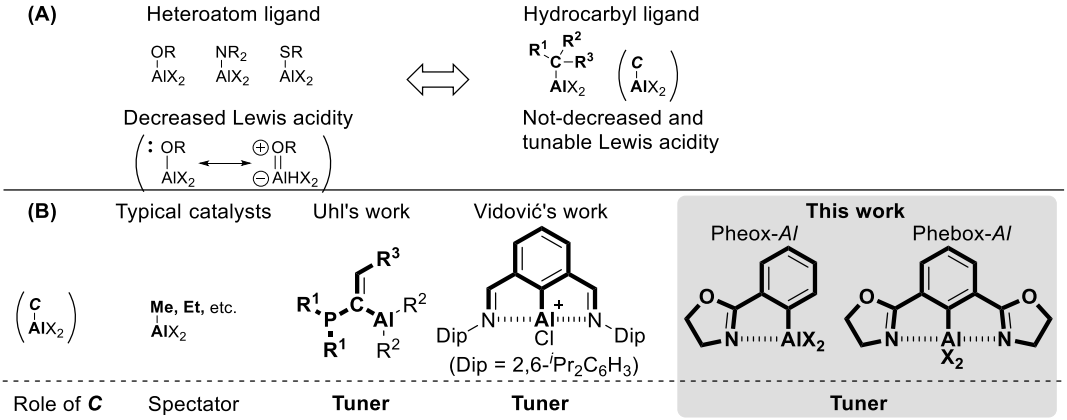

Figure 1. A) Comparison of hydrocarbyl and heteroatom ligands. B) Aluminum catalysts bearing a hydrocarbyl ligand.

Aluminum is one of the most abundant metals in the Earth's crust, with trivalent aluminum compounds being important Lewis acids in organic chemistry.[1] Indeed, to date, a number of aluminum catalysts with sophisticated covalent and/or dative ligands have been synthesized.[2] In terms of the covalent ligands, various well-defined alkoxy, aryloxy, amino, and thiolate ligands have been developed (Figure 1A); however, these ligands reduce the Lewis acidity by conjugation between an empty orbital of the Al atom and a lone pair of the ligand heteroatom. Thus, hydrocarbyl ligands are promising replacements, as this decrease in the Lewis acidity can be avoided, and modification of the carbon framework can precisely control the catalytic properties (Figure 1A). However, few aluminum catalysts with well-defined hydrocarbyl ligands have been reported,[3–5] and simple alkyl ligands behaving as spectators are often used (Figure 1B, typical catalysts).[1, 2] Due to the nucleophilic properties of hydrocarbyl ligands in addition to their sensitivities to moisture and air, the application of organoaluminum compounds as catalysts is challenging. Although Uhl reported that phosphine-substituted alkenylaluminums act as frustrated Lewis pair catalysts[6] and Vidovic´ synthesized and employed organoaluminum complexes supported by a bis(imino) aryl NCN pincer ligand,[7] the scope of applicable catalytic reactions was narrow (Figure 1B, Uhl's and Vidović's works). We therefore chose to adopt the 2-oxazolinylphenyl (Pheox) and 2,6-bis(oxazolinyl)phenyl (Phebox) ligands,[8, 9] as they can enhance the stability of complexes and tune the Lewis acidity by the intramolecular coordination of oxazoline moieties. Thus, we report the first synthesis, characterization, and catalytic property study of Pheox– and Phebox–Al complexes (Figure 1, this work). Through tuning of the Lewis acidity by using hydrocarbyl and heteroatom ligands, the Pheox– and Phebox–Al complexes

will be employed in the Mukaiyama aldol reaction and in the hydroboration of aldehydes. We also compare the substrate selectivity of the Pheox–Al catalyst with that of $AlCl_3$ in a hetero-Diels–Alder reaction.

2-2. Results and Discussion

For preparation of the desired Pheox– and Phebox–Al complexes, aryl lithium **1**-Li was initially formed by the treatment of **1**-Br with *n*-BuLi, and subsequent transmetalation with $AlCl_3$ gave pale brown precipitates. Pheox–$AlCl_2$ (**1**-$AlCl_2$) was obtained in 32% yield by further purification with diethyl ether extraction, concentration, and recrystallization from chloroform [Eq. (1)]. [10] Phebox–Al complex **2**-$AlCl_2$ was synthesized in 17% yield from **2**-Br by the similar method [Eq. (2)]. These Al complexes were characterized by X-ray diffraction, and the corresponding crystal structures are shown in Figure 2.[11] As indicated, the aluminum center of **1**-$AlCl_2$ adopts a distorted tetrahedral coordination geometry with intramolecular coordination of an oxazoline moiety, where the Al–C1 bond leans to the oxazoline moiety (Al–C1–C2 = 108.08°, Al–C1–C3 = 135.88°). Complex **2**-$AlCl_2$ has a trigonal bipyramidal geometry at the Al center. Three equatorial positions are occupied by two chlorines and a phenyl moiety, and both intramolecular oxazoline moieties coordinate at axial positions. The Al–C bond length in **1**-$AlCl_2$ (1.9697 Å) is comparable to that in **2**-$AlCl_2$ (1.964 Å), and both are close to a reported average value (C_{Ar}–Al 1.9998 Å).[12] Both complexes were stable over a few weeks under a nitrogen atmosphere.

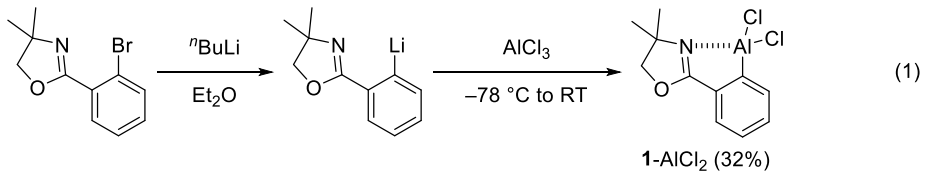

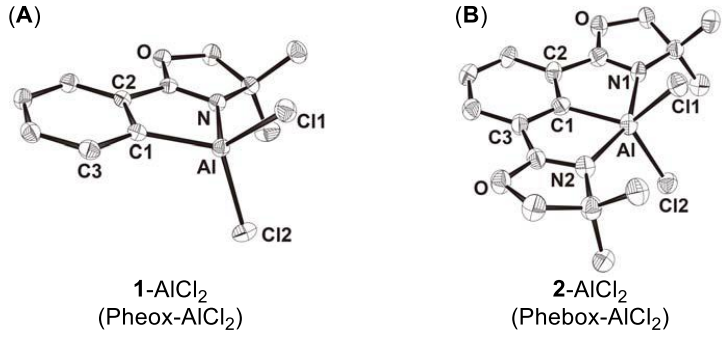

1-$AlCl_2$ (Pheox-$AlCl_2$) **2**-$AlCl_2$ (Phebox-$AlCl_2$)

Figure 2. X-ray crystallographic structures of: A) **1**-$AlCl_2$ and B) **2**-$AlCl_2$.

Treatment of **1**-$AlCl_2$ and **2**-$AlCl_2$ with $AgClO_4$ then gave **1**-$Al(ClO_4)_2$ and **2**-$Al(ClO_4)_2$,

respectively [Eq. (3) and (4)], and the corresponding crystal structures are given in Figure 3. The geometries of **1**-Al$(ClO_4)_2$ and **2**-Al$(ClO_4)_2$ are similar to those of **1**-$AlCl_2$ and **2**-$AlCl_2$, respectively, and all ClO_4 groups acted as ligands to the Al atoms. The lengths of the Al–C (1.937 Å) and Al–N (1.886 Å) bonds of **1**-Al$(ClO_4)_2$ were shorter than those of **1**-$AlCl_2$. In addition, the Al–C (1.931 Å) and two Al–N (2.101 and 2.080 Å) bonds of **2**-Al$(ClO_4)_2$ were also shorter. These results indicate an enhancement in the Lewis acidity. Additionally, **2**-Al$(OTf)_2$ was synthesized by using AgOTf [Eq. (4)].

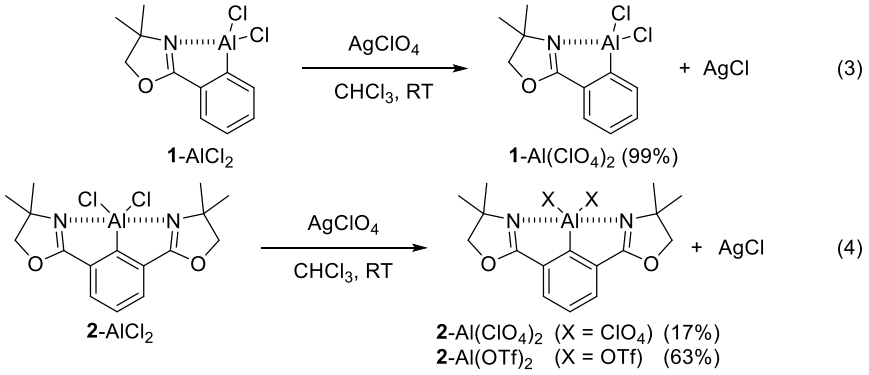

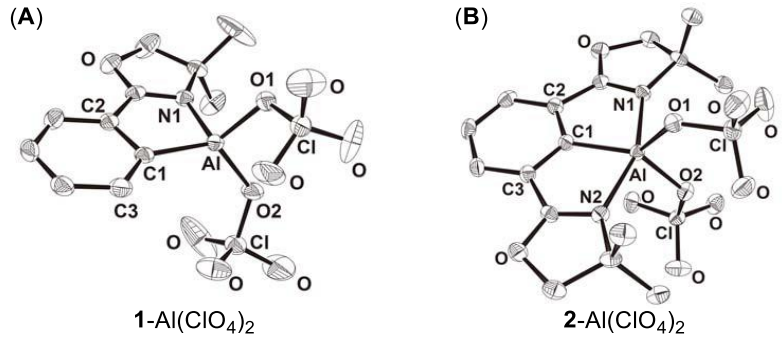

Figure 3. X-ray crystallographic structures of: A) **1**-Al$(ClO_4)_2$ and B) **2**-Al$(ClO_4)_2$.

We then investigated the Lewis acidic properties of the Pheox– and Phebox–Al complexes. In the ^{1}H NMR spectrum of **1**-$AlCl_2$ and 3,5-dibromopyridine **3**, the signals of **3** and the oxazoline moiety are shifted downfield and upfield, respectively [Eq. (5)]. X-ray diffraction measurements of Lewis acid–base adduct **1**-$AlCl_2$·**3** (Figure 4A) showed that the Al center possesses a trigonal bipyramidal geometry, and **3** coordinated to the Al center on the opposite side of an oxazoline moiety, occupying an axial position. Interactions between **2**-$AlCl_2$ and **3** were not confirmed by NMR measurements. In contrast, **2**-Al$(ClO_4)_2$ and **2**-Al$(OTf)_2$ interacted with **3** to give downfield shifts in the ^{1}H NMR signals of **3** [Eq. (6)], and X-ray diffraction measurement revealed the structure of the Lewis acid–base adduct **2**-Al$(OTf)_2$·**3** (Figure 4B), which suggested that ClO_4 and TfO ligands enhanced the Lewis acidity. The Al center of **2**-Al$(OTf)_2$·**3** displayed a distorted octahedral geometry with two TfO ligands, the Phebox ligand, **3**, and both oxazoline moieties coordinating to the Al atom. Pyridine ligand **3** occupied the coordination site over a square plane consisting of the Phebox and TfO ligands.

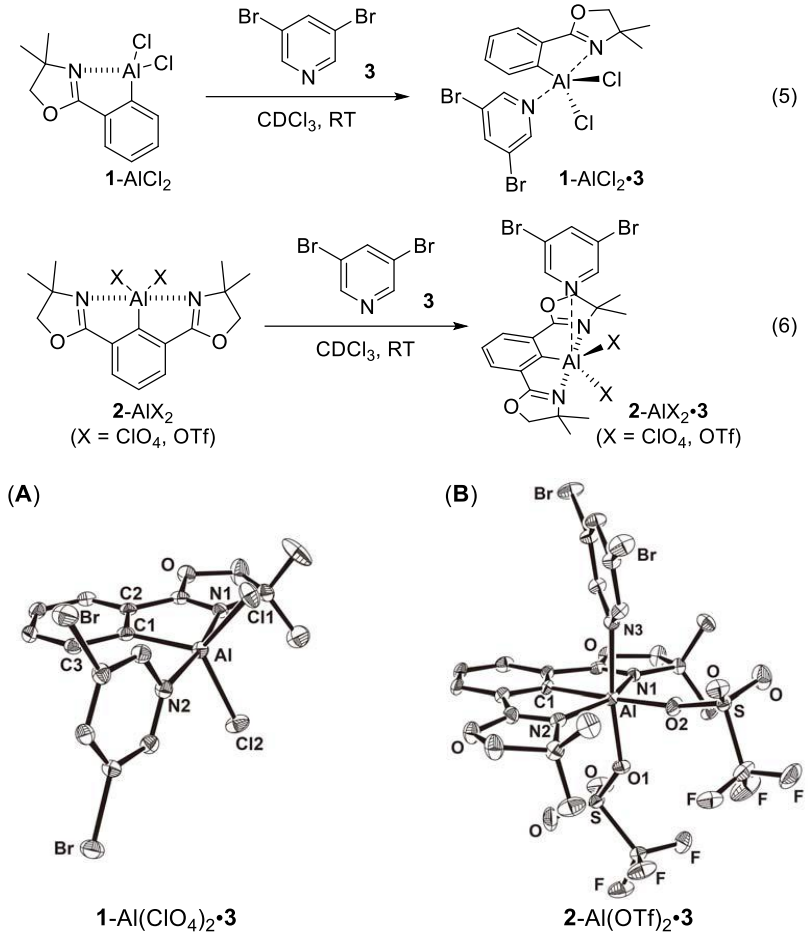

Figure 4. X-ray crystallographic structures of: A) **1**-$AlCl_2$·**3** and B) **2**-$Al(OTf)_2$·**3**.

In Lewis acid catalysis, the effective activation of substrates by Lewis acidity and the smooth release of products from a catalyst are essential for achieving a high turnover frequency, and so tuning of the Lewis acidity is necessary in efficient catalysis design. The Lewis acidities of **1**-AlX_2 and **2**-AlX_2 were estimated from the Δν(C=O) value of pyrone **4** in the complexation between aluminum compound Al and **4** (Table 1).[13] The observed values suggested that chloro complexes **1**-$AlCl_2$ and **2**-$AlCl_2$ have low and moderate Lewis acidities, respectively (Entries 1 and 2), and the perchlorate and triflate complexes (Entries 3–5) have high Lewis acidities comparable to those of $AlCl_3$, $Al(ClO_4)_3$, and $Al(OTf)_3$ (Entries 6–8).[14] Pentacoordinate **2**-$AlCl_2$ showed a lower Lewis acidity compared to the moderate Lewis acidity of tetracoordinate **1**-$AlCl_2$ (Entries 1 and 2), which is consistent with a lack of complexation between **2**-$AlCl_2$ and **3**. In contrast, **2**-$Al(ClO_4)_2$ showed a higher Lewis acidity than **1**-$Al(ClO_4)_2$ (Entries 3 and 4), which may be due to the dissociation of a ClO_4 ligand from the **2**-$Al(ClO_4)_2$·**4** complex to generate a cationic complex in the solution state. These results revealed that hydrocarbyl ligands have a significant influence on the Lewis acidity. Heteroatom ligands, Cl, ClO_4, and TfO, also change Lewis acidity. Larger p*K*a values for the conjugate acids of heteroatom ligands gave higher Lewis acidities in the corresponding aluminum complexes.[15]

Table 1. Complexation of aluminum compounds with pyrone **4**.[a]

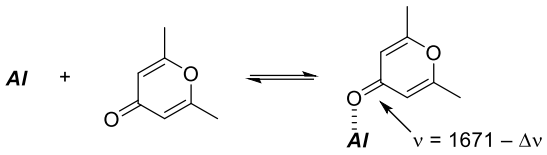

Entry	Al compound	Δν(C=O) [cm^{-1}]
1	**1**-$AlCl_2$	15
2	**2**-$AlCl_2$	0
3	**1**-$Al(ClO_4)_2$	19
4	**2**-$Al(ClO_4)_2$	22
5	**2**-$Al(OTf)_2$	19
6	$AlCl_3$	19
7	$Al(ClO_4)_3$	19
8	$Al(OTf)_3$	19

[a] IR spectra recorded in CH_2Cl_2 at room temperature.

For the further fine tuning of the Lewis acidity of aluminum complexes, substituents were introduced on the Phebox ligand. Methoxy-, chloro-, and *tert*-Bu-substituted Phebox aluminum complexes were synthesized (See Experimental Section) and their Lewis acidity were evaluated using pyrone **4** (Table 2). Pyrone **4** adducts of **2**-^{t}Bu-$Al(ClO_4)_2$ and **2**-Cl-$Al(ClO_4)_2$ have similar Δν(C=O) values with the adduct of **2**-$Al(ClO_4)_2$, which indicates these complexes have comparable Lewis acidities. In contrast, **2**-MeO-$Al(ClO_4)_2$ showed a lower Lewis acidity. According to these results, the substituents on Phebox ligand change the Lewis acidities of Phebox-Al complexes.

Table 2. Evaluation of Lewis acidities of substituted Phebox-Al complexes.[a]

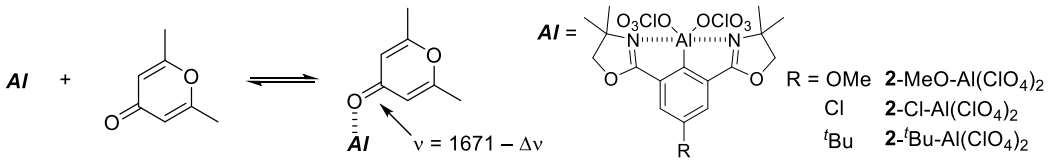

Entry	Al compound	Δν(C=O) [cm^{-1}]
1	**2**-$Al(ClO_4)_2$	22
2	**2**-^{t}Bu-$Al(ClO_4)_2$	21
3	**2**-Cl-$Al(ClO_4)_2$	21
4	**2**-MeO-$Al(ClO_4)_2$	18

[a] IR spectra recorded in CH_2Cl_2 at room temperature.

The catalytic activities of the synthesized organoaluminum complexes were then evaluated in the

Mukaiyama aldol reaction and in the hydroboration of aldehydes. A catalytic amount of **1**-$AlCl_2$ effectively accelerated the Mukaiyama aldol reaction of aldehyde **5** with silyl ketene acetal **6a** to give **7a** in 79% yield (Table 3, Entry 1). In contrast, **2**-$AlCl_2$ exhibited a poor catalytic activity due to its low Lewis acidity (Entry 2). In the aldol reaction using the less nucleophilic silyl enol ether **6b**,[16] no catalytic activity was observed for **1**-$AlCl_2$ or **2**-$AlCl_2$ (Entries 3 and 4). When the more Lewis acidic Pheox and Phebox complexes,**1**-Al(ClO4)$_2$, **2**-Al(ClO4)$_2$, and **2**-Al(OTf)$_2$ were examined, the desired reaction proceeded to give aldol product **7b** in high yields (Entries 5–7). When the reactions with $AlCl_3$, $Al(ClO_4)_3$, and $Al(OTf)_3$ were examined, $AlCl_3$ and $Al(OTf)_3$ afforded high yields (Entries 8–10) so Pheox and Phebox complexes were found to act as efficient catalysts to the same extent as classical aluminum salts.

Table 3. Mukaiyama aldol reaction of an aldehyde with silyl enolates.[a]

Entry	Si enolate		Al catalyst	Yield of **7** [%]	Recovery of **5** [%]
1	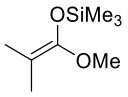	**6a**	**1**-$AlCl_2$	79 (**7a**)	21
2			**2**-$AlCl_2$	12 (**7a**)	63
3			**1**-$AlCl_2$	0 (**7b**)	77
4			**2**-$AlCl_2$	0 (**7b**)	88
5			**1**-$Al(ClO_4)_2$	99 (**7b**)	0
6	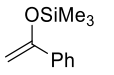	**6b**	**2**-$Al(ClO_4)_2$	97 (**7b**)	0
7			**2**-$Al(OTf)_2$	84 (**7b**)	14
8			$AlCl_3$	99 (**7b**)	0
9			$Al(ClO_4)_3$	8 (**7b**)[b]	7
10			$Al(OTf)_3$	95 (**7b**)	0

[a] Aldehyde **5** (0.5 mmol), silyl enolate **6** (0.75mmol), CH_2Cl_2 (1 mL), catalyst (0.025 mmol), reaction time 4 h. Yields determined by ^{1}HNMR spectroscopy by using an internal standard. [b] An enone product was obtained in 43% yield by the dehydration of aldol product **7**.

The hydroboration of aldehyde **8** with pinacolborane catalyzed by **1**-$AlCl_2$ and **2**-$AlCl_2$ resulted in low yields (Table 4, Entries 1 and 2).[17] **1**-Al(ClO$_4$)$_2$ also gave poor results (Entry 3),while **2**-Al(ClO$_4$)$_2$ and **2**-Al(OTf)$_2$ exhibited high catalytic activities (Entries 4 and 5). The catalytic activity of **2**-Al(OTf)$_2$ (Entry 6) was significantly higher than those of inorganic aluminum catalysts, $AlCl_3$,

$Al(OTf)_3$, and $Al(ClO_4)_3$ (Entries 7–9)[14] despite their similar high Lewis acidities (Scheme 1). The high Lewis acidities of conventional aluminum salts (e.g., $AlCl_3$) allow effective substrate activation, but these salts strongly associate with the products to reduce the turnover number. In contrast, **2**-$Al(OTf)_2$ can efficiently release the product due to the highly coordinated aluminum center, thereby giving an excellent catalytic activity. The investigation shown in Tables 3 and 4 demonstrated that hydrocarbyl and heteroatom ligands allow control of the catalytic activity.

Table 4. Hydroboration of benzaldehyde with HBpin catalyzed by aluminum compounds.[a]

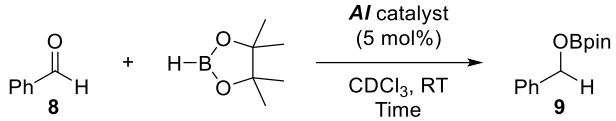

Entry	Al catalyst	Time [h]	Yield of **9** [%][b]	Recovery of **8** [%]
1	**1**-$AlCl_2$	8	30	68
2	**2**-$AlCl_2$	8	30	70
3	**1**-$Al(ClO_4)_2$	8	27	56
4	**2**-$Al(ClO_4)_2$	8	70	28
5	**2**-$Al(OTf)_2$	8	96	4
6	**2**-$Al(OTf)_2$	1	93	7
7	$AlCl_3$	1	5	95
8	$Al(OTf)_3$	1	6	94
9	$Al(ClO_4)_3$	1	47	52

[a] Benzaldehyde **8** (1.0 mmol), HBpin (1.1 mmol), $CDCl_3$ (1 mL), room temperature, 8h. [b] Yields were determined by ^{1}HNMR spectroscopy by using an internal standard.

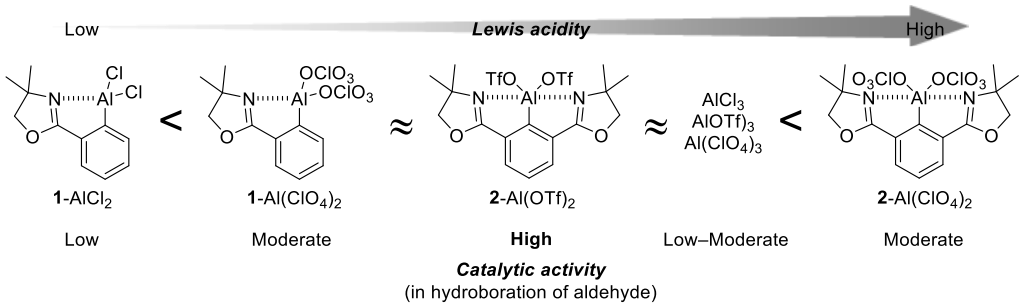

Scheme 1. Correlation between Lewis acidity and catalytic activity in the hydroboration reaction.

The successful tuning of the Lewis acidities and the catalytic activities of the Pheox– and Phebox–Al complexes (Scheme 1) encouraged us to address the challenging issue of recognition between similar substrates. We therefore examined competitive hetero-Diels–Alder reactions of

aldehydes with Danishefsky diene **12** (Table 5). In the $AlCl_3$-catalyzed competitive reaction between *p*-chlorobenzaldehyde **10** and *p*-anisaldehyde **11**, electron-rich aldehyde **11** preferentially reacted with **12**, giving a low product ratio (14/16 = 1:2.4; Entry 1). Other metal salts such as $Sc(OTf)_3$ and $InBr_3$ gave a similar selectivity to $AlCl_3$ (Entries 2 and 3). Surprisingly, **1**-$AlCl_2$ exhibited an inverse selectivity and high substrate recognition, with electron-deficient aldehyde **10** mainly undergoing **1**-$AlCl_2$-catalyzed cycloaddition, and giving a high product ratio (14/16 = 4.8:1; Entry 4). This inversion of the substrate selectivity between $AlCl_3$ and **1**-$AlCl_2$ was also observed in the competitive reaction between benzaldehyde **8** and *p*-anisaldehyde **11** (Entries 5 and 6). These results suggest that a strong Lewis acidic catalyst accelerates the reaction of an electron-rich aldehyde, while a weak Lewis acidic catalyst accelerates the reaction of an electron-deficient aldehyde. Considering the competitive reactions outlined in Scheme 2, this inversion can be explained by the change in the substrate-recognition step (see the Experimental section for an explanation of the substrate selectivity based on chemical kinetics). In the case of **1**-$AlCl_2$, a rapid equilibrium of coordination/dissociation exists between aldehydes and weak Lewis acidic **1**-$AlCl_2$, and the substrate selectivity is determined in the cycloaddition step; the more electrophilic aldehyde **16** preferentially undergoes the reaction to yield **17**. In contrast, in the case of strong Lewis acidic catalysts such as $AlCl_3$, $Sc(OTf)_3$, and $InBr_3$, the product ratio is determined during coordination of the aldehyde to the Lewis acid, as there is no association/dissociation equilibrium. Thus, the more electron-rich aldehyde **18** preferentially coordinates to a Lewis acid to give **19**. It is significant to successfully control the Lewis acidity and substrate selectivity of organoaluminum complexes by a hydrocarbyl ligand.

Table 5. Substrate recognition of aluminum complexes in competitive hetero-Diels–Alder reaction.[a]

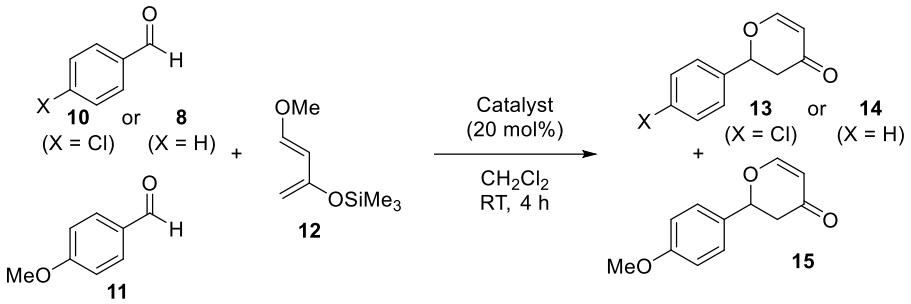

Entry	Substrates	Catalyst	Yield [%][b]	Ratio	
1	**10**, **11**	$AlCl_3$	43	1:2.4	(**13**/**15**)
2	**10**, **11**	$Sc(OTf)_3$	28	1:1.3	(**13**/**15**)
3	**10**, **11**	$InBr_3$	35	1:>99	(**13**/**15**)
4	**10**, **11**	**1**-$AlCl_2$	47	4.8:1	(**13**/**15**)
5	**8**, **11**	$AlCl_3$	44	1:1.4	(**14**/**15**)
6	**8**, **11**	**1**-$AlCl_2$	43	3.8:1	(**14**/**15**)

[a] Each aldehydes (0.5 mmol), **12** (0.25 mmol), CH_2Cl_2 (0.5 mL), RT, 4 h. Yields and ratios of products were determined by ^{1}HNMR spectroscopy by using an internal standard. [b] **13**+**15** or **14**+**15**.

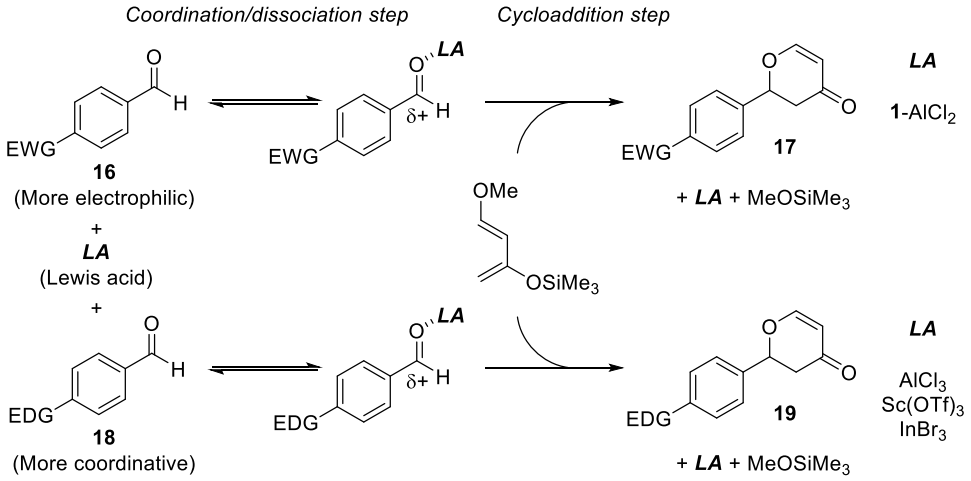

Scheme 2. Whole scheme of the competitive reaction.

2-3. Conclusion

In summary, we synthesized novel Pheox– and Phebox–aluminum complexes, **1**-$AlCl_2$, **1**-$Al(ClO_4)_2$, **2**-$AlCl_2$, **2**-$Al(ClO_4)_2$, and **2**-$Al(OTf)_2$. These complexes were successfully characterized by X-ray diffraction and NMR spectroscopy. They behaved as Lewis acid catalysts in the Mukaiyama aldol reaction and in the hydroboration of aldehydes. In addition, **1**-$AlCl_2$ exhibited the opposite selectivity from $AlCl_3$ in competitive hetero-Diels–Alder reactions between electron-rich and electron-deficient aldehydes. Furthermore, hydrocarbyl ligands and heteroatom ligands were found to control the catalytic activity. We are currently developing additional functionalized Pheox– and Phebox–aluminum catalysts to achieve new catalytic reactions.

2-4. Experimental Section

General

NMR spectra were recorded on a JEOL JNM-400 (400 MHz for ^{1}H NMR and 100 MHz for ^{13}C NMR, and 103 MHz for ^{27}Al NMR) spectrometer or a Bruker AVANCE III (600 MHz for ^{1}H NMR and 150 MHz for ^{13}C NMR) spectrometer. Chemical shifts were reported in ppm on the δ scale relative to tetramethylsilane (δ = 0 for ^{1}H NMR) and residual $CHCl_3$ (δ = 77.0 for ^{13}C NMR) as an internal reference, and $AlCl_3$ in D_2O (δ = 0 for ^{27}Al NMR) as an external reference. New compounds were characterized by ^{1}H, ^{13}C, ^{13}C off-resonance techniques, COSY, HMQC, and HMBC. Infrared (IR) spectra were recorded on a JASCO FT/IR-6200 Fourier transform infrared spectrophotometer or a METTLER TOLEDO ReactIR15. Column chromatographies were performed with silica gel. Purification by recycle HPLC was performed on a SHIMADZU recycle HPLC system (SPD-20A, RID-10A, DGU-20A, LC-6AD, and FCV-20H2) and Japan Analytical Industry Co. (NEXT recycling preparative HPLC). Reactions were carried out in dry solvents under nitrogen atmosphere, unless otherwise stated. Reagents were purchased from Aldrich or Tokyo Chemical Industry Co., Ltd. (TCI), Wako Pure Chemical Industries, Ltd., and used after purification by distillation or used without purification for solid substrates. X-ray diffraction analysis was carried out by a Rigaku XtaLAB Synergy with Hypix-6000HE.

Materials

Dehydrated solvents were purchased from Wako Pure Chemical Industries and used as obtained. 3,5-dibromopyridine **3**, pyrone **4**, aldehydes (**5**, **8**, **10**, **11**), silyl enolates (**6a**, **6b**, and **12**), and pinacolborane were purchased. The preparation and characterization of new compounds, **2**-Br and organoaluminum complexes were described below. $AlCl_3$ (aluminum chloride, 99.9%) was purchased from Wako Pure Chemical Industries and used as obtained. $Al(OTf)_3$ (aluminum trifluoromethanesulfonate, 99%) was purchased from Strem Chemicals, Inc. and used as obtained. $Al(ClO_4)_3 \cdot 9H_2O$ (aluminium perchlorate nonahydrate) was purchased from Strem Chemicals, Inc. and used as obtained. Compound **1**-Br was prepared according to the reported method.[18]

2,2'-(2-bromo-1,3-phenylene)bis(4,4-dimethyl-4,5-dihydrooxazole) (2-Br)

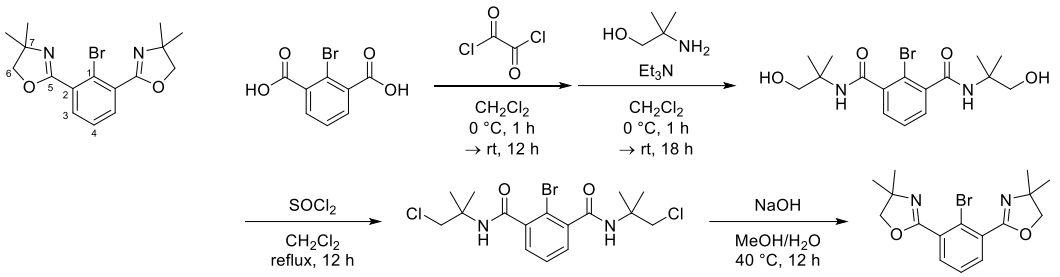

To a suspention of 2-bromoisophthalic acid (5.00 g, 20.4 mmol) in dichloromethane (60 mL) were added oxalyl chloride (8.5 mL, 100 mmol) and *N*,*N*-dimethylformamide (0.1 mL) at 0 °C. The reaction mixture was allowed to room temperature and stirred for 14 h to give a yellow solution. The solution was evaporated to remove the unreacted oxalyl chloride under a nitrogen atmosphere. Then, to the obtained 2-bromoisophthloyl dichloride was added CH_2Cl_2 (60 mL).

To a solution of triethylamine (7.55 g, 74.6 mmol) and 2-amino-2-methyl-1-propanol (6.09 g, 68.3 mmol) in dichloromethane (60 mL) was added the solution of 2-bromoisophthaloyl dichloride in dichloromethane at 0 °C via cannula. The reaction mixture was stirred for 1 h at 0 °C and stirred for 18 hours at room temperature to give the white suspension. The white suspension was evaporated and extracted with acetone. The filtrate was evaporated to give crude 2-bromo-*N*,*N'*-bis(1-hydroxy-2-methylpropn-2-yl)isophthalamide as a white solid (11.94 g). The crude product was carried through to the next step without further purification.

To a white suspension of the crude product of 2-bromo-*N*,*N'*-bis(1-hydroxy-2-methylpropn-2-yl)isophthalamide (11.94 g) in dichloromethane (40 mL) was slowly added thionyl chloride (7.25 mL, 100 mmol) at 0 °C. The reaction mixture was refluxed for 12 h and cooled to room temperature. The reaction mixture was quenched with 10% NaOH aq. The organic layer was separated and the aqueous layer was extracted with THF. The combined organic layer was dried over $MgSO_4$, filtered and condensed under the reduced pressure to yield crude 2-bromo-*N*,*N*'-bis(1-hydroxy-2-methylpropn-2-yl)isophthalamide as a brown solid (8.29 g). The crude product was carried through to the next step without further purification.

To a solution of 2-bromo-*N*,*N*'-bis(1-hydroxy-2-methylpropn-2-yl)isophthalamide (8.29 g) in methanol (20 mL) was added 10% NaOH aq (25 mL) and stirred at 40 °C for 12 h. The reaction mixture was diluted with H_2O/CH_2Cl_2 and extracted with dichloromethane. The combined organic layer was dried over $MgSO_4$. filtered and evaporated to obtain the crude product. The crude product was purified by flash silica gel columnchromatography (hexane/ethyl acetate = 50:50 ~ 20:80, column length 17 cm, diameter 48 mm silica gel) and recrystallization from EtOAc/hexane to give the colorless crystal (1.58g, 4.48 mmol, 22%).

^{1}H-NMR (400MHz, $CDCl_3$) 7.63 (d, *J* = 7.7 Hz, 2H, 3-H x 2), 7.37 (t, *J* = 7.7 Hz, 1H, 4-H), 4.16 (s, 4H, 6-H_2 x 2), 1.42 (s, 12H, 7-Me x 4).; ^{13}C-NMR (100 MHz, $CDCl_3$) 161.8 (s, C-5), 132.5 (d, C-3), 132.2 (s, C-2), 126.9 (d, C-4), 121.3 (s, C-1), 79.5 (t, C-6), 68.1 (s, C-7), 28.2 (q, 7-Me).; HRMS (DART) Calculated ($C_{16}H_{20}N_2O_2Br$) 351.07027 ($[M+H]^+$) Found: 351.07088; mp: 104–106 °C; IR: (KBr) 1664, 1645 cm^{-1}

Preparation of Aluminum Complexes

{2-(4,4-dimethyl-4,5-dihydrooxazol-2-yl)phenyl}aluminum dichloride (1-$AlCl_2$)

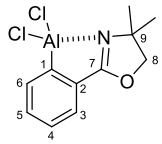

To a solution of 2-(2-bromophenyl)-4,4-dimethyl-4,5-dihydrooxazole (4.13 mmol, 1.05 g) in diethyl ether (16 mL) was added 1.6 M *n*-BuLi solution in hexane (4.4 mmol, 2.75 mL) at −78 ºC. The mixture was stirred at −78 ºC for 10 min, and then added to a solution of $AlCl_3$ (4.39 mmol, 0.586 g) in diethyl ether at −78 ºC *via* a cannula. The mixture was stirred at −78 ºC to room temperature over 12 h, and then pale brown precipitates were generated. The resulted mixture was brought into a glove box filled in dry nitrogen. The supernatant was separated by decantation, and then pale brown precipitates were extracted with ether. The supernatant solution was combined with the extraction ether. The combined solution was concentrated under reduced pressure. Chloroform was poured into the mixture to form white precipitates. The precipitates were filtered, and then the filtrate was concentrated to give crude product. The crude product was washed with cold ether and recrystallized from chloroform to give the product (colorless crystal, 0.355 g, 32%). The structure was identified by X-ray diffraction analysis.

^{1}H NMR: (400 MHz, $CDCl_3$) 7.80 (d, J = 7.3 Hz, 1H, 6-H), 7.72 (dt, J = 7.3, 1.0 Hz, 1H, 3-H), 7.59 (td, J = 7.3, 1.0 Hz, 1H, 5-H), 7.42 (td, J = 7.3, 1.0 Hz, 1H, 4-H), 4.71 (s, 2H, 8-H_2), 1.65 (s, 6H, 9-Me x 2).; ^{13}C NMR: (150 MHz, $CDCl_3$) 177.6 (s, C-7), 151.9 (br, C-1), 136.1 (d, C-6), 134.3 (d, C-5), 130.0 (s, C-2), 128.8 (d, C-4), 125.5 (d, C-3), 85.6 (t, C-8), 64.3 (s, C-9), 27.8 (q, 9-Me).

X-ray structure **1**-$AlCl_2$

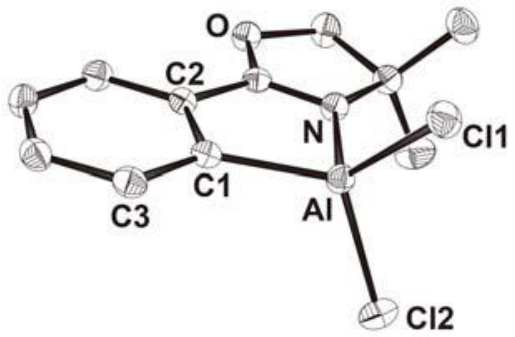

Selected bond lengths (Å) and angles (°); Al−C1 = 1.9697(15), Al−N1 = 1.9243(13), Al−Cl1 = 2.1386(6), Al–Cl2 = 2.1365(6), Al–C1–C2 = 108.00(10), Al–C1–C3 = 135.89(11), C1–Al–N1 = 87.98(6), C1–Al–Cl1 = 116.73(5), C1–Al–Cl2 = 118.73(5), Cl1–Al–Cl2 = 110.34(3)

{2,6-bis(4,4-dimethyl-4,5-dihydrooxazol-2-yl)phenyl}aluminum dichloride (2-$AlCl_2$)

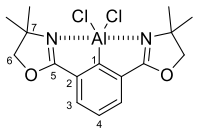

To a solution of 2,2'-(2-bromo-1,3-phenylene)bis(4,4-dimethyl-4,5-dihydrooxazole) (4.01 mmol, 1.41 g) in diethyl ether (16 mL) was added 1.6 M *n*-BuLi solution in hexane (4.4 mmol, 2.75 mL) at −78 ºC. The mixture was stirred at −78 ºC for 10 min, and then added to a solution of $AlCl_3$ (4.36 mmol, 0.582 g) in diethyl ether at −78 ºC via a cannula. The mixture was stirred at −78 ºC to room temperature over 12 h, and then pale brown precipitates were generated. The resulted mixture was brought into a glove box filled in dry nitrogen. The supernatant was separated by decantation, and then pale brown precipitates were extracted with ether. The supernatant solution was combined with the extraction ether. The combined solution was concentrated under reduced pressure. Chloroform was poured into the mixture to form white precipitates. The precipitates were filtered, and then the filtrate was concentrated to give crude product. The crude product was washed with cold ether and recrystallized from chloroform to give the product (colorless crystal, 0.252 g, 17%). The structure was identified by X-ray diffraction analysis.

^{1}H NMR (400 MHz, $CDCl_3$) 7.65 (d, J = 7.2 Hz, 2H, 3-H x 2), 7.40 (t, J = 7.2 Hz, 1H, 4-H), 4.54 (s, 4H, 6-H_2 x 2), 1.60 (s, 12H, 7-Me x 4); ^{13}C NMR (150 MHz, $CDCl_3$) 171.3 (d, C-5), 162.5 (br, C-1), 131.2 (s, C-2), 129.8 (d, C-4), 126.5 (d, C-3), 85.4 (t, C-6), 64.5 (s, C-7), 28.1 (q, 7-Me)

X-ray structure **2**-$AlCl_2$

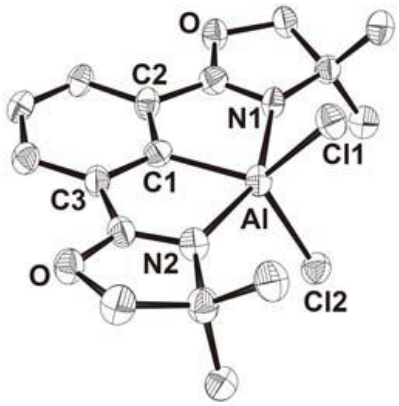

Selected bond lengths (Å) and angles(°); Al–C1 = 1.964(5), Al–N1 = 2.158(4), Al–N2 = 2.184(4), Al–Cl1 = 2.159(2), Al–Cl2 = 2.159(2), N1–Al–N2 = 155.42(16), C1–Al–Cl1 = 124.66(17), C1–Al–Cl2 = 124.72(18), Cl1–Al–Cl2 = 124.66(17).

{2-(4,4-dimethyl-4,5-dihydrooxazol-2-yl)phenyl}aluminum bisperchlorate (1-Al(ClO_4)$_2$)

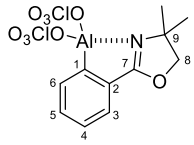

The mixture of Pheox-$AlCl_2$ (26.8 mg, 0.0985 mmol) and silver perchlorate (61.4 mg, 0.296 mmol) in chloroform was stirred vigorously for 2 h to form white precipitate. The suspension was filtered, and then the filtrate was concentrated under reduced pressure to give the product (white solid, 39.0 mg, 99%). This complex was recrystallized from chloroform and heptane. The structure was identified by X-ray diffraction analysis. This ligand exchange failed in CH_2Cl_2.

^{1}H NMR: (400 MHz, $CDCl_3$) 7.84 (d, *J* = 7.6 Hz, 1H, 6-H), 7.80 (dt, *J* = 7.6, 1.0 Hz, 1H, 3-H), 7.68 (dt, *J* = 7.6, 1.0 Hz, 1H, 5-H), 7.53 (td, *J* = 7.6, 1.2 Hz, 1H, 4-H), 4.77 (s, 2H, 8-H_2), 1.60 (s, 6H, 9-Me x 2).; ^{13}C NMR: (150 MHz, $CDCl_3$) 179.6 (s, C-7), 144.8 (br, C-1), 137.4 (d, C-6), 135.2 (d, C-5), 130.7 (s, C-2), 130.3 (d, C-4), 126.2 (d, C-3), 86.2 (t, C-8), 64.3 (s, C-9), 27.3 (q, 9-Me).

X-ray structure of **1**-Al(ClO_4)$_2$

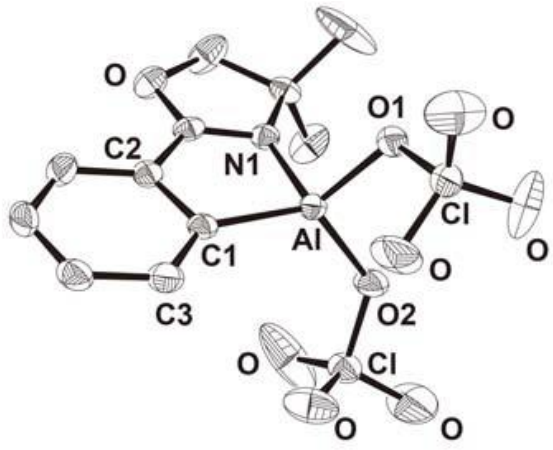

Selected bond lengths (Å) and angles (°); Al–C1 = 1.937(4), Al–N1 = 1.886(3), Al–O1 = 1.781(4), Al–O2 = 1.803(3), Al–C1–C2 = 107.2(3), Al–C1–C3 = 136.3(2), C1–Al–N1 = 89.42(13), C1–Al–O1 = 112.34(14), C1–Al–O2 = 124.04(18), O1–Al–O2 = 102.63(13)

{2,6-bis(4,4-dimethyl-4,5-dihydrooxazol-2-yl)phenyl}aluminum bisperchlorate (2-Al(ClO_4)$_2$)

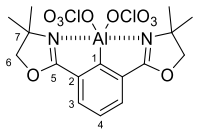

The mixture of Phebox-$AlCl_2$ (37.2 mg, 0.101 mmol) and silver perchlorate (62.2 mg, 0.300 mmol) in chloroform was stirred vigorously at room temperature for 2 h to form white precipitate. The suspension was filtered, and then the filtrate was concentrated under reduced pressure to give the product (white solid, 49.8 mg, 0.100 mmol, 99%). This ligand exchange failed in CH_2Cl_2. This complex was recrystallized from chloroform and heptane. The structure was identified by X-ray diffraction analysis.

^{1}H NMR (400 MHz, $CDCl_3$) 7.72 (d, J = 7.7 Hz, 2H, 3-H x 2), 7.48 (t, J = 7.7 Hz, 1H, 4-H), 4.66 (s, 4H, 6-H_2 x 2), 1.63 (s, 12H, 7-Me x 4); ^{13}C NMR (150 MHz, $CDCl_3$) 175.1 (s, C-5), 158.9 (br, C-1), 131.0 (d, C-4), 130.6 (s, C-2), 127.6 (d, C-3), 86.3 (t, C-6), 64.4 (s, C-7), 27.6 (q, 7-Me)

X-ray structure of **2**-Al(ClO_4)$_2$

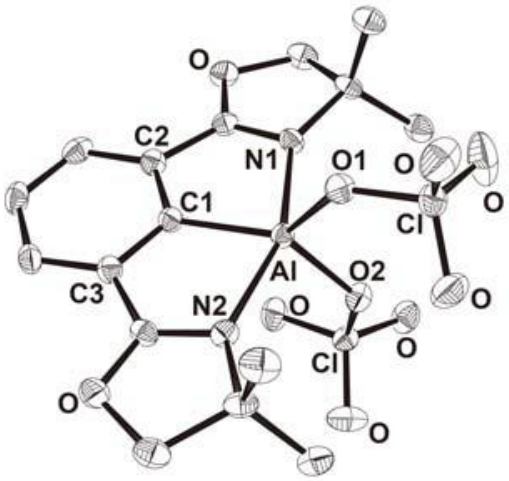

Selected bond lengths (Å) and angles(°); Al–C1 = 1.931(2), Al–N1 = 2.080(2), Al–N2 = 2.101(2), Al–O1 = 1.8231(17), Al–O2 = 1.8283(19), N1–Al–N2 = 159.83(8), C1–Al–O1 = 126.10(10), C1–Al–O2 = 132.40(9), O1–Al–O2 = 101.45(8).

{2,6-bis(4,4-dimethyl-4,5-dihydrooxazol-2-yl)phenyl}aluminum bistriflate (2-Al(OTf)$_2$)

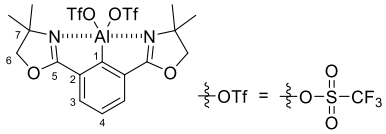

The mixture of Phebox-AlCl$_2$ (36.5 mg, 0.099 mmol) and silver triflate (60.5 mg, 0.235 mmol) in chloroform was stirred vigorously for 2 h to form white precipitate. The suspension was filtered, and then the filtrate was concentrated under reduced pressure to give the product (white solid, 37.2 mg, 0.062 mmol, 63%). This ligand exchange failed in CH_2Cl_2.

^{1}H NMR (400 MHz, $CDCl_3$)

7.74 (d, J = 7.7 Hz, 2H, 3-H x 2), 7.51 (t, J = 7.7 Hz, 1H, 4-H), 4.60 (s, 4H, 6-H$_2$ x 2), 1.58 (s, 12H, 7-Me x 4).

^{13}C NMR (150 MHz, $CDCl_3$)

174.5 (s, C-5), 157.5 (br, C-1), 131.3 (d, C-4), 131.0 (s, C-2), 127.5 (d, C-3), 118.7 (q, $^1J_{C–F}$ = 316.9 Hz, CF_3), 86.2 (t, C-6), 64.7 (s, C-7), 26.6 (q, 7-Me).

Pheox-$AlCl_2$-pyridine 3 complex (1-$AlCl_2$·3)

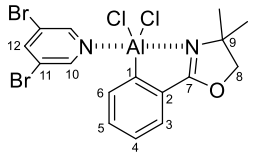

The mixture of Pheox-$AlCl_2$ (54.2 mg, 0.199 mmol) and 3,5-dibromopyridine (47.6 mg, 0.201 mmol) in $CDCl_3$ (0.5 mL) were stirred at room tempreture for 30 min to give the acid-base adduct quantitatively. This complex was recrystallized from chloroform. The structure was identified by X-ray diffraction analysis.

^{1}H-NMR: (400 MHz, $CDCl_3$) 9.06 (t, *J* = 1.9 Hz, 2H, 10-H x 2), 8.20 (t, *J* = 1.9 Hz, 1H, 12-H), 7.67 (dd, *J* = 7.4, 1.3 Hz, 1H, 3-H), 7.38-7.31 (m, 2H, 4-H, 5-H), 6.63 (d, *J* = 6.3 Hz, 1H, 6-H), 4.57 (s, 2H, 8-H_2), 1.67 (s, 6H, 9-Me x 2).; ^{13}C-NMR (100 MHz, $CDCl_3$) 173.8 (C-7), 153.4 (br, C-1), 148.6 (C-10), 143.2 (C-12), 136.1 (C-6), 132.9 (C-5), 131.7 (C-2), 128.4 (C-4), 124.8 (C-3), 120.9 (C-11), 85.0 (C-8), 65.0 (C-9), 27.7 (9-Me x 2).

X-ray structure of **1**-$AlCl_2$·**3**

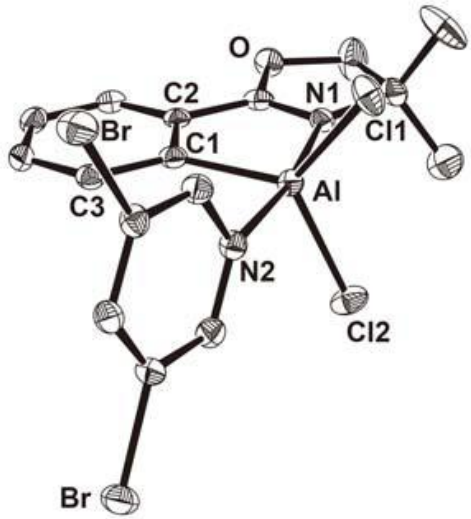

Selected bond lengths (Å) and angles (°); Al–C1 = 2.008(2), Al–N1 = 2.0602(19), Al–Cl1 = 2.1690(10), Al–Cl2 = 2.1777(9), Al–N2 = 2.1509(19), Al–C1–C2 = 111.65(16), Al–C1–C3 = 133.42(16), N1–Al–N2 = 170.70(7), C1–Al–Cl1 =123.91(7), C1–Al–Cl2 = 118.79(7), Cl1–Al–Cl2 = 117.30(4).

Phebox-Al(ClO_4)$_2$–pyridine 3 complex (2-Al(ClO_4)$_2$·3)

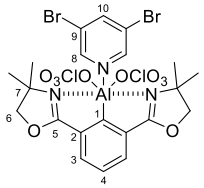

The mixture of Phebox-Al(ClO_4)$_2$ (48.7 mg, 0.098 mmol) and 3,5-dibromopyridine (23.8 mg, 0.100 mmol) in chloroform was stirred at room temperature for 30 min to give the acid-base adduct. This complex was recrystallized from chloroform and heptane. The structure was identified by X-ray diffraction analysis.

^{1}H NMR (400 MHz, $CDCl_3$); 8.57 (s, 2H, 8-H x 2), 8.07 (s, 1H, 10-H), 7.73 (d, J = 7.5 Hz, 2H, 3-H x 2), 7.47 (t, J = 7.6 Hz, 1H, 4-H), 4.62 (s, 4H, 6-H_2 x 2), 1.59 (s, 12H, 7-Me x 4).; ^{13}C NMR (100 MHz, $CDCl_3$); 174.7 (C-5), 162.69 (br, C-1), 148.9 (C-8), 142.1 (C-10), 130.7 (C-4), 130.2 (C-2), 127.5 (C-3), 121.0 (C-9), 86.0 (C-6), 64.5 (C-7), 27.5 (7-Me).

Phebox-Al(OTf)$_2$-pyridine 3 complex (2-Al(OTf)$_2$·3)

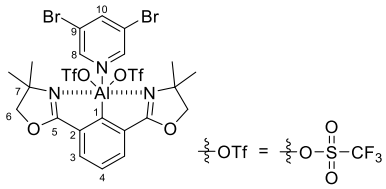

The mixture of Phebox-Al(OTf)$_2$ (96.7 mg, 0.162 mmol) and 3,5-dibromopyridine (38.6 mg, 0.163 mmol) in chloroform was stirred for 30 min to give the acid-base adduct. This complex was recrystallized from chloroform. The structure was identified by X-ray diffraction analysis.

^{1}H NMR (400 MHz, $CDCl_3$); 8.56 (d, J = 1.8 Hz, 2H, 9-H x 2), 8.12 (t, J = 1.8 Hz, 1H, 10-H), 7.74 (t, J = 7.6 Hz, 2H, 3-H x 2), 7.47 (t, J = 7.6 Hz, 1H, 4-H), 4.58 (s, 4H, 6-H_2 x 2), 1.55 (s, 12H, 7-Me x 4).; ^{13}C NMR (150 MHz, $CDCl_3$) 174.0 (C-5), 163.9 (br, C-1), 148.5 (C-8), 142.4 (C-10), 130.4 (C-4), 129.9 (C-2), 127.4 (C-3), 118.5 (q, $^1J_{C–F}$ = 317.3 Hz, CF_3), 120.8 (C-9), 85.7 (C-6), 64.6 (C-7), 26.6 (7-Me).

X-ray structure of **2**-Al(OTf)$_2$·**3**

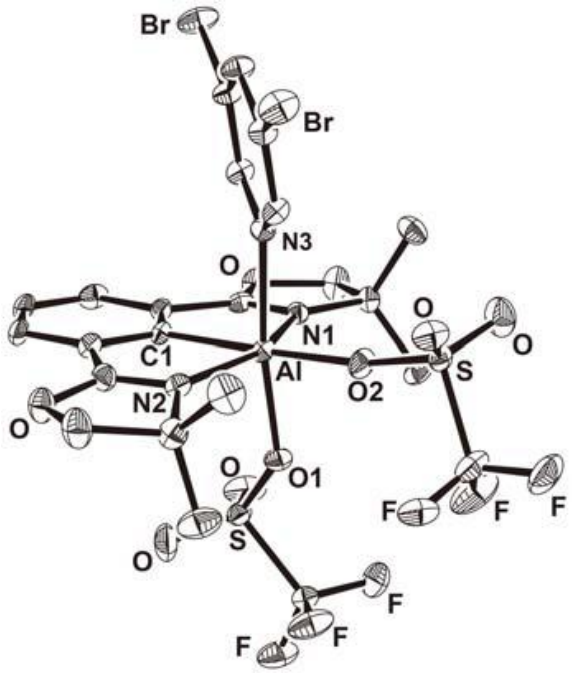

Selected bond lengths (Å) and angles (°); Al–C1 = 1.938(8), Al–N1 = 2.103(7), Al–N2 = 2.137(7), Al– N3 = 2.171(7), Al–O1 = 1.904(6), Al–O2 = 1.871(6), N3–Al–O1 = 165.6(3), C1–Al–N1 = 79.3(3), C1–Al–N2 = 78.6(3), N1–Al–O2 = 97.0(3), N2–Al–O2 = 104.7(3).

{2,6-bis(4,4-dimethyl-4,5-dihydrooxazol-2-yl)-4-methoxyphenyl}aluminum dichloride (2-MeO-$AlCl_2$)

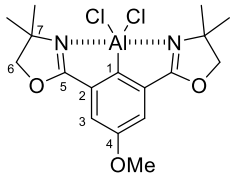

To a solution of 2,2'-(2-bromo-5-methoxy-1,3-phenylene)bis(4,4-dimethyl-4,5-dihydrooxazole) (61.2 mg, 1.60 mmol) in Et_2O (8 mL) was added 1.6 M *n*-BuLi solution in hexane (1.1 mL, 1.76 mmol, 1.1 equiv) at −78 °C and the resulted mixture were stirred at the same temperature for 10 minutes. The resulted mixture was added to a solution of $AlCl_3$ (238 mg, 1.78 mmol, 1.1 equiv) in Et_2O (8 mL) at −78 °C via cannula. The reaction mixture was stirred and allowed to warm up to room temperature over 12 h, and then pale-yellow precipitates were generated. The resulted mixture was brought into a glove box filled with dry nitrogen. The supernatant was separated by decantation, and then pale-yellow precipitates were washed with Et_2O. The combined solution was concentrated under the reduced pressure. Chloroform was poured into the resulted residue to form white precipitates. The precipitates were filtered, and the filtrate was concentrated under reduced pressure to give a crude product. The crude product was dispersed in Et_2O and then hexane was poured into the dispersion. The dispersion was stand overnight to give the product as colorless crystal (0.210 g, 0.527 mmol, 33%). The structure was identified by X-ray diffraction analysis.

^{1}H NMR (400 MHz, $CDCl_3$) 7.21 (s, 2H, 3-H x 2), 4.53 (s, 4H, 6-H_2 x 2), 3.84 (s, 3H, 4-OMe), 1.59 (s, 12H, 7-Me x 4); ^{13}CNMR (150 MHz, $CDCl_3$) 171.0 (s, C-5), 162.0 (s, C-4), 151.8 (br, C-1), 132.2 (s, C-2), 112.8 (d, C-3), 85.3 (t, C-6), 64.6 (s, C-7), 55.9 (q, 4-OMe), 28.0 (q, 7-Me).

{2,6-bis(4,4-dimethyl-4,5-dihydrooxazol-2-yl)-4-methoxyphenyl}aluminum bisperchlorate (2-MeO-$Al(ClO_4)_2$)

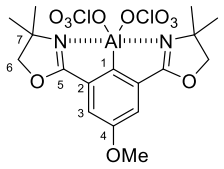

The mixture of **2**-MeO-$AlCl_2$ (20.0 mg, 0.050 mmol) and silver perchlorate (52.6 mg, 0.253 mmol) in chloroform was stirred vigorously at room temperature for 2 h to form white precipitate. The suspension was filtered, and then the filtrate was concentrated under reduced pressure to give the product (white solid, 25.6 mg, 0.0486 mmol, 97%). This complex was recrystallized from chloroform and heptane. The structure was identified by X-ray diffraction analysis.

^{1}H NMR (400 MHz, $CDCl_3$) 7.26 (s, 2H, 3-H x 2), 4.65 (s, 4H, 6-H_2 x 2), 3.86 (s, 3H, 4-OMe), 1.62 (s, 12H, 7-Me x 4); ^{13}CNMR (150 MHz, $CDCl_3$) 174.9 (s, C-5), 163.2 (s, C-4), 148.2 (br, C-1), 131.8 (s, C-2,), 114.1 (d, C-3), 86.4 (t, C-6), 64.7 (s, C-7), 56.1 (q, 4-OMe), 27.8 (q, 7-Me).

{2,6-bis(4,4-dimethyl-4,5-dihydrooxazol-2-yl)-4-chlorophenyl}aluminum dichloride (2-Cl-AlCl$_2$)

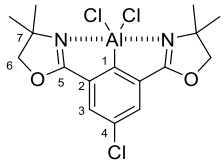

To a solution of 2,2'-(2-bromo-5-chloro-1,3-phenylene)bis(4,4-dimethyl-4,5-dihydrooxazole) (3.20 mmol, 1.23 g) in Et_2O (12 mL) was added 1.6 M *n*-BuLi solution in hexane (3.52 mmol, 2.2 mL) at −78 ºC. The mixture was stirred at −78 ºC for 10 min, and then added to a solution of $AlCl_3$ (3.51 mmol, 0.582 g) in Et_2O (12 mL) at −78 ºC via cannula. The mixture was stirred at −78 ºC to room temperature over 12 h, and then pale brown precipitates were generated. The resulted mixture was brought into a glove box filled in dry nitrogen. The supernatant was separated by decantation, and then pale brown precipitates were extracted with ether. The supernatant solution was combined with the extraction ether. The combined solution was concentrated under reduced pressure. Chloroform was poured into the mixture to form white precipitates. The precipitates were filtered, and then the filtrate was concentrated to give crude product. The crude product was washed with cold ether and recrystallized from chloroform to give the product (colorless crystal, 0.472 g, 1.17 mmol, 37%). The structure was identified by X-ray diffraction analysis.

^{1}H NMR (400 MHz, $CDCl_3$) 7.63 (s, 2H, 3-H), 4.55 (s, 4H, 6-H_2 x 2), 1.60 (s, 12H, 7-Me x 4); ^{13}CNMR (150 MHz, $CDCl_3$) 170.5 (s, C-5), 160.2 (br, C-1), 135.9 (s, C-2 or 4), 132.6 (s, C-2 or 4), 126.8 (d, C-3), 85.7 (t, C-6), 65.0 (s, C-7), 28.2 (q, 7-Me).

{2,6-bis(4,4-dimethyl-4,5-dihydrooxazol-2-yl)-4-chlorophenyl}aluminum bisperchlorate (2-Cl-Al(ClO$_4$)$_2$)

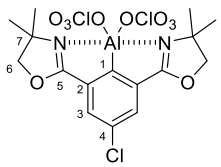

The mixture of **2**-Cl-$AlCl_2$ (40.5 mg, 0.100 mmol) and silver perchlorate (0.1050 mg, 0.506 mmol) in chloroform was stirred vigorously at room temperature for 2 h to form white precipitate. The suspension was filtered, and then the filtrate was concentrated under reduced pressure to give the product (white solid, 50.9 mg, 0.0957 mmol, 95%). This complex was recrystallized from chloroform and heptane. The structure was identified by X-ray diffraction analysis.

^{1}H NMR (400 MHz, $CDCl_3$) 7.70 (s, 2H, 4-H x 2), 4.68 (s, 4H, 6-H_2 x 2), 1.63 (s, 12H, 7-Me x 4); ^{13}CNMR (150 MHz, $CDCl_3$) 174.2 (s, C-5), 156.7 (br, C-1), 137.3 (s, C-2 or 4), 131.9 (s, C-2 or 4), 128.0 (d, C-3), 86.6 (t, C-6), 64.9 (s, C-7), 27.8 (q, 7-Me).

{2,6-bis(4,4-dimethyl-4,5-dihydrooxazol-2-yl)-4-*tert*-Butyl-phenyl}aluminum dichloride (2-^{t}Bu-$AlCl_2$)

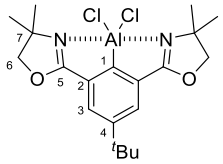

To a solution of 2,2'-(2-bromo-5-*tert*-butyl-1,3-phenylene)bis(4,4-dimethyl-4,5-dihydrooxazole) (3.20 mmol, 1.30 g) in Et_2O (12 mL) was added 1.6 M *n*-BuLi solution in hexane (3.52 mmol, 2.2 mL) at −78 ºC. The mixture was stirred at −78 ºC for 10 min, and then added to a solution of $AlCl_3$ (3.56 mmol, 0.475 g) in Et_2O (12 mL) at −78 ºC via cannula. The mixture was stirred at −78 ºC to room temperature over 12 h, and then pale brown precipitates were generated. The resulted mixture was brought into a glove box filled in dry nitrogen. The supernatant was separated by decantation, and then pale brown precipitates were extracted with ether. The supernatant solution was combined with the extraction ether. The combined solution was concentrated under reduced pressure. Chloroform was poured into the mixture to form white precipitates. The precipitates were filtered, and then the filtrate was concentrated to give crude product. The crude product was washed with cold ether and recrystallized from chloroform to give the product (white solid, 0.794 g, 1.15 mmol, 58%).

^{1}H NMR (600 MHz, $CDCl_3$) 7.71 (s, 2H, 3-H), 4.53 (s, 4H, 6-H_2 x 2), 1.59 (s, 12H, 7-Me x 4), 1.33 (s, 9H, 4-CMe_3); ^{13}CNMR (150 MHz, $CDCl_3$) 171.7 (s, C-5), 159.0 (br, C-1), 154.2 (s, C-4), 131.4 (s, C-2), 123.8 (d, C-3), 85.5 (t, C-6), 64.6 (s, C-7), 35.4 (s, 4-*C*Me_3), 31.5 (q, 4-C*Me*$_3$), 28.2 (q, 7-Me).

{2,6-bis(4,4-dimethyl-4,5-dihydrooxazol-2-yl)-4-*tert*-Butyl-phenyl}aluminum bisperchlorate (2-^{t}Bu-$Al(ClO_4)_2$)

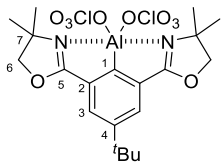

The mixture of **2**-^{t}Bu-$AlCl_2$ (42.3 mg, 0.099 mmol) and silver perchlorate (104.1 mg, 0.502 mmol) in chloroform was stirred vigorously at room temperature for 2 h to form white precipitate. The suspension was filtered, and then the filtrate was concentrated under reduced pressure to give the product (white solid, 42.3 mg, 0.0764 mmol, 77%).

^{1}H NMR (400 MHz, $CDCl_3$) 7.76 (s, 2H, 4-H), 4.65 (s, 4H, 6-H_2 x 2), 1.62 (s, 12H, 7-Me x 4), 1.35 (s, 9H, 4-CMe_3); ^{13}CNMR (150 MHz, $CDCl_3$) 175.5 (s, C-5), 155.7 (s, C-4), 155.3 (br, C-1), 130.8 (s, C-2), 125.0 (d, C-3), 86.4 (t, C-6), 64.5 (s, C-7), 35.6 (s, 4-*C*Me_3), 31.5 (q, 4-C*Me*$_3$), 27.8 (q, 7-Me x 4).

Products

All products in Mukaiyama aldol reaction (Table 3), hydroboration (Table 4), and competitive Diels-Alder reactions are known compounds (Table 5). These products are identified by following papers. Compound **7a**,[19] Compound **7b**,[20] Compound **9**,[21] Compound **14**,[22] Compound **15**,[23] Compound **16**.[24]

General procedures

Evaluation of Lewis acidity by complexation of aluminum compounds with 2,6-dimethyl-γ-pyrone (4)

The solution of an aluminum compound (0.1 mmol) and 2,6-dimethyl-γ-pyrone **4** (0.1 mmol) in CH_2Cl_2 was prepared under a nitrogen atmosphere. The solution was stirred at room temperature for 10 min, and then, infrared spectra of the aluminum compound with **4** were recorded.

Mukaiyama aldol reaction of aldehyde with silyl enolates

To a solution of an aluminum catalyst (0.025 mmol) and silyl enolate **6** (0.75 mmol) in CH_2Cl_2 (1 mL) was added *p*-tolualdehyde **5** (0.5 mmol) at room temperature. Then, the reaction mixture was stirred at room temperature for 4 h. The aqueous solution of KH_2PO_4 (1 M, 3 mL) and the aqueous solution of KF (saturated, 3 mL) were poured into the reaction mixture. The reaction mixture was extracted with CH_2Cl_2 (5 mL x 3), and the combined organic layers were dried over $MgSO_4$, filtrated, concentrated under reduced pressure. The yield of the desired product was determined by ^{1}H NMR using 1,1,2,2-tetrachloroethane as an internal standard.

Hydroboration of benzaldehyde with HBpin catalyzed by aluminum compounds

To a solution of an aluminum catalyst (0.01 mmol) and pinacol borane (HBpin) (1.1 mmol) in $CDCl_3$ (1 mL) was added benzaldehyde **8** (1 mmol) at room temperature. The reaction mixture was stirred at room temperature for 1 or 8 h. After 1,1,2,2-tetrachloroethane was added as an internal standard, a yield of product **9** was determined by ^{1}H NMR.

Substrate recognition of aluminum complexes in competitive hetero-Diels–Alder reaction

To a solution of two aldehydes (0.25 mmol each) and Danishefsky diene **12** (0.125 mmol) in CH_2Cl_2 (0.5 mL) was added a catalyst (0.025 mmol) at room temperature. Then, the reaction mixture was stirred at room temperature for 4 h. The aqueous solution of $NaHCO_3$ (saturated, 3 mL) were poured into the reaction mixture. The reaction mixture was extracted with CH_2Cl_2 (5 mL x 3), and the combined organic layers were dried over $MgSO_4$, filtrated, concentrated under reduced pressure. The yields of products were determined by ^{1}H NMR using 1,1,2,2-tetrachloroethane as an internal standard. Results are shown in Tables 6 and 7. Experiments for **1**-$AlCl_2$- and $AlCl_3$-catalyzed reactions were carried out each twice. Average values are shown in Table 5 of the manuscript.

(annotation) In the reaction using **1**-$AlCl_2$, $AlCl_3$, $InBr_3$, and $Sc(OTf)_3$ which are shown in Table 5, opened products (acyclic aldol products) were not obtained. Actually, we have experiences of observing opened products in the examinations using some other metal salt catalysts ($BF_3 \cdot OEt_2$, $ZnCl_2$, and $GaBr_3$), so we carefully analyzed reaction products in the hetero-Diels–Alder reaction. In addition, material balances between a production of cyclic compounds (**13**, **14**, and **15**) and a recovery of starting aldehydes were reasonable (Tables 6 and 7). Therefore, comparisons in Table 5 are correctly illustrated.

Table 6. Competitive hetero-Diels–Alder reaction between *p*-chlorobenzaldehyde **10** and *p*-anisaldehyde **11**.

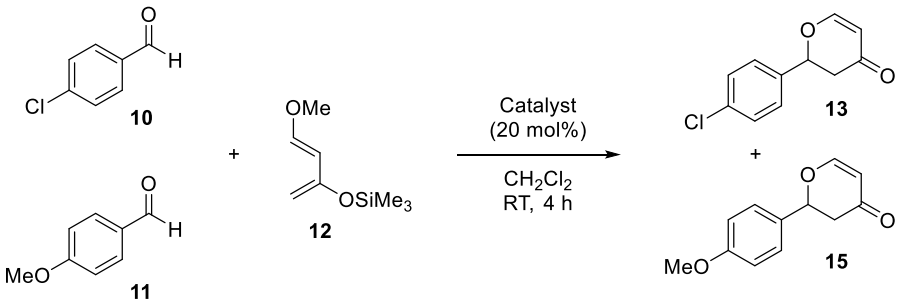

Entry	Catalyst	Yield [%]		Ratio (**13**/**15**)	Recovery [%]	
		13	**15**		**10**	**11**
1	**1**-$AlCl_2$	38	7	5.4:1	53	85
2	**1**-$AlCl_2$	39	9	4.3:1	54	93
3	$AlCl_3$	11	29	1:2.6	75	70
4	$AlCl_3$	14	31	1:2.	84	64
5	$Sc(OTf)_3$	7	21	1:3	84	64
6	$InBr_3$	0	35	–	92	56

Table 7. Competitive hetero-Diels–Alder reaction between benzaldehyde **10** and *p*-anisaldehyde **12**.

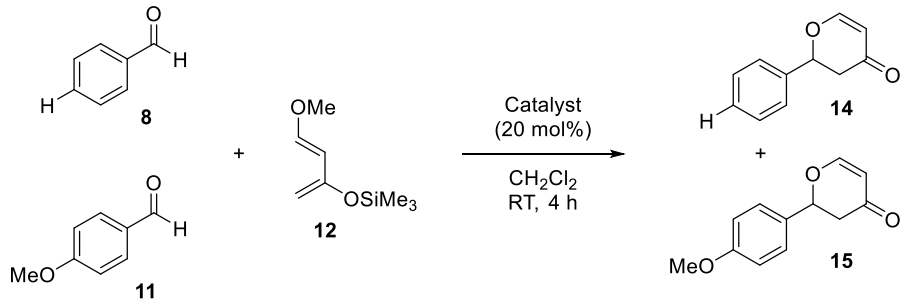

Entry	Catalyst	Yield [%]		Ratio	Recovery [%]	
		14	**15**	**(14/16)**	**8**	**11**
1	**1**-$AlCl_2$	33	11	3:1	52	95
2	**1**-$AlCl_2$	35	7	5:1	53	89
3	$AlCl_3$	17	25	1:1.5	47	70
4	$AlCl_3$	19	27	1:1.4	71	71

Explanation of inversion of the substrate-selectivity

The competitive hetero-Diels–Alder reaction between aldehydes A and B is outlined in Scheme 3, and the corresponding schematic energy diagram is illustrated in Scheme 4. The reaction rates, $v_{\mathrm{Pro}\mathbf{A}}$ and $v_{\mathrm{Pro}\mathbf{B}}$ are expressed by equations 1 and 2, respectively. Coordination/dissociation between an aldehyde and a Lewis acid (LA) is under equilibrium (equations 3 and 4), and so the concentrations [LA·**A**] and [LA·**B**] are expressed by equations 5 and 6, respectively. Equations 1 and 5 then furnish equation 7 for $v_{\mathrm{Pro}A}$, which is expressed using [**A**], [**C**], K_1, and k_2. Equation 8 for $v_{\mathrm{Pro}\mathbf{B}}$ is also established. The ratio of $v_{\mathrm{Pro}\mathbf{A}}$ to $v_{\mathrm{Pro}\mathbf{B}}$ is then expressed using [**A**], [**B**], K_1, K_3, k_2, and k_4 (equation 9).

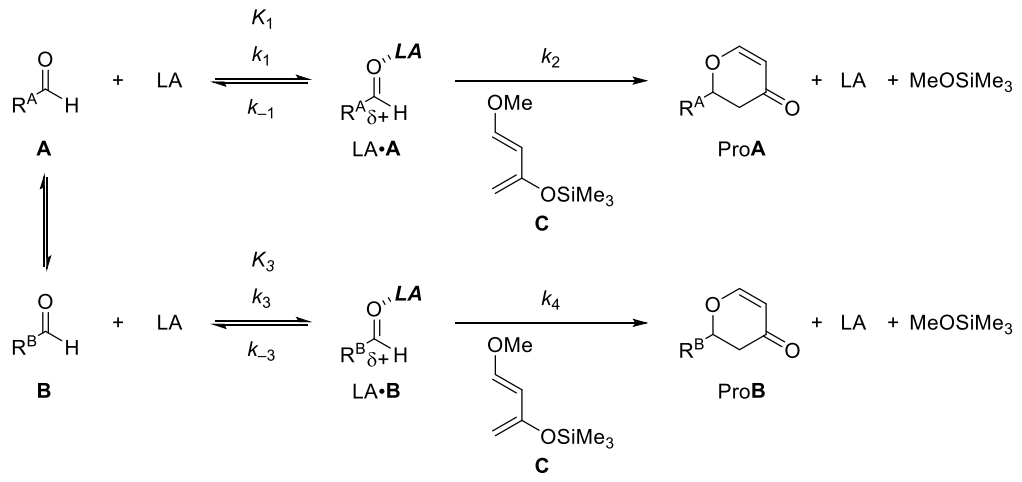

Scheme 3. The overall reaction scheme of competitive hetero-Diels–Alder reaction.

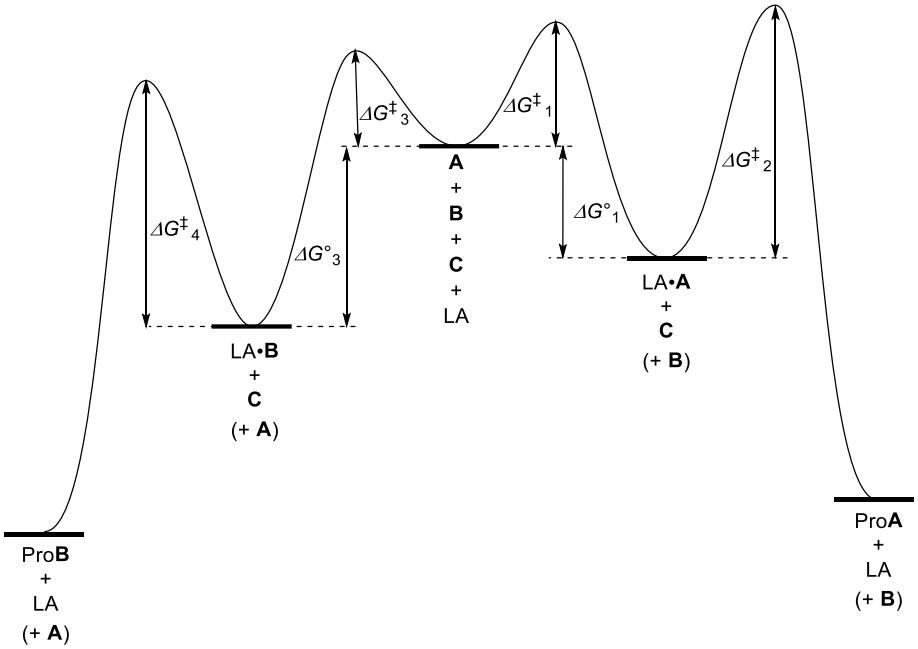

Scheme 44. The energy diagram of hetero-Diels–Alder reaction.

$$v_{\mathrm{Pro}\mathbf{A}} = \frac{d[\mathrm{Pro}\mathbf{A}]}{dt} = k_2[\mathrm{LA}\cdot\mathbf{A}][\mathbf{C}] \tag{1}$$

$$v_{\mathrm{Pro}\mathbf{B}} = \frac{d[\mathrm{Pro}\mathbf{B}]}{dt} = k_4[\mathrm{LA}\cdot\mathbf{B}][\mathbf{C}] \tag{2}$$

$$k_1[\mathbf{A}][\mathrm{LA}] = k_{-1}[\mathrm{LA}\cdot\mathbf{A}] \tag{3}$$

$$k_3[\mathbf{B}][\mathrm{LA}] = k_{-3}[\mathrm{LA}\cdot\mathbf{B}] \tag{4}$$

$$[\mathrm{LA}\cdot\mathbf{A}] = K_1[\mathbf{A}][\mathrm{LA}] \left(K_1 = k_1/k_{-1}\frac{[\mathrm{LA}\cdot\mathbf{A}]}{[\mathbf{A}][\mathrm{LA}]}\right) \tag{5}$$

$$[\mathrm{LA}\cdot\mathbf{B}] = K_3[\mathbf{B}][\mathrm{LA}] \left(K_3 = k_3/k_{-3}\frac{[\mathrm{LA}\cdot\mathbf{B}]}{[\mathbf{B}][\mathrm{LA}]}\right) \tag{6}$$

$$v_{\mathrm{Pro}\mathbf{A}} = \frac{d[\mathrm{Pro}\mathbf{A}]}{dt} = k_2[\mathrm{LA}\cdot\mathbf{A}][\mathbf{C}] = K_1k_2[\mathbf{A}][\mathrm{LA}][\mathbf{C}] \tag{7}$$

$$v_{\mathrm{Pro}\mathbf{B}} = \frac{d[\mathrm{Pro}\mathbf{B}]}{dt} = k_4[\mathrm{LA}\cdot\mathbf{B}][\mathbf{C}] = K_3k_4[\mathbf{B}][\mathrm{LA}][\mathbf{C}] \tag{8}$$

$$\frac{v_{\mathrm{Pro}\mathbf{A}}}{v_{\mathrm{Pro}\mathbf{B}}} = \frac{K_1k_2[\mathbf{A}][\mathrm{LA}][\mathbf{C}]}{K_3k_4[\mathbf{B}][\mathrm{LA}][\mathbf{C}]} = \frac{K_1k_2[\mathbf{A}]}{K_3k_4[\mathbf{B}]} \tag{9}$$

When the concentrations [**A**] and [**B**] are significantly larger than that of [LA] and the changes in concentration (d[**A**] and d[**B**]) are negligibly smaller than the initial concentrations ([**A**]$_0$ and [**B**]$_0$) in the early or middle stage of the reaction, the approximation shown below can be drawn (equations 10

and 11). Therefore, the rate ratio ($v_{\mathrm{Pro}\mathbf{A}}/v_{\mathrm{Pro}\mathbf{B}}$) can be expressed by $[\mathbf{A}]_0$, $[\mathbf{B}]_0$, K_1, K_3, k_2, and k_4 (equation 12).

$$[\mathbf{A}] = [\mathbf{A}]_0 + d[\mathbf{A}] \approx [\mathbf{A}]_0 \tag{10}$$

$$[\mathbf{B}] = [\mathbf{B}]_0 + d[\mathbf{B}] \approx [\mathbf{B}]_0 \tag{11}$$

$$\frac{v_{\mathrm{Pro}\mathbf{A}}}{v_{\mathrm{Pro}\mathbf{B}}} = \frac{K_1 k_2 [\mathbf{A}]_0}{K_3 k_4 [\mathbf{B}]_0} \tag{12}$$

Based on the experimental conditions, equation $[\mathbf{A}]_0 = [\mathbf{B}]_0$ can be established (equation 13). Therefore, the rate ratio ($v_{\mathrm{Pro}\mathbf{A}}/v_{\mathrm{Pro}\mathbf{B}}$) can be expressed using only K_1, K_3, k_2, and k_4 (equation 14).

$$[\mathbf{A}]_0 = [\mathbf{B}]_0 \tag{13}$$

$$\frac{v_{\mathrm{Pro}\mathbf{A}}}{v_{\mathrm{Pro}\mathbf{B}}} = \frac{K_1 k_2 [\mathbf{A}]_0}{K_3 k_4 [\mathbf{B}]_0} \tag{14}$$

K_1 and K_3 can be expressed by ΔG°_1 and ΔG°_3, respectively (equations 15 and 16).

$$K_1 = \exp(-\Delta G^\circ{}_1/\mathrm{RT}) \tag{15}$$

$$K_3 = \exp(-\Delta G^\circ{}_3/\mathrm{RT}) \tag{16}$$

Based on the Arrhenius equation, k_2 and k_4 are expressed as shown in equations 17 and 18, respectively. In the same type of reaction, each pre-exponential factor is comparable (equation 19).

$$k_2 = \mathrm{A}_2 \exp\left(-\Delta G_2^{\ddagger}/\mathrm{RT}\right) \tag{17}$$

$$k_4 = \mathrm{A}_4 \exp\left(-\Delta G_4^{\ddagger}/\mathrm{RT}\right) \tag{18}$$

$$\mathrm{A}^2 \approx \mathrm{A}^4 \tag{19}$$

Substitution of equations 15, 16, 17, 18, and 19 into equation 14 furnishes equation 20 for the rate ratio ($v_{\mathrm{Pro}\mathbf{A}}/v_{\mathrm{Pro}\mathbf{B}}$) which is expressed by ΔG°_1, ΔG°_3, $\Delta G^{\ddagger}_2$, and $\Delta G^{\ddagger}_4$.

$$\begin{aligned}\frac{v_{\mathrm{Pro}\mathbf{A}}}{v_{\mathrm{Pro}\mathbf{B}}} &= \frac{\exp(-\Delta G^\circ{}_1/\mathrm{RT}) \cdot \mathrm{A}^2 \exp\left(-\Delta G_2^{\ddagger}/\mathrm{RT}\right)}{\exp(-\Delta G^\circ{}_3/\mathrm{RT}) \cdot \mathrm{A}^4 \exp\left(-\Delta G_4^{\ddagger}/\mathrm{RT}\right)} \\ &= \exp\left\{\frac{\left(-\Delta G^\circ{}_1 + \Delta G^\circ{}_3 - \Delta G_2^{\ddagger} + \Delta G_4^{\ddagger}\right)}{\mathrm{RT}}\right\} \\ &= \exp\left[-\frac{\left\{(\Delta G^\circ{}_1 - \Delta G^\circ{}_3) + \left(\Delta G_2^{\ddagger} - \Delta G_4^{\ddagger}\right)\right\}}{\mathrm{RT}}\right]\end{aligned} \tag{20}$$

Therefore, the rate ratio ($v_{\mathrm{Pro}\mathbf{A}}/v_{\mathrm{Pro}\mathbf{B}}$) depends on an association/dissociation-equilibrium-factor (ΔG°_1 and ΔG°_3) and an activation Gibbs energy factor ($\Delta G^{\ddagger}_2$ and $\Delta G^{\ddagger}_4$).

The situation in which A is an electron-deficient aldehyde and B is an electron-rich aldehyde, isconsidered.

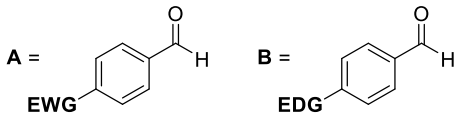

(1) In the case of a low Lewis acidity

The energy diagram for this system is illustrated in Scheme 5. As a coordination/dissociation equilibrium is established significantly faster than a cycloaddition reaction takes place due to the weak interactions between an aldehyde and a weak Lewis acid, the following inequality (equation 21) and the approximation given in equation 22 can be established.

$$\Delta G^{\circ}{}_1, \Delta G^{\circ}{}_3 \ll \Delta G_2^{\ddagger}, \Delta G_4^{\ddagger} \tag{21}$$

$$(\Delta G^{\circ}{}_1 - \Delta G^{\circ}{}_3) + \left(\Delta G_2^{\ddagger} - \Delta G_4^{\ddagger}\right) \approx \Delta G_2^{\ddagger} - \Delta G_4^{\ddagger} \tag{22}$$

Therefore, the rate ratio ($v_{\mathrm{Pro}\mathbf{A}}/v_{\mathrm{Pro}\mathbf{B}}$) depends on an activation Gibbs energy ($\Delta G^{\ddagger}{}_2$ and $\Delta G^{\ddagger}{}_4$) (equation 23).

$$\frac{v_{\mathrm{Pro}\mathbf{A}}}{v_{\mathrm{Pro}\mathbf{B}}} = \exp\left[\frac{-\left(\Delta G_2^{\ddagger} - \Delta G_4^{\ddagger}\right)}{\mathrm{RT}}\right] \tag{23}$$

Thus, the electron-deficient aldehyde **A** undergoes the cycloaddition reaction with diene **C** in preference to electron-rich aldehyde **B** because of higher electrophilicity of **A** compared to **B**, and so the inequality outlined in equation 24 is established. Therefore, the rate ratio ($v_{\mathrm{Pro}\mathbf{A}}/v_{\mathrm{Pro}\mathbf{B}}$) is >1 (equation 25), and equation 26, which indicates that the product ratio (**A**/**B**) is >1, is deduced.

$$\Delta G_2^{\ddagger} < \Delta G_4^{\ddagger} \tag{24}$$

$$\frac{v_{\mathrm{Pro}\mathbf{A}}}{v_{\mathrm{Pro}\mathbf{B}}} > 1 \tag{25}$$

$$\mathrm{ratio}(\mathbf{A}/\mathbf{B}) > 1 \tag{26}$$

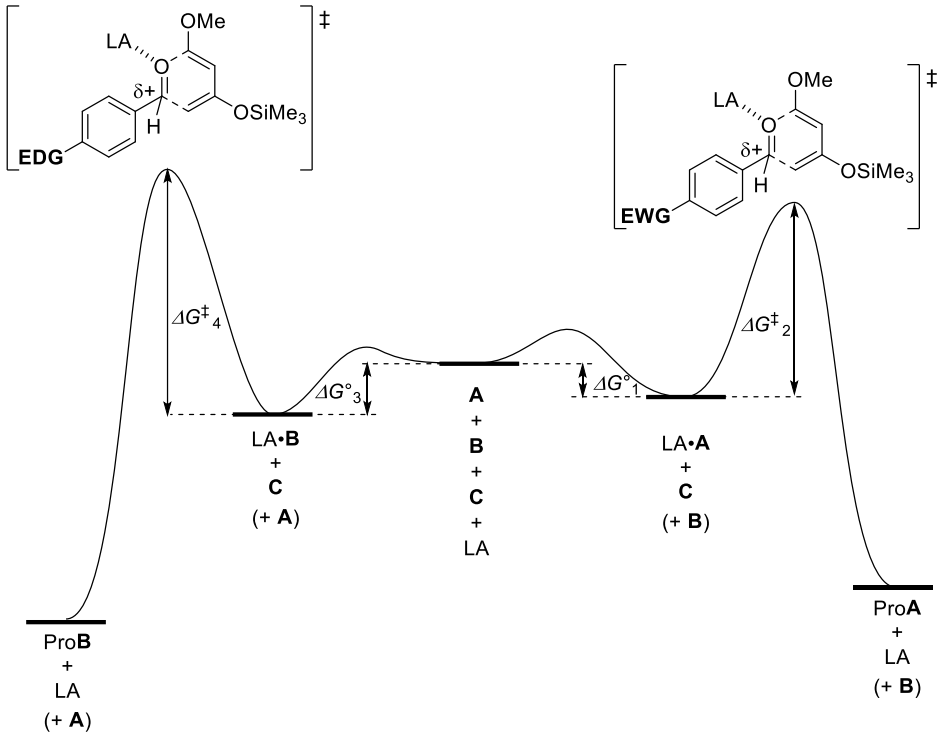

Scheme 5. The energy diagram in the case of a high Lewis acidity.

(2) In the case of a high Lewis acidity

In the case of a high Lewis acidity, there is no equilibrium in the coordination/dissociation between an aldehyde and a Lewis acid, because the aldehyde strongly coordinates to a strong Lewis acid. The overall reaction scheme and the corresponding energy diagram for this system are illustrated in Schemes 6 and 7, respectively.

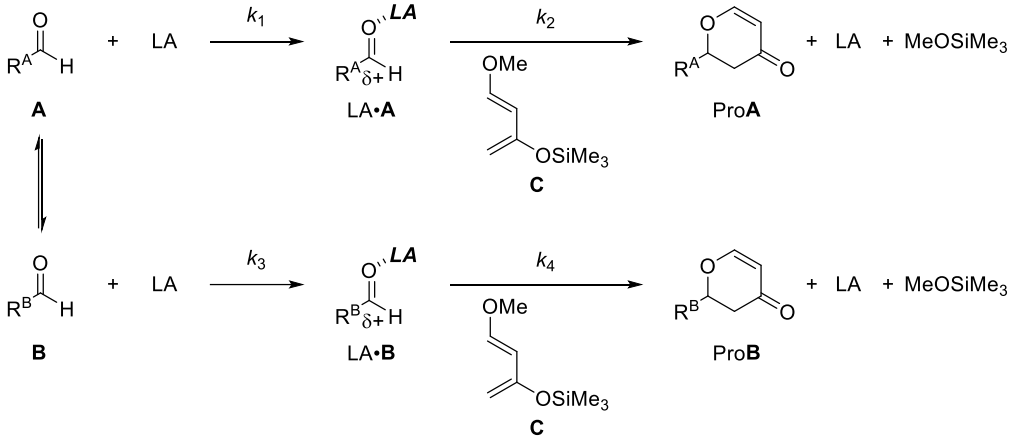

Scheme 65. The overall reaction scheme in the case of a high Lewis acidity.

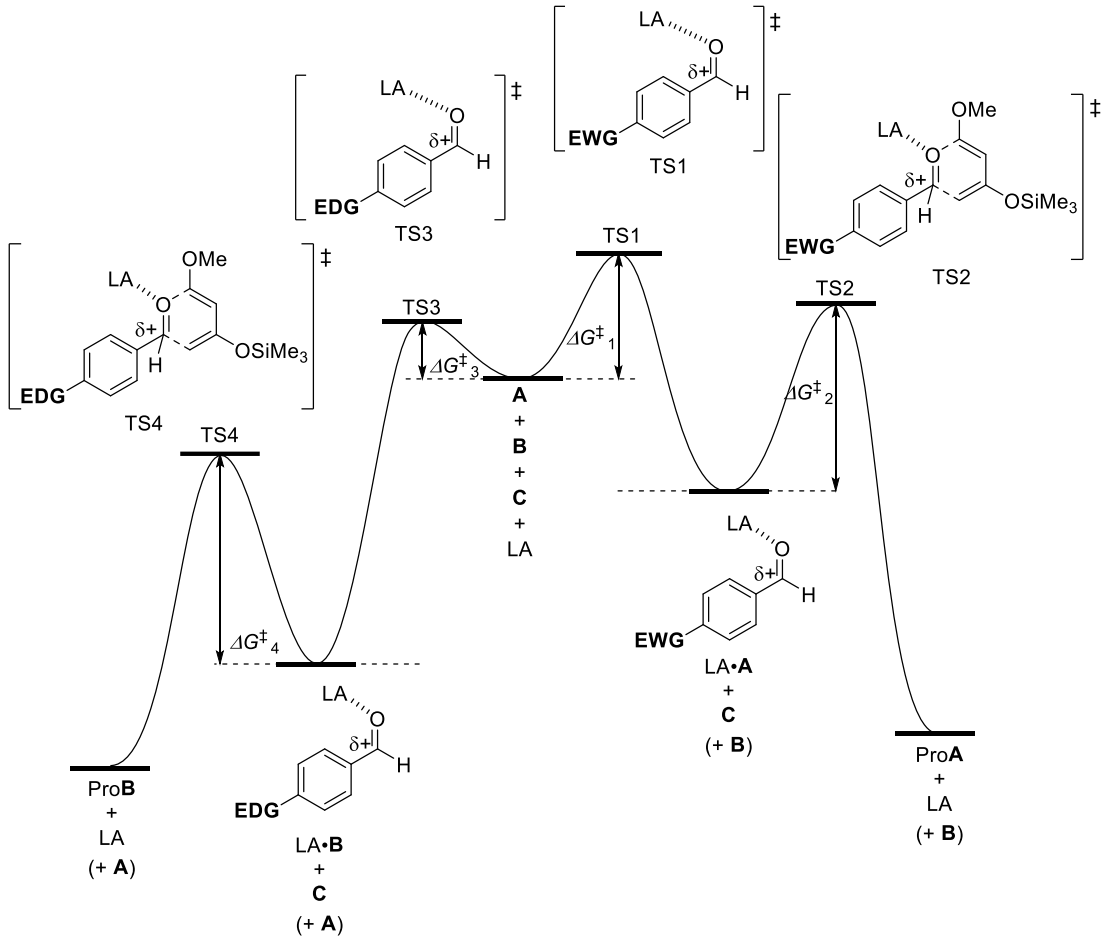

Scheme 76. The energy diagram in the case of a high Lewis acidity.

Equations 27–30 are then established, and so equations 12 and 20 are converted to give equation 31. Therefore, the rate ratio ($v_{\mathrm{ProA}}/v_{\mathrm{ProB}}$) can be expressed using $\Delta G^{\ddagger}_1$, $\Delta G^{\ddagger}_2$, $\Delta G^{\ddagger}_3$, and $\Delta G^{\ddagger}_4$. Therefore, the rate ratio ($v_{\mathrm{ProA}}/v_{\mathrm{ProB}}$) depends on activation Gibbs energy factors for the coordination of aldehydes to a Lewis acid ($\Delta G^{\ddagger}_1$ and $\Delta G^{\ddagger}_3$) and the addition reaction of diene **C** with aldehydes ($\Delta G^{\ddagger}_2$, and $\Delta G^{\ddagger}_4$).

$$[\mathrm{LA}\cdot\mathbf{A}] = k_1[\mathbf{A}][\mathrm{LA}] \tag{27}$$

$$[\mathrm{LA}\cdot\mathbf{B}] = k_3[\mathbf{B}][\mathrm{LA}] \tag{28}$$

$$k_2 = \mathrm{A}_2 \exp\left(-\Delta G_2^{\ddagger}/\mathrm{RT}\right) \tag{29}$$

$$k_4 = \mathrm{A}_4 \exp\left(-\Delta G_4^{\ddagger}/\mathrm{RT}\right) \tag{30}$$

$$\frac{v_{\mathrm{ProA}}}{v_{\mathrm{ProB}}} = \frac{k_1 k_2 [\mathbf{A}]_0}{k_3 k_4 [\mathbf{B}]_0} = \exp\left[-\frac{\left\{(\Delta G^{\circ}{}_1 - \Delta G^{\circ}{}_3) + \left(\Delta G_2^{\ddagger} - \Delta G_4^{\ddagger}\right)\right\}}{\mathrm{RT}}\right] \tag{31}$$

In addition, we note that a larger positive charge on a carbonyl carbon in a transition state during the addition step results in a smaller activation energy, i.e., $\Delta G^{\ddagger}_2$, and $\Delta G^{\ddagger}_4$ (Figure 1). The Lewis acidity of a Lewis acid (LA) and the electron-withdrawing ability of a substituent (R) are the main factors responsible for increasing the positive charge. When the Lewis acidity is particularly strong, the effect

of the substituent (R) becomes relatively small, and so an increase in the positive charge depends only on the Lewis acidity. In other words, the activation energy of an addition reaction accelerated by a strong Lewis acid becomes almost the same value regardless of the substituents (R) present. Therefore, approximation (32) is possible, and the rate ratio ($v_{\mathrm{Pro}\mathbf{A}}/v_{\mathrm{Pro}\mathbf{B}}$) can be expressed using $\Delta G^{\ddagger}_1$ and $\Delta G^{\ddagger}_3$ (equation 33).

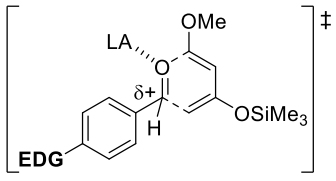

Figure 5.

$$\Delta G_2^{\ddagger} \approx \Delta G_4^{\ddagger}, \Delta G_2^{\ddagger} - \Delta G_4^{\ddagger} \approx 0 \tag{32}$$

$$\frac{v_{\mathrm{Pro}\mathbf{A}}}{v_{\mathrm{Pro}\mathbf{B}}} = \exp\left[-\frac{\left(\Delta G_1^{\ddagger} - \Delta G_3^{\ddagger}\right)}{\mathrm{RT}}\right] \tag{33}$$

Finally, electron-rich aldehyde **B** coordinates to a Lewis acid faster than electron-deficient aldehyde **A**, meaning that $\Delta G^{\ddagger}_3$ is smaller than $\Delta G^{\ddagger}_1$ (equation 34). Therefore, the rate ratio ($v_{\mathrm{Pro}\mathbf{A}}/v_{\mathrm{Pro}\mathbf{B}}$) is <1 (equation 35), and the product ratio (**A**/**B**) is also <1 (equation 36).

$$\Delta G_1^{\ddagger} > \Delta G_3^{\ddagger} \tag{34}$$

$$\frac{v_{\mathrm{Pro}\mathbf{A}}}{v_{\mathrm{Pro}\mathbf{B}}} < 1 \tag{35}$$

$$\mathrm{ratio}(\mathbf{A}/\mathbf{B}) < 1 \tag{36}$$

2-5. References

[1] a) “Aluminum-Based Catalysis”: Mark R. Mason, in *Encyclopedia of Inorganic and Bioinorganic Chemistry*, Wiley, Chichester, **2015**; b) P. Knochel, G. A. Molander, *Comprehensive Organic Synthesis*, 2nd ed., Elsevier, Amsterdam, **2014**; c) S. Aldridge, A. J. Downs, *The Group 13 Metals Aluminium, Gallium, Indium and Thallium: Chemical Patterns and Peculiarities*, Wiley, Chichester, **2008**.

[2] a) T. Taguchi, H. Yanai in *Acid Catalysis in Modern Organic Synthesis, Vol. 1* (Eds.: H. Yamamoto, K. Ishihara), Wiley-VCH, Weinheim, **2008**, pp. 241–331; b) T. Ooi, K. Maruoka in *Lewis Acids in Organic Synthesis* (Ed.: H. Yamamoto), Wiley-VCH, Weinheim, **2000**, pp. 191–282; c) W. D. Wulff in *Lewis Acids in Organic Synthesis* (Ed.: H. Yamamoto), Wiley-VCH, Weinheim, **2000**, pp. 283–354.

[3] Some aluminum complexes with a functionalized hydrocarbyl ligand were used as co-catalysts for polymerization reactions; a) A. Eisenhardt, B. Heuer, W. Kaminsky, K. Kçhler, H. Schumann, *Adv. Synth. Catal.* **2003**, *345*, 1299; b) H. Schumann, S. Dechert, S. Schutte, J.-Y. Hyeon, M. Hummert, B. C. Wassermann, *Organometallics* **2003**, *22*, 1391.

[4] Many frustrated Lewis pairs based on organoaluminum Lewis acids have been reported, but they have not been used as catalysts in catalytic reactions. Reviews: a) D. W. Stephan, G. Erker, *Angew. Chem. Int. Ed.* **2015**, *54*, 6400; *Angew. Chem.* 2015, *127*, 6498; b) D. W. Stephan, G. Erker, *Science* **2016**, *354*, aaf7229; c) W. Uhl, E.-U. Wurthwein in *Frustrated Lewis Pairs II* (Eds.: G. Erker, D. W. Stephan), Springer, Heidelberg, **2013**, pp. 101–119. d) Selected recent papers: M. Lange, J. C. Tendyck, P. Wegener, A. Hepp, E.-U. Werthwein, W. Uhl, *Chem. Eur. J.* **2018**, *24*, 12856; e) S. Chen, B. Li, X. Wang, Y. Huang, J. Li, H. Zhu, L. Zhao, G. Frenking, H. W. Roesky, *Chem. Eur. J.* **2017**, *23*, 13633; f) K. Martinewski, T. Holtrichter-Rçßmann, C. Rçsener, A. Hepp, E.-U. Werthwein, W. Uhl, *Chem. Eur. J.* **2017**, *23*, 6129.

[5] A recent review of organoaluminum complexes: L. Micouin, I. Marek, Z. Rappoport, *The Chemistry of Organoaluminum Compounds*, Wiley, Chichester, **2017**.

[6] Application of aluminum complexes with a functionalized hydrocarbyl ligand to catalytic reactions: a) C. Appelt, J. C. Slootweg, K. Lammertsma, W. Uhl, *Angew. Chem. Int. Ed.* **2012**, *51*, 5911; *Angew. Chem.* **2012**, *124*, 6013; b) C. Appelt, J. C. Slootweg, K. Lammertsma, W. Uhl, *Angew. Chem. Int. Ed.* **2013**, *52*, 4256; *Angew. Chem.* **2013**, *125*, 4350.

[7] Z. Liu, R. Ganguly, D. Vidović, *Dalton Trans.* **2017**, *46*, 753.

[8] Phebox–metal complexes: A pioneering work, a) Y. Motoyama, H. Narusawa, H. Nishiyama, *Chem. Commun.* **1999**, 131; A review: b) H. Nishiyama, *Chem. Soc. Rev.* **2007**, *36*, 1133.

[9] Pheox–metal complexes: A pioneering work, a) A. Abu-Elfotoh, K. Phomkeona, K. Shibatomi, S. Iwasa, *Angew. Chem. Int. Ed.* **2010**, *49*, 8439; *Angew. Chem.* 2010, 122, 8617; b) A review: S. Chanthamath, S. Iwasa, *Acc. Chem. Res.* **2016**, *49*, 2080.

[10] Crude yields of **1**-$AlCl_2$ and **2**-$AlCl_2$ were ca. 60–80 %. However, recrystallization to remove unreacted $AlCl_3$ reduced isolated yields.

[11] The downfield shift for protons in the oxazoline moieties of **1**-$AlCl_2$ and **2**-$AlCl_2$ in the ^1H NMR spectrum suggest that the oxazoline moieties coordinate to an Al center in the solution state as in the solid state.

[12] The average value was calculated by the Cambridge Structural Database System.

[13] We established a method for evaluation of the Lewis acidity using the Δν(C=O) value of 2,6-dimethyl-g-pyrone **4** in the complexation between a Lewis acid and **4**. A. Konishi, R. Yasunaga, K. Chiba, M. Yasuda, *Chem. Commun.* **2016**, *52*, 3348.

[14] Commercially available $Al(ClO_4)_3 \cdot 9H_2O$ was used

[15] The p*K*a value of the conjugate acid of a counter anion: $HClO_4 \approx HOTf > HCl$. A. Trummal, L. Lipping, I. Kaljurand, I. A. Koppel, I. Leito, *J. Phys. Chem. A* **2016**, *120*, 3663. H. Mayr, B. Kempf, A. R. Ofial, *Acc. Chem. Res.* **2003**, *36*, 66.

[16] Recent reports for the Al-catalyzed hydroboration of carbonyl compounds: a) Y. Liu, X. Ma, Y. Ding, Z. Yang, H. W. Roesky, *Organometallics* **2018**, *37*, 3839; b) A. Bismuto, M. J. Cowley, S. P. Thomas, *ACS Catal.* **2018**, *8*, 2001; c) L. E. Lemmerz, R. McLellan, N. R. Judge, A. R. Kennedy, S. A. Orr, M. Uzelac, E. Hevia, S. D. Robertson, J. Okuda, R. E. Mulvey, *Chem. Eur. J.* **2018**, *24*, 9940.

[17] The involvement of Me_3SiOTf and Me_3SiClO_4, which could be generated in situ, in the reaction mechanism cannot be avoided at this stage. a) T. K. Hollis, B. Bosnich, *J. Am. Chem. Soc.* **1995**, *117*, 4570; b) S. Lin, G. V. Bondar, C. J. Levy, S. Collins, *J. Org. Chem.* **1998**, *63*, 1885.

[18] X. Tanga, D. Zhanga, S. Jiea, W.-H. Suna, J. Chen, *J. Organomet. Chem.* **2005**, *690*, 3918.

[19] S. Matsukawa, K. Fukazawa, J. Kimura, *RSC Adv.* **2014**, *4*, 27780.

[20] G. Onodera, T. Toeda, N. Toda, D. Shibagishi, R. Takeuchi, *Tetrahedron* **2010**, *66*, 9021.

[21] S. Chen, D. Yan, M. Xue, Y. Hong, Y. Yao, Q. Shen, *Org. Lett.* **2017**, *19*, 3382.

[22] L. Fang, M. Li, W.-B. Lin, C.-F. Chen, *Tetrahedron* **2018**, *74*, 7164.

[23] H. J. Edwards, S. Goggins, C. G. Frost, *Molecules* **2015**, *20*, 6153.

[24] W. Chaładaj, R. Kowalczyk, J. Jurczak, *J. Org. Chem.* **2010**, *75*, 1740.

Chapter 3. Phebox–Al Catalyzed Hydrodebromination Reaction under Visible Light Irradiation: Ligand-to-Ligand Charge Transfer through Aluminum Center

3-1. Introduction

Visible-light photocatalysis has played a vital role in organic chemical reactions to achieve different molecular transformations from thermal reactions.[1] Thus, various organic dyes and transition-metal complexes have been developed as photocatalysts (PCs). Single electron transfer (SET) between substrates and PCs to generate reactive intermediates is one of the most important events, and the two kinds of SET process are generally considered (Scheme 1A). One is SET between substrates and an excited photocatalyst (PC*) generated by visible-light irradiation. In another process, reduction or oxidation of PC* by quenching-agents generates PC radical anion or cation, respectively, to cause SET with substrates. The SET efficiency suffers from diffusion-controlled collision process because these processes are outer sphere electron transfer. And, the substrate-recognition by PCs is a challenging issue due to the dependence on difference in the redox potentials. In that kind of background, installing a substrate binding site into PCs could provide the good solution to these issues. Thus, we focused on the Lewis acidic metal moiety not only to work as a binding site for various types of Lewis basic functional groups and to improve the SET efficiency by proximity effect but also to influence on redox potential of substrates.[2] Electron transfer between a chromophore and a substrate on the same metal center is recognized ligand-to-ligand charge transfer (LLCT) (Scheme 1B). Light-induced LLCT has been reported for various types of main-group metal complexes in contrast to the fact that MLCT or LMCT (metal-to-ligand or ligand-to-metal charge transfer), in which d-orbital electrons are involved, in prior to LLCT often causes in transition metal complexes. For example, the emission mechanism of tris(8-hydroxyquinoline) aluminum (Alq3), which is one of the most famous organic electro-luminescence materials[3], involves LLCT between quinolone ligands[4]. Hashmi reported that the adducts of $B(C_6F_5)_3$ with tolane derivatives bearing a formyl group exhibited aggregation-induced luminescence due to LLCT from HOMO on the tolane moiety to LUMO localized on C_6F_5 group.[5] In contrast to the application to luminescent materials, utilization as a photocatalyst were underdeveloped. König reported Flavin–zinc(II)–cyclen complex[6] to work as a sensitizer for the photo-oxidation of 4-methoxybenzyl alcohol to the corresponding aldehyde, in which the Lewis acidic zinc center captured the alcohol molecule to accelerate intramolecular electron transfer to the excited Flavin (Scheme 1C). Recently, Ooi reported LLCT in Lewis adducts between $B(C_6F_5)_3$ and aniline derivatives mediated the generation of the corresponding α-aminoalkyl radicals and their additions to enones.[7] In this study, we discovered the photocatalytic ability of 2,6-bis(oxazolinyl)phenylaluminum (Phebox-Al) complexes, which we previously reported as tunable Lewis acids,[8] for hydrodebromination of aryl bromides under visible-light irradiation. The Lewis acidic aluminum center acts as a binding site to aryl bromides and the Phebox ligand is a chromophore

to undergo LLCT with the captured aryl bromides. The present photocatalysis achieved the substrate-recognition via Lewis acid–Lewis base interaction without relying on the difference in the reduction potential of substrates in contrast to the previous LLCT catalysis.

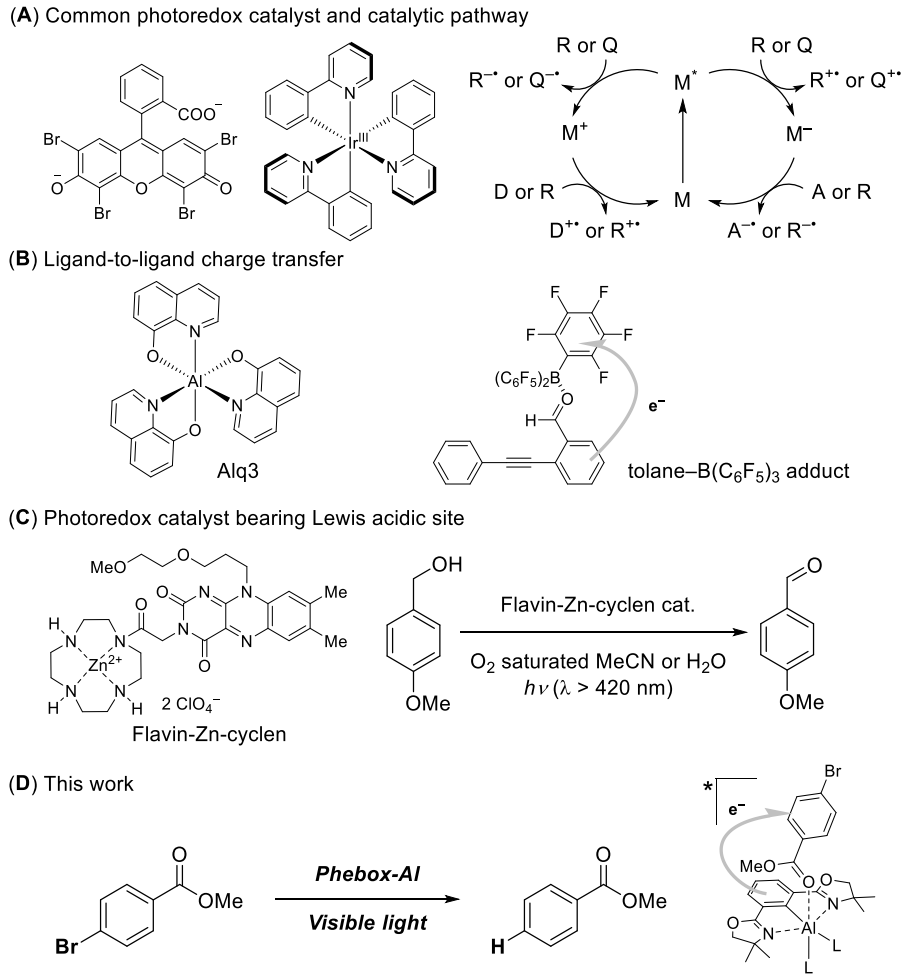

Scheme 1. Photoredox catalysis

Our group has studied on the syntheses and properties of 2-oxazolinylphenylaluminum (Pheox–Al) and 2,6-bis(oxazolinyl)phenylaluminum (Phebox–Al) complexes, and discovered the tunable Lewis acidic properties and its application to Lewis acid catalysts in organic reactions. During this research, we noticed that Phebox–Al$(ClO_4)_2$ in the solution exhibited a weak violet emission to visually confirm under a black light irradiation, which motivated us to investigate photochemical properties of Phebox–Al and Pheox–Al complexes.

3-2. Results and Discussions

Hydrodebromination reaction of methyl 4-bromobenzoate **5a** was carried out with *N*,*N*-diisopropyl ethylamine as a sacrificial reductant and a hydrogen donor under 405 nm LED irradiation. The reduction of the substrate **5a** proceeded in 26% yield in the absence of a catalyst (Entry 1).

Complex **1**-Al$(ClO_4)_2$ without a substituent at the *para*-position in the Phebox ligand showed a small effect to promote the hydrodebromination (Entry 2), whereas the introduction of *tert*-butyl, chloro, or methoxy groups at the *para*-position significantly increased the yield of **6a** (Entries 3–5). The hydrodebromination did not proceed without photoirradiation (Entry 6). On the other hand, no catalytic effect was observed for the inorganic aluminum perchlorate salt (Entry 7). This indicates that the aluminum complex worked not only as a Lewis acid, but also as a photoredox catalyst.

Table 14. Hydrodebromination of **5a** under visible light irradiation.[a]

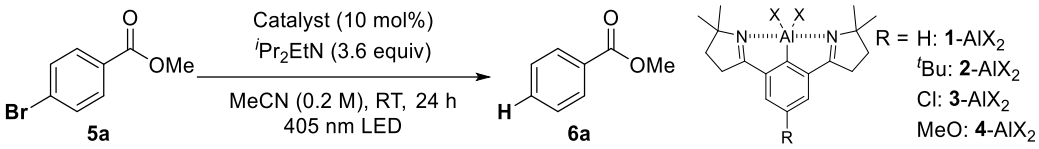

Entry	Catalyst	Yield[b] of **5a** [%]	Recovery[b] of **6a** [%]
1	None	26	48
2	**1**-Al$(ClO_4)_2$	38	31
3	**2**-Al$(ClO_4)_2$	51	20
4	**3**-Al$(ClO_4)_2$	54	10
5	**4**-Al$(ClO_4)_2$	56	16
6[c]	**4**-Al$(ClO_4)_2$	0	70
7	Al$(ClO_4)_3 \cdot 9H_2O$	25	42

[a] Standard conditions: **5a** (0.20 mmol), ^{i}Pr$_2$EtN (0.64 mmol), catalyst (0.02 mmol), RT, 24 h, 405 nm LED irradiation. [b] Yields and recoveries were determined by GC analysis using hexadecane as an internal standard. [c] In dark conditions.

Substrate scopes of hydrodebromination of aryl bromides bearing Lewis basic moieties were demonstrated using **4**-Al$(ClO_4)_2$ as a catalyst (Scheme 2). In the case of benzoic acid ester derivatives, *para*- or *ortho*-brominated compounds were efficiently reduced (**5b** and **5c**). In contrast, hydrodebromination of *meta*-brominated aryl esters **5d** and **5e** were not efficient to give the product in lower yield. Instead of benzoic acid ester derivatives, 4-bromobenzamides **5f** and **5g** were reduced to give the corresponding reduced products in moderate yields. 4-Bromopivalophenone **5h** and 4-bromobenzonitrile **5i** were also applicable to give the products in high yields. Benzyl 2-bromoacetate **5j** afforded the corresponding product.

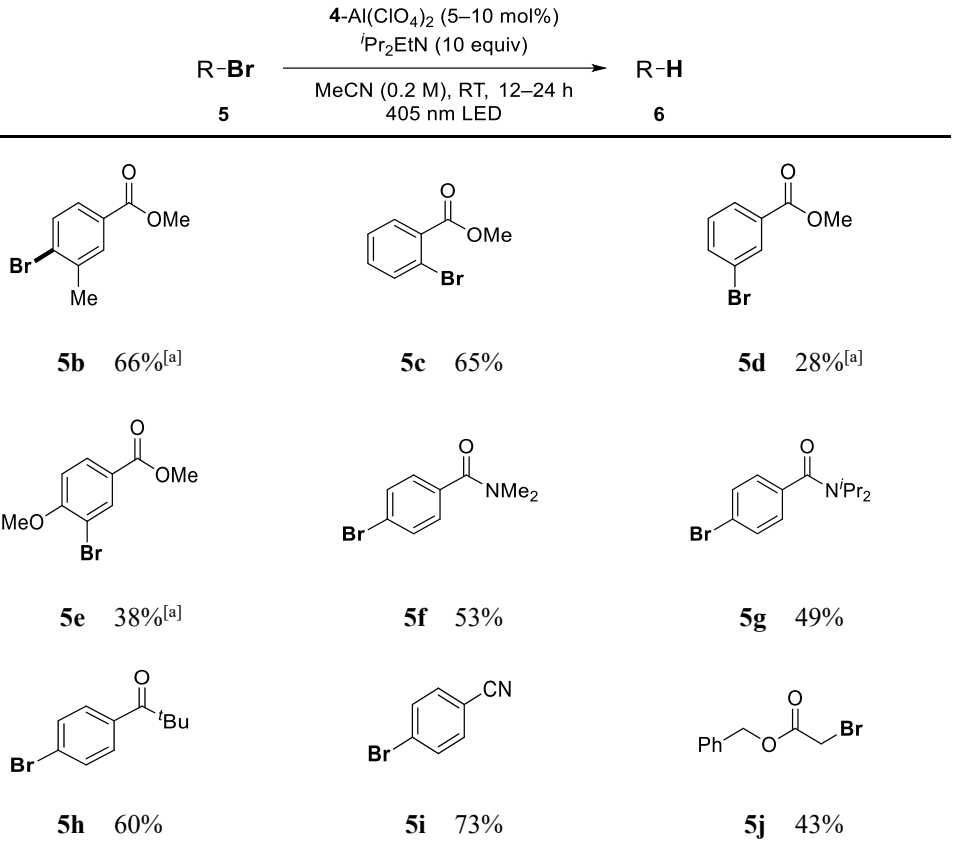

Scheme 27. Scope of aryl or alkyl bromides. Reaction conditions. **5** (0.2 mmol), $^{i}Pr_2EtN$ (2.0 mmol), **4**-$Al(ClO_4)_2$ (0.01 mmol), MeCN (1.0 mL), 12 h. Yields were determined by GC analysis using hexadecane as internal standard. [a] 24 h.

UV/vis absorption spectra of the solution of Phebox–Al complexes **1**-, **3**-, and **4**-$Al(ClO_4)_2$ in dichloromethane are shown in Figure 1A. These complexes have absorption bands in the ultraviolet region and the substituents on Phebox ligand changes the absorption band. **1**-$Al(ClO_4)_2$ has the longest absorption wavelength at 300 nm. TD-DFT calculation of **4**-$Al(ClO_4)_2$ revealed the longest absorption is corresponding to the π–π* transition based on π- and π*-orbitals are delocalized on the benzene ring (Figure 1B).

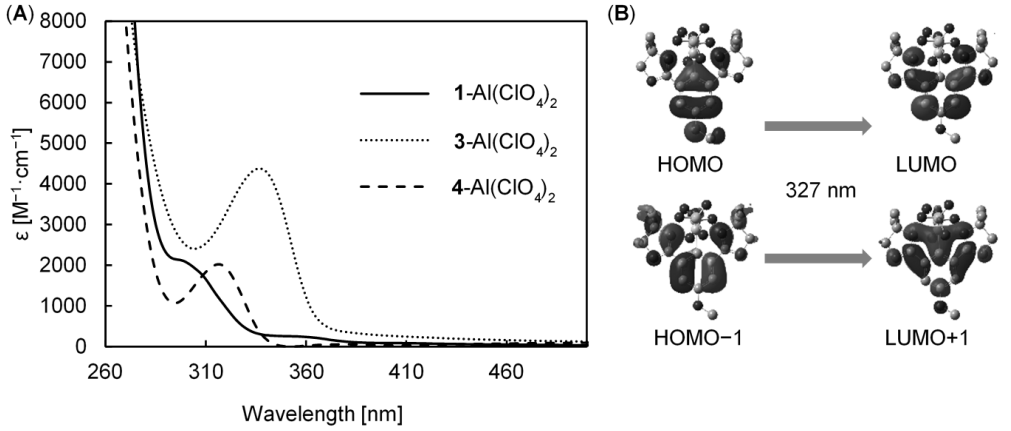

Figure 1. A) UV/vis absorption spectra of Phebox–$Al(ClO_4)_2$. B) Calculated S1 transition of **4**-$Al(ClO_4)_2$.

The addition of an equimolar amount of methyl benzoate **6a** to the solution of **1**-$Al(ClO_4)_2$ in dichloromethane led to a new absorption band around 350 nm while the absorption band around 300 nm remains (Figure 2A). A DFT calculation (B3LYP/6-31G+(d,p) level of theory) was carried out for Lewis acid–base adduct **1**-$Al(ClO_4)_2$–**6a** (Figure 2B). The HOMO of **1**-$Al(ClO_4)_2$–**6a** is mainly localized on the benzene ring of a Phebox ligand. On the other hand, the LUMO is localized on the benzene ring of the methyl benzoate. Based on a TD-DFT calculation at the same level of theory, the S1 of **1**-$Al^+(ClO_4)\cdot$**6a** has an intramolecular charge transfer character from the Phebox ligand moiety into the methyl benzoate moiety. The longest absorption wavelength of **1**-$Al(ClO_4)_2$ with an equivalent of **6a** observed by UV/vis absorption spectroscopy is consistent with the calculated S1 transition.

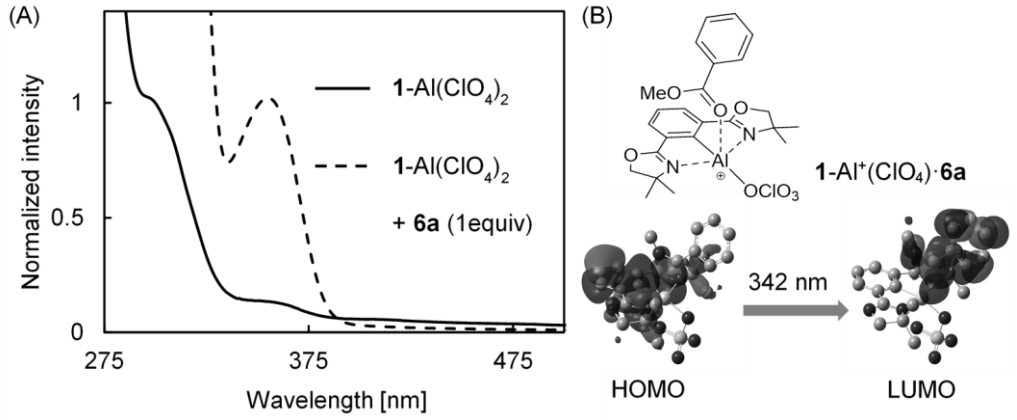

Figure 2. A) UV/vis absorption spectra B) TD-DFT calculation of **1**-$Al^+(ClO_4)\cdot$**6a**.

According to the results of UV/vis absorption spectra and TD-DFT calculations, plausible mechanism is shown in Scheme 3. Aryl bromide **5a** coordinates to aluminum center to form Lewis acid–base pair **1**–**5a**. Photoirradiation to **1**–**5a** causes single electron transfer from Phebox ligand to aryl bromide moiety to generate charge-separated complex $\mathbf{1}^{\cdot+}$–$\mathbf{5a}^{\cdot-}$. Then dissociation of the charge-

separated complex gives aryl bromide radical anion **5a**$^{\bullet-}$, and then a bromo anion eliminates to an aryl radical.[9] The aryl radical abstracts a hydrogen atom from diisopropylethylamine radical cation to yield reduced product **6a**. On the other hand, the radical cationic aluminum complex **1**$^{\bullet+}$ is reduced by diisopropylethylamine to regenerate **1**.

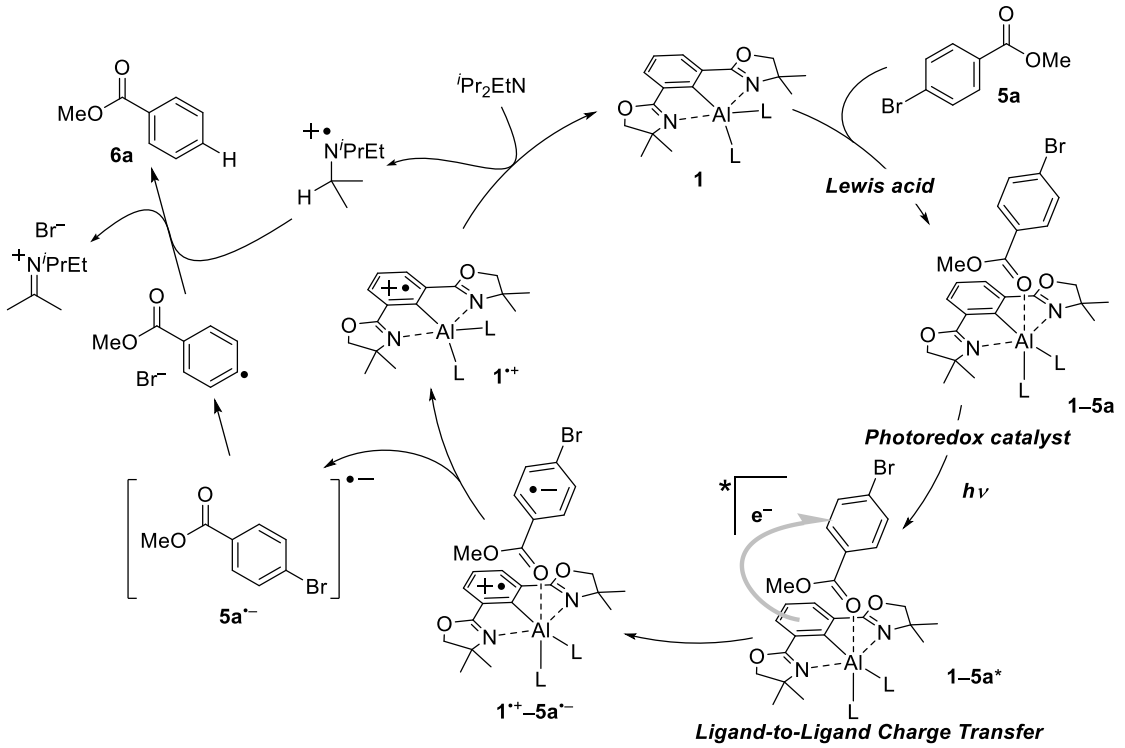

Scheme 3. Plausible reaction mechanism

Then, this aluminum complexes catalyzed reaction system was compared with the reported methods of hydrodebromination under visible light irradiation. Hydrodebromination of aryl bromides **7** bearing two bromine groups in the same molecule was performed. This reaction can give three types of compounds **8**, **9**, and **10**. Using the aluminum catalyst **4**-Al$(ClO_4)_2$, only the bromine atom on the benzene ring bearing a carbonyl group was selectively reduced to obtain a single product **8** in high yield (Entry 1). On the other hand, Method A using an iridium complex[10] yielded product **9** in which both bromo groups were reduced (Entry 2). Method B using tris(trimethylsilyl)silane[11] gave a mixture of three products **8**–**10** (Entry 3).

Table 2. Hydrodebromination of aryl bromide bearing two different bromine atoms in a molecule

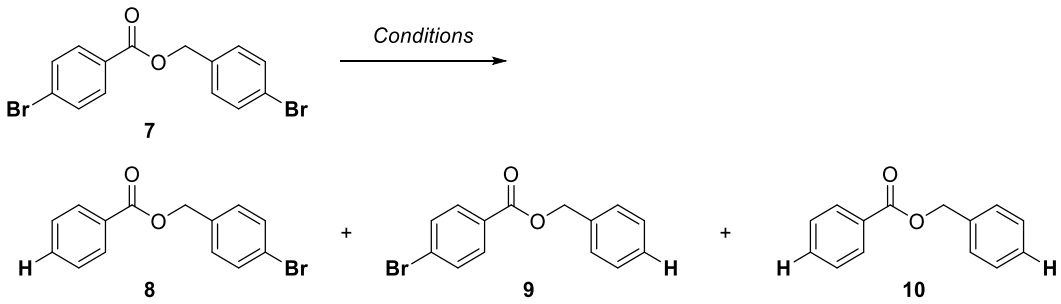

Entry	Conditions	Yield [%][a]		
		8	**9**	**10**
	<u>This work</u>			
1	**4**-Al(ClO_4)$_2$ (5 mol%), ^{i}Pr$_2$EtN (10 equiv) MeCN (0.2 M), RT, 24 h, 405 nm LED	84	0	0
	<u>Method A</u>			
2	[Ir(dtbbpy)(ppy)$_2$]PF_6[b] (0.5 mol%l) ^{i}Pr$_2$EtN (2.2 equiv), (Me_3Si)$_3$Si–H (2.2 equiv) MeCN (0.1 M), RT, 4 h, Open air, 455 nm LED	0	0	88
	<u>Method B</u>			
3	(Me_3Si)$_3$Si–H (1.0 equiv) MeCN (0.2 M), RT, 8 h, 405 nmLED	35	16	13

[a] 0.2 mmol of **7** was used. Yields and recovery were determined by NMR analysis using 1,1,2,2-tetrachloroethane as an internal standard. [b] [Ir(dtbbpy)(ppy)$_2$]PF_6: (4,4'-di-*tert*-butyl-2,2'-bipyridine)bis[(2-pyridinyl)phenyl]iridium(III) Hexafluorophosphate.

Then, a competition experiment between two substrates with similar reduction potentials and different steric hindrances around the coordination site was conducted. In the Phebox–Al catalysis (Entry 1), dimethylamide **5f** which has less steric hindrance, was preferentially reduced, whereas Method A and Method B showed almost no selectivity (Entries 2 and 3). Method C, the catalytic system using perylene diimide reported by König et al.,[12] also showed no selectivity and the reaction rarely progressed. Thus, the Phebox–Al complexes in this study have a Lewis acid moiety and thus recognize differences in the presence or absence of substrate coordination sites and steric hindrance.

Table 3. Competitive reduction between aryl bromides.[a]

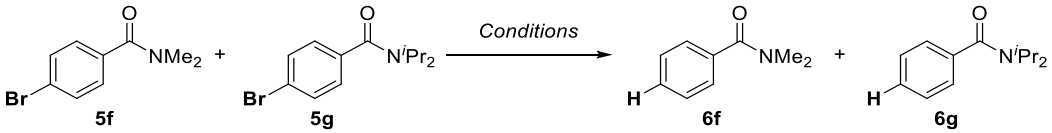

Entry	Conditions	Yield [%][b]	
		6f	**6g**
	This work		
1	**4**-Al(ClO_4)$_2$ (0.01 mmol), ^{i}Pr$_2$EtN (2.0 mmol) MeCN (1.0 mL), RT, 4 h, 405 nm LED	66	17
	Method A		
2	[Ir(dtbbpy)(ppy)$_2$]PF_6[c] (0.001 mmol) ^{i}Pr$_2$EtN (0.44 mmol), (Me_3Si)$_3$Si–H (0.44 mmol) MeCN (2 mL), RT, 15 min, Open air, 455 nm LED	39	48
	Method B		
3	(Me_3Si)$_3$Si–H (0.1 mmol) MeCN (1.0 mL), RT, 12 h, 405 nmLED	51	43
	Method C		
4	PDI[d] (0.005 mmol), Et_3N (0.8 mmol) DMF (6.0 mL), RT, 12 h, 455 nmLED	7	5

[a] An equimolar amount (0.1 mmol) of **5f** and **5g** were used. [b] Yields were determined by GC analysis using hexadecane as an internal standard. [c] [Ir(dtbbpy)(ppy)$_2$]PF_6: (4,4'-di-*tert*-butyl-2,2'-bipyridine)bis[(2-pyridinyl)phenyl]iridium(III) hexafluorophosphate. [d] PDI: *N*,*N*′-bis(2,6-diisopropylphenyl)-3,4,9,10-perylenetetracarboxylic diimide

3-3. Conclusion

A hydrodebromination reaction of aryl bromides catalyzed by Phebox–Al complexes under visible light irradiation was developed. Various aryl bromides bearing Lewis basic coordination site were applicable for this reaction. UV/vis absorption spectra and TD-DFT calculations suggested ligand-to-ligand charge transfer from a Phebox ligand to an aryl bromide occurred under photo irradiation. Substrate recognition without depending on the redox potential of the substrates was achieved due to the Lewis acid–base interaction between Phebox–Al complexes and substrates.

3-4. Experimental Section

General

NMR spectra were recorded on aJEOL JNM-400 (400 MHz for ^{1}H NMR and 100 MHz for ^{13}C NMR, and 103 MHz for ^{27}Al NMR) spectrometer or aBruker AVANCE III (600 MHz for ^{1}H NMR and 150 MHz for ^{13}C NMR) spectrometer. Chemical shifts were reported in ppm on the δ scale relative to tetramethylsilane (δ = 0 for ^{1}H NMR) and residual $CHCl_3$ (δ = 77.0 for ^{13}C NMR) as an internal reference, and $AlCl_3$ in D_2O (δ = 0 for ^{27}Al NMR) as an external reference. New compounds were characterized by ^{1}H, ^{13}C, ^{13}C off-resonance techniques, COSY, HMQC, and HMBC. Infrared (IR) spectra were recorded on a JASCO FT/IR-6200 Fourier transform infrared spectrophotometer or a METTLER TOLEDO ReactIR15. Column chromatographies were performed with silica gel. Purification by recycle HPLC was performed on a SHIMADZU recycle HPLC system (SPD-20A, RID-10A, DGU-20A, LC-6AD, and FCV-20H2) and a Japan Analytical Industry Co. (NEXT recycling preparative HPLC). Reactions were carried out in dry solvents under nitrogen atmosphere, unless otherwise stated. Reagents were purchased from Aldrich or Tokyo Chemical Industry Co., Ltd. (TCI), Wako Pure Chemical Industries, Ltd., and used after purification by distillation or used without purification for solid substrates. X-ray diffraction analysis was carried out by a Rigaku XtaLAB Synergy with Hypix-6000HE. EvoluChem P206-18-8 was used as 405 nm LED light. Kessil A160WE Tuna Blue was used as 455 nm LED light.

Materials

Dehydrated solvents were purchased from Wako Pure Chemical Industries and used as obtained. Aryl bromides (**5a**, **5b**, **5c**, **5d**, **5e**, **5i, 5j**) were purchased. *N*,*N*-diisopropylethylamine and triethyl amine were used after purification by drying with CaH_2, distillation, and Freeze-Pump-Thaw cycling. Tris(trimethylsilyl)silane was used after distillation. Other aryl bromides (**5f**,[13] **5g**,[14] **5h**,[15] **7**[16]) were prepared by the reported method, and spectroscopic data matches that were reported in the literature. All metal salt catalysts were purchased used as obtained.

Products

All products in hydrodebromination (Scheme 2) are known compounds. Hydrodebrominated products **6** are identified with standard samples by GC analysis. Standard samples (**6a**, **6b**, **6c**, **6d**, **6e**, **6f**, **6h**, **6i**, **6j**) were purchased and **6g**[17] was prepared by the reported procedure. **8**,[18] **9**[19], and **10**[19] are identified by the reported papers.

General procedures

Hydrodebromination of aryl bromides

In N_2-filled glove box, to a solution of aryl bromide **5** (0.2 mmol) and *N*,*N*-diisopropylethylamine in acetonitrile (0.5 mL), a solution of catalytic amount of organoaluminum complex in acetonitrile (0.5 mL) was added and the resulted mixture was stirred at ambient temperature under photoirradiation

(purple LED, λ_{max} = 405 nm). After the reaction, hexadecane was added as an internal standard, and then a yield of hydrodebrominated product and a recovery of starting material were determined by GC analysis.

Competitive hydrodebromination of 7

Method A.

In N_2-filled glove box, to a solution of aryl bromide **7** (0.2 mmol) and $[Ir(dtbbpy)(ppy)_2]PF_6$ (0.001 mmol) in acetonitrile (2.0 mL), tris(trimethylsilyl)silane (0.44 mmol) and then *N*,*N*-diisopropylethylamine (0.44 mmol) were added. The reaction vial was brought out of the glove box to expose to the air and the resulted mixture was stirred at ambient temperature under photoirradiation (blue LED, λ_{max} = 455 nm). After the reaction, 1,1,2,2-tetrachloroethane was added as an internal standard, and then a yield of hydrodebrominated product and a recovery of starting material was determined by NMR analysis.

Method B

In N_2-filled glove box, to a solution of aryl bromide **7** (0.2 mmol) in acetonitrile (1.0 mL), tris(trimethylsilyl)silane (0.2 mmol) was added. The resulted mixture was stirred at ambient temperature under photoirradiation (purple LED, λ_{max} = 405 nm). After the reaction, 1,1,2,2-tetrachloroethane was added as an internal standard, and then a yield of hydrodebrominated product and a recovery of starting material was determined by NMR analysis.

Competitive hydrodebromination of 5f and 5g

Method A

In N_2-filled glove box, to a solution of aryl bromides **5f** (0.1 mmol) and **5g** (0.1 mmol) in acetonitrile (1.0 mL), a solution of $[Ir(dtbbpy)(ppy)_2]PF_6$ (0.001 mmol) in acetonitrile (1.0 mL), tris(trimethylsilyl)silane (0.44 mmol) and *N*,*N*-diisopropylethylamine (0.44 mmol) were added. The reaction vial was brought out of the glove box to expose to the air and the resulted mixture was stirred at ambient temperature under photoirradiation (blue LED, λ_{max} = 455 nm). After the reaction, hexadecane was added as an internal standard, and then a yield of hydrodebrominated product and a recovery of starting material was determined by GC analysis.

Method B

In N_2-filled glove box, to a solution of aryl bromides **5f** (0.1 mmol) and **5g** (0.1 mmol) in acetonitrile (1.0 mL), tris(trimethylsilyl)silane (0.2 mmol) was added. The resulted mixture was stirred at ambient temperature under photoirradiation (purple LED, λ_{max} = 405 nm). After the reaction, hexadecane was added as an internal standard, and then a yield of hydrodebrominated product and a recovery of starting material was determined by GC analysis.

Method C

In N_2-filled glove box, to a solution of *N*,*N*′-bis(2,6-diisopropylphenyl)-3,4,9,10-perylenetetracarboxylic Diimide (PDI) (0.005 mmol) and triethylamine (0.8 mmol) in *N*,*N*-dimethylformamide (3.0 mL), a solution of aryl bromides **5f** (0.1 mmol) and **5g** (0.1 mmol) in *N*,*N*-dimethylformamide (3.0 mL) was added. The resulted mixture was stirred at ambient temperature under photoirradiation (blue LED, λ_{max} = 455 nm). After the reaction, hexadecane was added as an internal standard, and then a yield of hydrodebrominated product and a recovery of starting material was determined by GC analysis.

Computational chemistry

All computations were performed using the Gaussian 16 program. Optimization of the geometry was performed at the B3LYP/6-31G(d,p) level of theory, the starting geometries were based on the crystallographic coordinates. TD-DFT calculation was performed at the B3LYP/6-31G(d,p) level of theory using the optimized structure.

3-5. References

[1] C. Stephenson, T. Yoon, D. W. C. MacMillan, *Visible Light Photocatalysis in Organic Chemistry*, Wiley-VCH Verlag GmbH & Co. KGaA, Weinheim, Germany, **2018**.

[2] K. L. Skubi, T. R. Blum, T. P. Yoon, *Chem. Rev.* **2016**, *116*, 10035–10074.

[3] C. W. Tang, S. A. Vanslyke, *Appl. Phys. Lett.* **1987**, *51*, 913–915.

[4] A. Popczyk, A. Aamoum, A. Migalska-Zalas, P. Płóciennik, A. Zawadzka, J. Mysliwiec, B. Sahraoui, *Nanomaterials* **2019**, *9*, 1–15.

[5] M. M. Hansmann, A. López-Andarias, E. Rettenmeier, C. Egler-Lucas, F. Rominger, A. S. K. Hashmi, C. Romero-Nieto, *Angew. Chemie Int. Ed.* **2016**, *55*, 1196–1199.

[6] R. Cibulka, R. Vasold, B. König, *Chem. Eur. J.* **2004**, *10*, 6223–6231.

[7] Y. Aramaki, N. Imaizumi, M. Hotta, J. Kumagai, T. Ooi, *Chem. Sci.* **2020**, *11*, 4305–4311.

[8] Y. Nishimoto, S. Nakao, S. Machinaka, F. Hidaka, M. Yasuda, *Chem. Eur. J.* **2019**, *25*, 10792–10796.

[9] C. Costentin, M. Robert, J. M. Savéant, *J. Am. Chem. Soc.* **2004**, *126*, 16051–16057.

[10] J. J. Devery, J. D. Nguyen, C. Dai, C. R. J. Stephenson, *ACS Catal.* **2016**, *6*, 5962–5967.

[11] H. Jiang, J. R. Bak, F. J. López-Delgado, K. A. Jørgensen, *Green Chem.* **2013**, *15*, 3355–3359.

[12] I. Ghosh, T. Ghosh, J. I. Bardagi, B. König, *Science* **2014**, *346*, 725–728.

[13] G. H. Chan, D. Y. Ong, Z. Yen, S. Chiba, *Helv. Chim. Acta* **2018**, *101*, 2–9.

[14] K. D. Otley, J. A. Ellman, *Org. Lett.* **2015**, *17*, 1332–1335.

[15] R. Mandal, B. Emayavaramban, B. Sundararaju, *Org. Lett.* **2018**, *20*, 2835–2838.

[16] T. Werner, J. Koch, *Eur. J. Org. Chem.* **2010**, 6904–6907.

[17] D. Ach, V. Reboul, P. Metzner, *Eur. J. Org. Chem.* **2003**, 3398–3406.

[18] D. Ye, Z. Liu, H. Chen, J. L. Sessler, C. Lei, *Org. Lett.* **2019**, *21*, 6888–6892.

[19] H. Huang, J. Y. Kang, *Org. Lett.* **2017**, *19*, 544–547.

Conclusion

This thesis reported the development of Lewis acid-catalyzed reactions and novel Lewis acid catalysts based on fine tuning of Lewis acidity and catalytic activity of indium or *C*,*N*-chelated organoaluminum complexes.

Chapter 1 revealed the coupling reaction of electron-deficient alkenyl ethers with silicon nucleophiles was catalyzed by indium salts. Various alkenyl ethers and silicon nucleophiles were applicable in this reaction. Strong Lewis acid $TiCl_4$ and strong nucleophiles, a fluoride anion-activated Si enolate, a Li enolate, and a Zn enolate, were not suitable for this coupling reaction. These results indicate both the moderate Lewis acidity of indium salts and the moderate nucleophilicity of silicon nucleophiles are essential for this reaction. The observation of an intermediate by VT-NMR proposed an addition–elimination reaction mechanism. This reaction gave 1,5-dioxo-alk-2-ene products with a perfect stereoselectivity, and the reduction of the product provided 1,5-dihydroxy-alk-2-ene with retention of the stereochemistry of the carbon–carbon double bond, which is a partial structure of bioactive natural products.

Chapter 2 focused on aluminum which is inexpensive and abundant in the earth's crust. I synthesized *C*,*N*-chelated organoaluminum complexes, Pheox– and Phebox–Al, and characterized by spectroscopic analysis. These ligands stabilized organoaluminum complexes and maintained their Lewis acidity. Their Lewis acidities were estimated experimentally and theoretically. Lewis acidity was precisely controlled by counteranions, the oxazoline coordination, and substituents on carbon ligands. Tuning of the Lewis acidity improved the catalytic activity for the hydroboration reaction of benzaldehyde and showed the opposite selectivity to $AlCl_3$ in the competitive hetero Diels–Alder reaction.

In Chapter 3, Phebox–Al complexes, which were developed in Chapter 2, promoted the hydrodebromination reaction of aryl bromides under visible light irradiation. Phebox–Al complexes acted as not only Lewis acids, but also photoredox catalysts. Various aryl bromides bearing Lewis basic coordination groups were suitable for this reaction. UV/vis absorption spectra and TD-DFT calculations suggested ligand-to-ligand charge transfer from Phebox ligand to an aryl bromide occurred under photo irradiation. The Lewis acid–photoredox cooperative catalyst achieved substrate recognition without relying on the redox potential substrates.

Chapter 1 shows an importance of moderate Lewis acidity of indium salts and the new coupling reaction was developed by choosing proper metal center. In chapters 2 and 3, focusing on the modification of ligands, fine tuning of a Lewis acidity of organoaluminum complexes and the metal–ligand cooperation are demonstrated.

The obtained knowledge provides an opportunity to develop main-group metal Lewis acid catalysts.